Università degli Studi della Tuscia di Viterbo
IFO – Istituto Regina Elena IRE

Corso di Dottorato di Ricerca in

Ecologia e gestione Sostenibile delle Risorse Ambientali

XXXIV Ciclo

Role of telomeric protein TRF2 in aging and cancer

Settore scientifico-disciplinare
BIO/11

Tesi di dottorato di:

Serena Di Vito

Coordinatore del corso

Prof. Claudio Carere

Tutor

Dott.ssa Annamaria Biroccio

Dott. Carlo Leonetti

Co-tutor

Prof.ssa Carla Caruso

A.Y. 2021/22

INDEX

1. ABREVIATIONS

AFM, Atomic force microscopy

ALT, Alternative Lengthening of Telomeres

APB, ALT-associated PML body

ATM, Ataxia Telangiectasia mutated

ATR, ATM and rad3-related

BC, Breast cancer

BC, Black carbon

BLM, Bloom syndrome protein, RecQ helicase-like

BRCA1/2, Breast cancer type 1/2 susceptibility protein

CRISPR-Cas9, Clustered Regularly Interspaced Short Palindromic Repeats

CTE, C-terminal domain

DDR, DNA damage response

DDT, Para-dichlorodiphenyltrichloroethane

DSB, Double strand breaks

dsDNA, Double-stranded DNA

ECM, Extracellular matrix

EGFR, Epidermal Growth Factor Receptor

EPA, Environmental Protection Agency

ER, Estrogen receptor

γH2AX, H2A histone family member X

GPC6, Glypican 6

GST, Glutathione S-transferases

HER2, Human epidermal growth factor-2 receptor

HR, Homologous recombination

HS3ST4, Heparan Sulfate-Glucosamine 3-Sulfotransferase 4

hTR, Human telomerase RNA

IARC, International Research Agency on Cancer

IFNγ, Interferon γ

IHC, Immunohistochemistry

ITS, Interstitial telomeric sequences

LINC, Linker of Nucleoskeleton and Cytoskeleton

LPA, Lysophosphatidic acid

MDSC, Myeloid-derived suppressor cells

MRE11, meiotic recombination 11

mRNA, Messenger RNA

MYB, Myeloblastosis

NAF1, Nuclear Assembly Factor 1

NBS1, Nijmegen breakage syndrome

NHEJ, Non-homologous end joining

NK, Natural Killer

NMR, Nuclear magnetic resonance spectroscopy

NSG, NOD scid gamma

OS, Oxidative stress

p53, Tumor suppressor p53

PAH, Polycyclic aromatic hydrocarbons

PARP1/2, Poly [ADP-ribose] polymerase 1/2

PLA, Proximity Ligation Assay

PM, particulate matter

PML, promyelocytic leukemia

POP, Persistent organic pollutants

POT1, Protection of Telomere Protein 1

PR, Progesterone

RAD50, Double strand break repair protein

RAP1, Repressor-activator protein 1

RCT, C-terminal

RNA, RiboNucleic Acid

RNP, Ribonucleoprotein

ROS, Reactive oxygen species

RPA, Replication protein A

RT, Reverse transcriptase

SES, Socioeconomic status

shRNA, Short Hairpin RNA

SULF2, Sulfatase 2

TCAB1, Telomerase Cajal body protein 1

TCGA, The Cancer Genome Atlas

TEN, N-terminal

TERRA, Telomeric repeat-containing RNA

TERT, Telomerase reverse transcriptase

TIF, Telomere dysfunction induced DNA damage foci

TIN2, TERF1-interacting nuclear factor 2

TLR2, Toll Like Receptor 2

TMM, Telomere maintenance mechanism

TNBC, Triple negative breast cancer

TPE, Telomere position effect

TPP1, Tripeptidyl Peptidase 1

TR, Telomerase RNA component

TRBD, Telomerase RNA binding domain

TRF1, Telomere Repeat binding Factor 1

TRF2, Telomere Repeat binding Factor 2

TRFH, TRF homology

TUNEL, Terminal deoxynucleotidyl transferase dUTP nick end labeling

VCAN, Versican

VEGF-A, Vascular-Endothelial Growth Factor-A

WRN, Werner syndrome ATP-dependent helicase

WT, Wild-type

WT1, Wilms Tumor 1

2. GENERAL INTRODUCTION

2.1. ENVIRONMENT AND CANCER

2.1.1. Environmental tumor-promoting factors

Cancer is the major public health problem worldwide, both industrialized countries and under-developed countries, with 81-100% increase projected by 2030 (Ding *et al.*, 2015). It is a multifactorial disease, with environmental and genetic factors representing risk factors for developing cancer.

About 90-95% of all cancers are thought to be related to environment and lifestyle, while 5-10% have their roots in heredity (Figure 1) (Anand *et al.*, 2008).

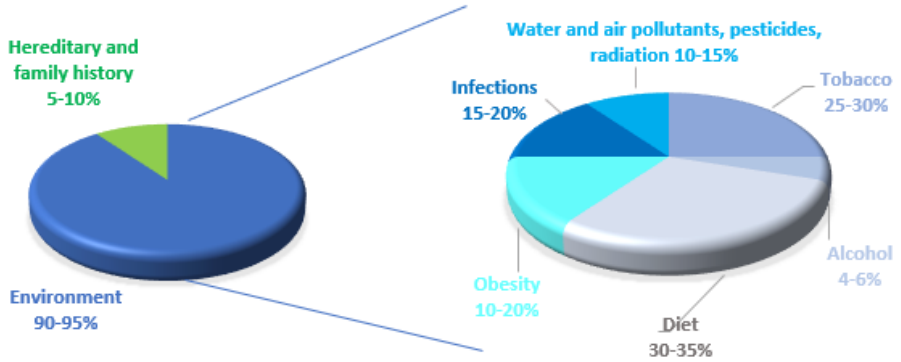

Figure 1. Risk factors of cancer.

Environmental factors include lifestyle choices such as cigarette smoking, excessive alcohol consumption, poor diet, lack of exercise and excessive exposure to sunlight (Figure 2) (Ng *et al.*, 2020). Other factors include exposure to certain drugs, hormones, X-rays, gamma rays, radioactive materials, aniline type dyes, free radicals, asbestos,

silica dust, air pollution, food additives, chemicals used in perfumes, oncogenic viruses and bacteria (Kaleli, Deveci and Guney Eskiler, 2018). They can be present in air, water, food and workplace. Many environmental chemicals have been identified through studies of occupational groups that have higher exposures to these chemicals compared to the general population. Various environmental exposures are linked to specific types of cancer (Belpomme *et al.*, 2007; Parsa, 2012). For example, exposure to asbestos is mainly linked to lung cancer (Nielsen *et al.*, 2014), while exposure to benzidine, a chemical found in some dyes, has been associated with bladder cancer (Bi *et al.*, 1992; Tan, Goedegebuure and Eberlein, 2012). The effect of smoking is linked to tumors of the lung, bladder, mouth, colon, kidneys, throat, esophagus, stomach, cervix, liver and pancreas (Loeb *et al.*, 1984; Sasco, Secretan and Straif, 2004; U.S.DHSS, 2010; Macacu *et al.*, 2015; Alexandrov *et al.*, 2016; Conlon *et al.*, 2020; Mori *et al.*, 2020).
Over time, environmental substances can cause genetic alterations, which accumulate in our body. Although many alterations have no effect on a person's health, there are permanent mutations in some genes that can lead to cancer. The possibility that a person develops cancer in response to a certain environmental agent depends on the interaction between several factors, including time of exposure to a substance, exposure to additive agents, genetic factors, diet, lifestyle, health, age and gender. For this reason, the correlation between environmental exposure and the risk of developing cancer cannot be predicted.
It has been described in several studies that diagnostic/therapeutic X-rays can cause mutations and be related to the onset of tumors. For example, radiation treatment in childhood with acne or head and neck diseases produce an increased risk of thyroid cancer or head and neck cancers. Also, the children whose mothers received diagnostic radiographs during pregnancy were found to be at increased risk for childhood leukemia. Additional studies in women who received weekly chest x-rays for prolonged periods to monitor Tubercolosis therapy showed an increased risk of radiation-related breast cancer (BC) (Kohn, 1990; Lin, 2010).

Dietary factors have been associated with 30% of cancers in Western countries (Key *et al.*, 2002). In fact, having a healthy diet is a great way of prevention. It has been demonstrated that some synthetic additives used have carcinogenic effects, such as cinnamyl anthranilate and thiourea, the use of which has now been banned. Other substances, potentially carcinogenic, including nitrite salts, sodium nitrite and potassium nitrite are still widely used today in various food products (Kaleli, Deveci and Guney Eskiler, 2018; M Waheed, Aleksandra and Matthias, 2018; Mentella *et al.*, 2019; Key *et al.*, 2020).

Nowadays industrial expansion causes an increasing rate of toxic pollution as highly toxic waste and extremely harmful to nature and human health are released into the environment (Okunola A *et al.*, 2019; Manisalidis *et al.*, 2020; Naidu *et al.*, 2021). Many of these waste products are mutagenic and, like ionizing radiation, cause genetic disease mutations and contribute to the onset of cancer. For this reason, the management of environmental resources turns out to be one an issue of increasing importance due to its consequences on public health. The main natural resources affected are water, air and the atmosphere in general (Figure 2).

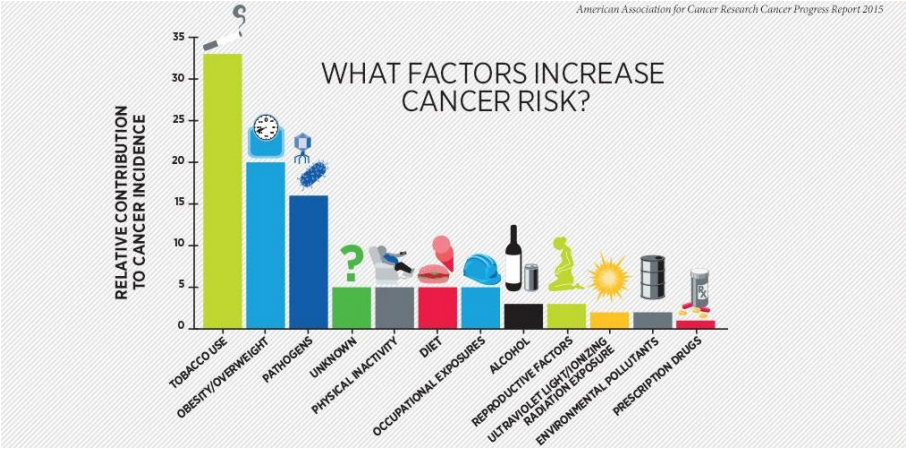

Figure 2. Factors that increase the risk of developing cancer, including cigarette smoking, body weight, infection with pathogens, physical activity, diet, ultraviolet (UV) exposure, pollutants and drugs (American Association for Cancer Research, Cancer Progress Report 2017).

Pollutants are organic and inorganic substances due to human activity. There are many different types of industrial waste that are released by industries. For example, caustic soda and chlorine factories release heavy metals such as cadmium, a dangerous risk factor for cancer (Huff *et al.*, 2007).

Exposure to heavy metals is associated with cancer risk depending on dose, genetics, immune system, age, nutrition level, and general health of the person exposed. When metals enter the body through air, food, water or skin exposure, exert their enzymatic and genotoxic effects on different organs. Some heavy metals such as chromium, copper, lead, nickel, zinc and mercury can affect human health as far as the food chain (Kim *et al.*, 2015).

Drinking water used for domestic use is often polluted with arsenic, leading to an increased risk in develop lung, bladder, breast and skin cancers (Mendez *et al.*, 2017). In 2001, the Environmental Protection Agency (EPA), responsible for water control, established the maximum concentration of arsenic present in drinking water as <10μg / l. However, recent studies have proved that such a concentration is associated with a higher incidence of skin cancer. Other sources of water pollution are fertilizers and herbicides used in agriculture. The most widely used herbicide is glyphosate, but only recently the International Research Agency on Cancer (IARC) in March 2015 decided to reclassify the compound in category 2A (probably carcinogenic to humans). Subsequent studies performed in humans and rodents confirmed a link between glyphosate-based herbicide and the development of different tumors, thus supporting the potential role of glyphosate as carcinogenic (Zhang *et al.*, 2019; Portier, 2020).

2.1.2. Environmental effects on breast cancer risk

Breast cancer (BC) is one of the most frequently diagnosed cancers in women. Mortality is associated mainly with the development of metastases (Koual *et al.*, 2020). Environmental factors, in combination with genetic predisposition, are believed to be a major cause of the

increased incidence of BC. Recent studies have shown that cadmium, even in low doses, acts as an estrogen mimic, suggesting the need to study the effects of metals on BC risk (Coyle, 2004; Eriksen *et al.*, 2014). Among risk factors, chemical environment and pollution are increasingly suggested to have a relevant effect on the signaling pathways involved in metastatic tumor progression.

There are many environmental factors that influence the eventual tumorigenesis of BC throughout the lifespan, from prenatal exposures in utero through puberty and maturity in the postmenopausal years. At every stage of life, there are multi-level influences, from individual behavior to social factors to broader environmental factors. Particular importance assumes puberty, as it is clinically defined by the first signs of breast development, pubic hair and other secondary sex features (Hiatt, Haslam and Osuch, 2009). *Hiatt et al* break down the environmental factors that can influence the onset of BC into three main categories (Figure 3):

a) physical environment - exposure to environmental pollutants or toxic substances;

b) built environment, or the places where you live;

c) social environment - social norms of behavior and culture.

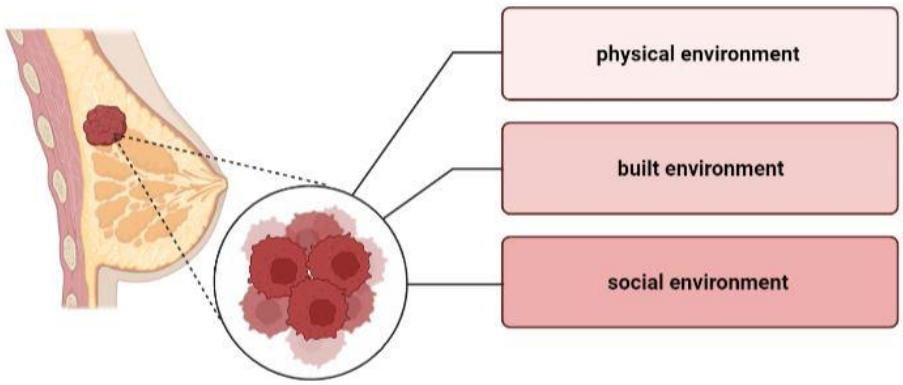

Figure 3. Main categories of environmental factors that influence the BC developing.

Synthetic and natural agents, such as xenoestrogens, are referred as endocrine disruptors because of them ability to disrupt normal hormone

levels. Sources of these substances are personal care products, cosmetics and food-grade plastic wrappers. Recent studies have shown that girls who had been exposed to pesticides like DDT (para-dichlorodiphenyltrichloroethane) before the age of 14 have a higher incidence of BC compared to those who had not been exposed (Baveye and Laba, 2008). Polycyclic Aromatic Hydrocarbons (PAHs) are a class of chemicals that are generated by incomplete combustion of coal, oil and gas, as well as tobacco smoke and other substances to which humans are continuously exposed. These substances are known to be potential breast carcinogens, genotoxic substances that damage DNA through oxidative stress; in particular, puberty is considered to be the period during which the breast is more sensitive to these effects (Jeffy, Chirnomas and Romagnolo, 2002; Korsh *et al.*, 2015; White *et al.*, 2016). Finally, exposure to ionizing radiation has always been recognized as a risk factor for BC, probably due to induction of double-stranded DNA breaks (Ronckers, Erdmann and Land, 2005).

Also influencing the incidence and mortality of BC are various aspects of the built environment, such as the availability of transport to clinics or location of hospitals for screening and treatment (Akinyemiju *et al.*, 2015; Cheng *et al.*, 2015). Sometimes, in fact, the therapeutic structures are located outside the neighborhoods where low-income minorities live and this can represent an obstacle for the prevention and treatment of pathologies (Coughlin and King, 2010; S. Coughlin, 2015).

At last, there is a known direct relationship between a woman's socioeconomic status (SES) and the onset of BC (Lee and Cubbin, 2002; Pudrovska, Anishkin and Shen, 2012). Socioeconomic determinants that appear to influence BC incidence include income, education, unemployment, immigration, inadequate housing, and geographic factors such as proximity to health services (Chagpar and Coccia, 2012; Coughlin, 2019). In particular, low socioeconomic status may be associated with an increased risk of aggressive premenopausal BCs, as well as late diagnosis and a lower survival rate. A study on a group of African American women showed that low socioeconomic status and psychosocial stress in early childhood and adulthood may

contribute to an increased risk of BC (Williams, Mohammed and Shields, 2016). At the same time, it has been seen that women with higher socioeconomic status tend to have their first child later in life, have fewer children and have menopause later, which increases the risk of BC (Hiatt, Haslam and Osuch, 2009).

2.1.2.1. Breast cancer subtypes and therapies

BC is the most common cancer among women and one of the most important causes of death among them. The prognosis is good when the cancer is localized in the breast (5-year survival rate, 99%), but the survival rate decreases significantly with disseminated disease (survival of 26% frequency if distant metastases are present) (Siegel, Miller and Jemal, 2020). BC progression is defined by an increase in the rate of growth and invasiveness of the tumor. This leads to the acquisition of metastatic potential in cancer cells. Metastasis involves the spread of cancer cells from the primary tumor to the surrounding tissues and, as well as to distant organs, and represents the main cause of mortality (90%) (Koual *et al.*, 2020). Drug resistance to chemotherapy is not uncommon, especially in some subtypes of BC, so an in-depth analysis of this aspect represents a great challenge to improve the lives of patients with BC.

Therapeutic concepts follow a multidisciplinary context, taking into account the molecular subtype.

BC has four primary molecular subtypes (Figure 4), defined in large part by hormone receptors (HR) and other types of proteins involved (or not involved) in each cancer:

- Luminal A or HR+/HER2- (HR-positive/HER2-negative);
- Luminal B or HR+/HER2+ (HR-positive/HER2-positive);
- Triple-negative or HR-/HER2- (HR/HER2-negative);
- HER2-positive.

A fifth subtype, known as normal-like BC, closely resembles luminal A.

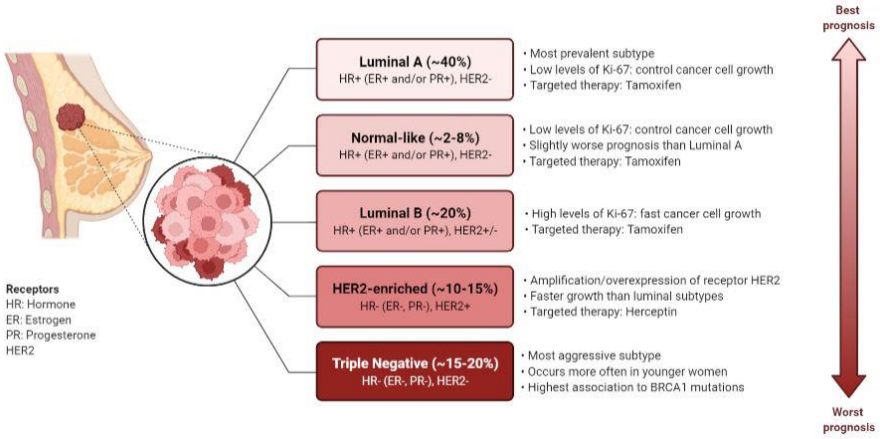

Figure 4. Subtypes of BC, characteristics and prognosis (from Dai *et al.*, 2015).

About 15% of breast carcinomas is represented by triple negative BC (TNBC) (Denkert *et al.*, 2017; Harbeck and Gnant, 2017; Pernaut, Lopez and Ciruelos, 2018), a particularly aggressive and heterogeneous subtype. TNBC is defined as a BC type with negative expression of estrogen (ER), progesterone (PR) and human epidermal growth factor-2 receptor (HER2) (Wolff *et al.*, 2014). Germinal mutations in breast and ovarian cancer susceptibility genes were identified in 14.6 % of all patients and have been associated with TNBC. Of these, 11.2 % had mutations in the BRCA1 (8.5 %) and BRCA2 (2.7 %) genes (Kumar and Aggarwal, 2016). The development of metastases in TBNC represents a highly complex process that includes different steps such as genetic and epigenetic alterations, angiogenesis, tumor-stroma interactions, intravasation through the basement membrane, survival in the circulation and extravasation in the distal tissues (Al-Mahmood *et al.*, 2018).

Epidemiological data show that TNBC mainly occurs in young premenopausal women under 40, which account for about 15-20% of the whole BC patients. Compared to other types of BC, TNBC patient survival time is shorter and the mortality rate is 40% within the first 5 years after diagnosis (Dent *et al.*, 2007). TNBC is highly invasive, the

average survival time after the onset of metastases is very low, and the recurrence rate after surgery reaches 25%. Compared to other types of BC, TNBC has limited treatment options and the chemotherapy remains the main approach (Wahba and El-Hadaad, 2015). Recently the literature has shown that the use neoadjuvant chemotherapy regimens in treatment of TNBC can significantly improve the prognosis of TNBC patients. The guidelines of the Comprehensive National Cancer Network recommend the use of combination regimens based on taxane, anthracycline, cyclophosphamide, cisplatin and fluorouracil (L. Yin *et al.*, 2020). Despite the difficulty in discovering new targeted therapies due to the high heterogeneity of TNBC, there are currently a large number of clinical trials ongoing targeting specific receptors or targeted therapies based on immunohistochemical staining results. Examples are EGFR-targeted treatment, PARP inhibitors and immunotherapy (Du *et al.*, 2015; Vagia, Mahalingam and Cristofanilli, 2020).

2.2. TELOMERES, CANCER AND ENVIRONMENTAL FACTORS

2.2.1. Telomeres: general features

2.2.1.1. Structure and function of telomeres

Telomeres are nucleoprotein structures present at the chromosomal endings, composed of 5’-TTAGGG-3’ tandem repeats (G-rich strand) and a complementary sequence 3’-AATCCC-5’ (C-rich strand). The telomere terminus is not blunt, but consists of a single filament protrusion of the G-strand, called "G overhang ", which varies from a length of 50 nt to 500 nt (McElligott and Wellinger, 1997; Paeschke, McDonald and Zakian, 2010). By conducting experiments to investigate the physical structure of the ends of the chromosome, *Griffith et al* demonstrated that telomere DNA is organized in a large

structure called "t-loop" (Griffith *et al.*, 1999). The strand called G-overhang invades a region of double-stranded telomeric DNA (dsDNA) to form a displacement loop (D-loop) and a double-stranded telomeric loop (T-loop) region (Nikitina and Woodcock, 2004). The T-loop has the purpose of masking the DNA terminus from the DNA double strand break repair (DSB) machinery.

Associated to telomeric DNA there is a protein component, the Shelterin complex, formed by six different proteins, TRF1, TRF2, POT1, RAP1, TIN2 and TPP1 in mammalian cells (Palm and De Lange, 2008; Schmutz and De Lange, 2016; Chen, 2019) (Figure 5).

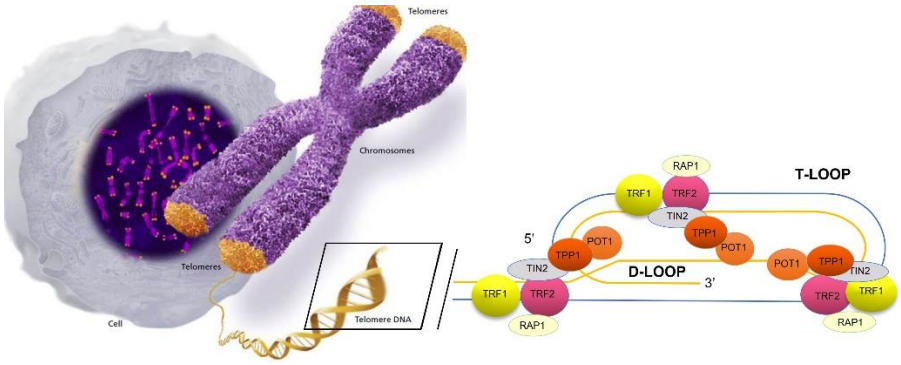

Figure 5. Telomere structure and Shelterin complex.

The Shelterin complex function is crucial for telomere maintenance and genome integrity. Knockout experiments in mouse cells have proved that shelterin protects telomeres from DNA damage signaling and DNA repair and it also promotes the semi-conservative telomeric DNA replication. Also, shelterin regulates the telomerase mediated maintenance of telomeric DNA (Schmutz and De Lange, 2016).

The main interaction interfaces of the Shelterin subunits were established on the basis of co-immunoprecipitation experiments, two yeast hybrids analysis, and structural studies. TRF1 and TRF2 bind to TIN2 using distinct interaction surfaces. TIN2 also binds to TPP1, which in turn binds to POT1. RAP1 binds TRF2, completing the six-subunit complex (Erdel *et al.*, 2017).

TRF1 and TRF2 exist as homodimers and bind the double-stranded DNA regions of telomeres with high affinity and specificity. TRF1 negatively regulates telomere length by a counting mechanism promotes efficient DNA replication of telomeres (Steensel and Lange, 1997; Sfeir *et al.*, 2009). TRF2 protects telomeres from being recognized as double-stranded DNA breaks (DSBs) by inhibiting the DNA damage signaling pathway and the non-homologous end-joining repair pathway (NHEJ) (Karlseder *et al.*, 2004; Celli and de Lange, 2005; De Lange, 2009; Doksani *et al.*, 2013). It has been shown to induce higher order structures of DNA in vitro, including T-loops (Stansel, De Lange and Griffith, 2001; Gaullier *et al.*, 2015; Benarroch-Popivker *et al.*, 2016). The formation of T-loops by TRF2 may explain why the ATM kinase is unable to recognize telomeres. The ATM kinase pathway arises from the recognition of DNA end by the MRE11 / RAD50 / NBS1 (MRN) complex, which probably does not recognize the telomere in the T-loop configuration. Likewise, c-NHEJ depends on the DNA-end-binding complex, which is unable to gaining access to the telomere end in the t-loop structure (Schmutz and De Lange, 2016).

RAP1 is recruited into telomeres through interaction with TRF2 and, in combination with the latter, inhibits homologous recombination (Sfeir *et al.*, 2010). POT1 interacts with TPP1 to form a stable heterodimer to repress the Rad3-related signaling pathway (ATR) and together regulate telomerase activity (Denchi and De Lange, 2007). The repression of ATR signaling by POT1 involve the protection of the single-stranded DNA from replication protein A (RPA), a single-stranded DNA-binding protein that acts as a sensor in the ATR pathway (Schmutz and De Lange, 2016). Importantly, deletion of TPP1 from mouse embryonic fibroblasts resulted in the release of POT from telomere (Kibe *et al.*, 2010). Also, telomere dysfunction phenotypes associated with TPP1 deletion were similar to those of POT knockdown cells, in particular are noticeable suppression of the DNA damage response at telomere and 3 'overhang elongation (Takai *et al.*, 2011).

TIN2 is a bridging molecule that interacts simultaneously with TRF1, TRF2 and TPP1 and facilitates the assembly of an intact Shelterin

complex (Bandaria *et al.*, 2016). Its deletion in mouse cells led to the loss of TPP1/POT1a at telomeres causing induction of ATR pathway (Takai *et al.*, 2011).

Not much is known about the stoichiometry of the shelterin complex in vivo. In human cells, TRF1, TRF2, TIN2 and RAP1 are approximately 10 times more abundant than TPP1 and POT1 (Takai *et al.*, 2010). Therefore, the shelterin nucleus is likely to be a complex of the four most abundant subunits with a fraction of the complexes also containing TPP1 and POT1. Although the TIN2 bridge stabilizes TRF1 and TRF2 on telomeres (Liu *et al.*, 2004), it is not excluded that there are separate subcomplexes based on TRF1 or TRF2 at telomeres. For example, when TRF2 is eliminated, a subcomplex consisting of TRF1, TIN2, TPP1, and POT1 continues to be functional (Denchi and De Lange, 2007). The nucleus abundance of shelterin is sufficient to bind all ds TTAGGG repeats and there is a tenfold excess of TPP1 / POT1 on its ss TTAGGG binding sites, suggesting that most telomeric DNA is associated with shelterin proteins.

X-ray crystallography and NMR studies revealed the structure of many domains of shelterin subunits. The structures of the Myb / SANT and TRFH domains of TRF1 and TRF2 (Fairall *et al.*, 2001), as well as the OB folds of POT1 and TPP1 (Lei, Podell and Cech, 2004; Wang *et al.*, 2007) have been resolved. The structure of a TIN2 peptide that binds to the TRFH domain of TRF1 has also been resolved as well as the C-terminal TRF2 interaction domain (the RCT) of RAP1 (Chen *et al.*, 2011). Finally, an N-terminal domain of TIN2 and its interactions with TRF2 and TPP1 peptides were crystallized (Hu *et al.*, 2017).

Together, these data demonstrate a well-established role of telomeres in the protection of genome from nucleolytic degradation, unnecessary recombination, repair, and interchromosomal fusion and, therefore, a key role in preserving the information of our genome.

Telomere function is tightly regulated and depends on a minimum length of telomeric repeats and the associated shelterin complex.

As a normal cellular process, during cell division, telomeres progressively shortens and, when telomere length reaches a critical

limit, the cell undergoes senescence and/or apoptosis. Telomere length may therefore serve as a biological clock to determine the lifespan of a cell and an organism (Lu *et al.*, 2013). In some cases, thanks to the telomerase enzyme, telomeres are regenerated. Telomerase is activated via multiple genetic and epigenetic mechanisms in most cancers and immortalized cells, its activity allows cancer cells to have unlimited replication (Bernardes de Jesus and Blasco, 2013; Trybek *et al.*, 2020). Rarely, in ~5-15% of tumors, another DNA recombination mechanism called alternative lengthening of telomeres (ALT) is used (De Vitis, Berardinelli and Sgura, 2018; Yuan, Larsson and Xu, 2019; Claude and Decottignies, 2020).

2.2.1.2. Telomere shortening in aging and diseases

Eukaryotic chromosomes are duplicated during the S phase via semiconservative replication with a leading (continuous synthesis at the 3′ end of the nascent leading strand) and lagging (discontinuous Okazaki fragment synthesis at the 5′ end of the nascent lagging strand) elongating strands (Prioleau and MacAlpine, 2016; Guilliam and Yeeles, 2020). In chromosomal semiconservative replication, the short 5′ RNA primer is removed from the nascent strand and the gap is filled in by DNA that is ligated to the adjacent nascent DNA. However, at the end of the chromosome, the gap after removal of the 5′ terminal RNA primer on the lagging strand cannot be filled in, and telomeres shorten by 50-100 base pairs at each round of replication, a phenomenon called the End Replication Problem (Lingner, Cooper and Cech, 1995; Wellinger, 2014). In most eukaryotes, this problem is solved by the 3′ extension of telomeres by a reverse transcriptase called telomerase and subsequent filling with conventional DNA replication machinery (Wellinger, 2014).

When telomeres reach a critical length, lose the capping function at the chromosome terminals. These dysfunctional telomeres are recognized as DNA damage and induce DNA damage checkpoints (D'Adda Di Fagagna *et al.*, 2003). Two checkpoints that limit cellular lifespan in

response to telomere dysfunction have been identified (Figure 6): the first checkpoint (first stage of mortality = M1) is characterized by a permanent arrest of the cell cycle (Wright and Shay, 1992), leads to senescence and depends on the activation of tumor suppressor gene like p53 and Rb. It occurs after about 50-70 cell divisions. Cells with p53 mutated manage to bypass the senescence checkpoint and continue to proliferate despite the presence of critically short and dysfunctional telomeres. However, continuous shortening of telomeres leads to a further increase in telomere dysfunction, inducing a second checkpoint (second stage of mortality = M2), called crisis. The crisis is independent of p53 and it is characterized by strong chromosomal instability, leading to cell death (Figure 6) (Wright and Shay, 1992; Von Morgen and Maciejowski, 2018).

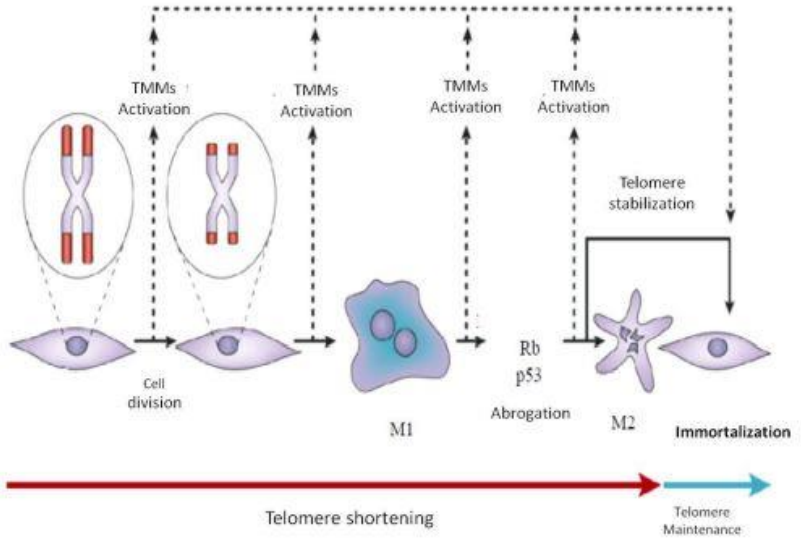

Figure 6. Cell fate in response to telomere shortening. Somatic cells can divide for a limited number of cell divisions. When cells reach Hayflick limit, they enter into cell cycle arrest (senescence), called M1 phase. The cells can bypass M1 phase by the abrogation of Rb and p53. Thus, telomeres get shorter finally leading to cell death, called M2 phase. Telomerase re-activation or induction of ALT mechanism in M2 phase lead to telomere maintenance with consequent cell immortalization (modified from Shay and Wright, 2005)

The processes of senescence and apoptosis limit the replicative lifespan of the cells, thus acting as a tumor suppressor mechanism in limiting the growth of transformed cells. However, these processes can

contribute to the depletion of cellular function and to reduce maintenance of organs during aging. Indeed, most human tissues and organs show noticeable shortening of telomeres during aging (Djojosubroto *et al.*, 2003), although there are also organs, such as the brain, that do not show significant telomeric shortening. There is emerging evidence that telomere shortening has a functional impact on aging and diseases associated with aging. Individuals with short telomeres showed a 3.18-fold increase in death rate from heart disease and 8.54 times for infectious diseases versus those with relatively long telomeres. However, telomere shortening is not considered a sufficient prognostic factor to establish human survival beyond 85 years and over (Martin-Ruiz *et al.*, 2005). Several studies have clearly demonstrated the association between telomere shortening and the onset of numerous diseases. Among these, there is dyskeratosis congenita, a disease that presents with a progressive insufficiency of the bone marrow and with a series of symptoms affecting the skin and mucous membranes. Others are diabetes, hypertension, Alzheimer's disease and disorders such as fatal aplastic anemia, pulmonary fibrosis and liver cirrhosis which, together with bone marrow failure, can be a significant cause of early death (Rizvi, Raza and Mahdi, 2015; Chakravarti, LaBella and DePinho, 2021; Di Micco *et al.*, 2021).

In addition to numerous known pathologies, the incidence of cancer greatly increases during aging. The reason for this is explained by several studies that show how the crisis phase M2, in which telomeres reach the critical length that leads to cell death, can be considered the prelude to cell transformation and malignancy, given the strong instability of the genome that arises at this stage. Therefore, escape from the crisis is an essential prerequisite for tumorigenesis. The crisis could contribute to tumorigenesis by creating a permissive environment for the acquisition of genetic and epigenetic alterations. These changes may allow a minority of cells to emerge from this phase and progress into invasive cancer (Parkinson, 1996; Maciejowski *et al.*, 2015). Human cells move towards immortalization by activating the so-called telomere maintenance mechanisms (TMM). Most cancers reactivate

telomerase reverse transcriptase or use alternative telomere elongation (ALT) (Nassour, Schmidt and Karlseder, 2020).

2.2.1.3. Telomere length maintaining mechanisms

Telomeres gradually shorten with each cell division and, after a certain number of divisions, the chromosomes become genetically unstable and guide the cells towards the processes of senescence and apoptosis. Cancer cells avoid these processes by telomere length maintaining mechanisms and accumulate genomic instability, becoming immortal cells. Therefore telomeres are crucial for the survival of cancer cells (Jafri *et al.*, 2016).

2.2.1.3.1. The telomerase complex

The best known telomere elongation mechanism is telomerase, a ribonucleoprotein (RNP) enzyme that synthesizes new DNA (Figure 7). Telomerase is a complex molecule with two main subunits: a reverse transcriptase (TERT) and a RNA template known as telomerase RNA component (hTR). In addition, other proteins regulate the biogenesis and correct assembly of telomerase in vivo: TCAB1, dyskerin and its associated proteins NHP2, NOP10, GAR1 (Chan and Blackburn, 2004; Smogorzewska and De Lange, 2004; Cohen *et al.*, 2007). One more protein which may be transiently involved in telomerase assembly is NAF1, which initially binds the disc and accompanies it to the nascent RNA before being replaced by GAR1 to produce mature RNP (Reddel, 2014). Human telomerase consists of two subunits of TERT and two of TR (Cohen *et al.*, 2007). The catalytic subunit is a 127 kDa protein that contains different functional domains: N-terminal domain (TEN), a RNA binding domain (TRBD), the reverse transcriptase domain (RT) and the conserved C-terminal domain (CTE). The second telomerase component TR is transcribed by RNA polymerase II and has a size of 451 nucleotides in humans. TR contains a core domain that includes the template for reverse transcription (5'-CUAACCCUAAC-3') and

conserved regions (CR3, CR4, CR6, CR7, CR8) that are used as anchor points for the sequence alignment (Feng *et al.*, 1995).

Telomere length maintenance by telomerase is a multistep complex process (Rouda and Skordalakes, 2007). In the first step of DNA synthesis, the 3′ end of the G-overhang is positioned in the active site of TERT aligning on the RNA template in TR through base pair formation. In a second elongation step, nucleotide addition takes place to synthesize the telomeric DNA repeat. In a third step the telomerase translocates to restart telomeric repeat synthesis (Figure 7) (Blackburn and Collins, 2011; Pfeiffer and Lingner, 2013).

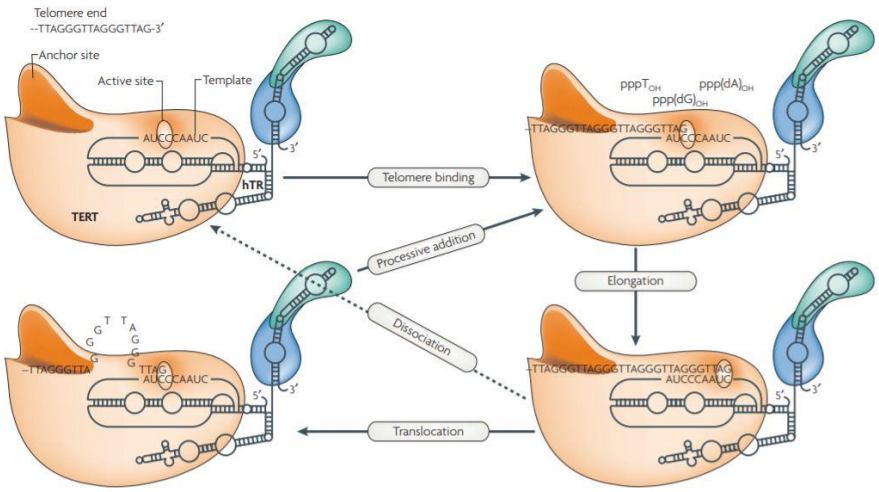

Figure 7. Telomerase is an RNA-dependent reverse transcriptase in which the templating RNA (telomerase RNA component (hTR)) is integral to the enzyme. Two protein structures are schematically illustrated: the larger one represents telomerase reverse transcriptase (TERT), the smaller protein structure represents dyskerin and other members. The sequence of the hTR template region is shown (from Harley, 2008).

Many studies conducted on mice with TR mutations demonstrate the importance of telomerase in the development of various diseases. TR knockout mice are prone to telomere shortening, even in subsequent generations (Blasco, 2005). This leads to an early onset of aging and often related diseases such as alopecia, intestinal atrophy, infertility, cardiac dysfunction, bone marrow aplasia, renal dysfunction and proliferative defects of neural stem cells (Herrera, Samper and Blasco, 1999; Leri *et al.*, 2003; García-Cao *et al.*, 2006).

Conversely, overexpression of telomerase reverse transcriptase in mice results in increased proliferation of skin cells which increases susceptibility to skin carcinogenesis (Cayuela, Flores and Blasco, 2005; Flores, Cayuela and Blasco, 2005).

Activation of telomerase as a mechanism to ensure unlimited cell proliferation is a hallmark of nearly all human cancers. Several oncogenes such as Myc and Wnt are capable of activate telomerase transcriptionally (Greider, 2012; Hoffmeyer *et al.*, 2012), as well as epigenetic alterations or mechanisms involving alternative splicing (Kyo and Inoue, 2002).

Furthermore, studies conducted on melanomas reveal mutations that increase the transcriptional activity of the TERT promoter (Horn *et al.*, 2013). Telomerase is active from the beginning of tumor development, however its activity is essential for cancer growth and progression by allowing telomere length to be maintained above a critically short length (Begus-Nahrmann *et al.*, 2012). Given the crucial role of telomerase in supporting tumor growth, telomerase inhibitors are considered a potential cancer therapy. However, the therapy that targets telomerase can activate alternative telomere lengthening (ALT) (Hu *et al.*, 2012).

2.2.1.3.2. Mechanism of ALT

Another telomere length maintenance mechanism that some cancers, such as breast carcinomas, use is an alternative telomere lengthening mechanism (ALT) (Figure 8). ALT involves the synthesis of new telomeric DNA from a DNA template using homologous recombination. The template could be the telomere of another chromosome or another region of the same telomere via t-loop or sister telomere recombination (Zhang and Zou, 2020). The first step of the process involves that the single-stranded protrusion G at the end of the telomere invading the homologous DNA, forming an intermediate structure. Then there is the direct synthesis from the telomeric DNA model, by the δ or ζ polymerases (Maloisel, Fabre and Gangloff, 2008).

A third phase consists in the processing of intermediate products, before chromosomal segregation. Finally, a final phase of filling of the complementary strand was hypothesized. Cancer types in which ALT is very common include osteosarcomas, undifferentiated pleomorphic sarcomas, and astrocytic brain tumors, but it is also common in some other types of glioblastomas, neuroblastomas and in many types of carcinomas recombination of telomeres (Figure 8) (Hakin-Smith *et al.*, 2003; Henson *et al.*, 2005; Subhawong *et al.*, 2009).

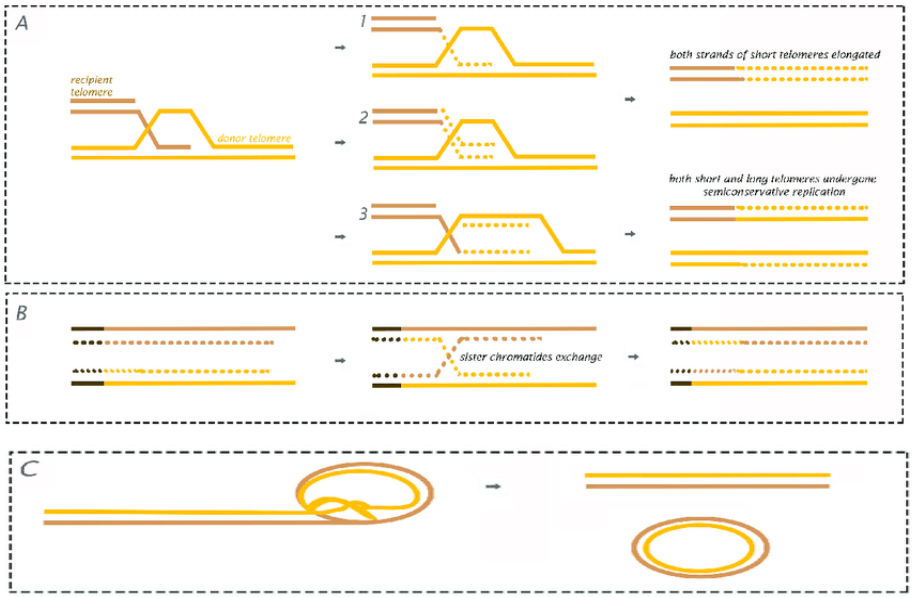

Figure 8. Theoretical models for ALT mechanism: (A) Break-induced replication loss from the donor telomere (1 and 2 without loss from the donor telomere). In this model, there is a unidirectional replication fork with semi-conservative replication of the telomeres. (B) Unequal telomeric sister chromatid exchange (T-SCE) model. (C) Rolling circle and t-circle formation after t-loop resolution providing a linear double strand break for subsequent HR-mediated activation into the homologous templates (from Amorim *et al.*, 2016).

ALT cells show peculiar characteristics, such as the presence of extrachromosomal DNA with telomeric sequences. This DNA takes many forms, including double-stranded telomeric circles (T-circles) (Cesare and Griffith, 2004; Wang, Smogorzewska and De Lange, 2004), partially single-stranded circles (referred to as C-circles or G-circles depending on whether they are C-rich or G-rich) (Henson *et al.*, 2005; Nabetani and Ishikawa, 2009), linear double-stranded DNA and

very high molecular weight "t complex" DNA that is likely to contain highly branched abnormal structures (Nabetani and Ishikawa, 2009).
Moreover, telomeric DNA (chromosomal or extrachromosomal) and associated binding proteins can be found in a subset of nuclear bodies of promyelocytic leukemia (PML nuclear bodies). PMLs containing telomeric chromatin are highly characteristic of ALT cells and are therefore referred to as ALT-associated PML bodies (APBs) (Yeager *et al.*, 1999). Other features of ALT cells include highly heterogeneous telomeres with lengths ranging from very short to extremely long (Bryan *et al.*, 1995), rapid changes in telomere length (Murnane *et al.*, 1994; Perrem *et al.*, 2001) and an increased level of telomere recombination (Londoño-Vallejo *et al.*, 2004).
These phenotypic features of ALT may be useful markers for the presence of ALT activity.

2.2.1.4. The impact of the environment on telomeres

Many studies have shown that telomere length is associated with diseases, such as tumors and cardiovascular diseases, influenced by environmental factors (Blackburn, Epel and Lin, 2015). Oxidative stress and inflammation are the two main routes for the development of diseases and are also risk factors for telomeres shortening. Over the years, many demonstrations have accumulated that support the thesis that exposure to the environmental chemicals and telomere length are closely related, with most studies reporting shorter telomeres due to exposure. In particular, in vitro and in vivo studies have analyzed the negative influence of chemicals and atmospheric pollution, as well as particular lifestyles (Choi, Fauce and Effros, 2008; Martens and Nawrot, 2016; Walton *et al.*, 2016; Schmidt, 2020).
Other chemicals analyzed are polycyclic aromatic hydrocarbons (PAH), which at high doses in the workplace can cause a noticeable telomeric shortening and, moreover, are known carcinogens that could modify DNA and cause genetic mutations (Denissenko *et al.*, 1997). Indeed, it has been demonstrated the presence of telomeric shortening

in men who are exposed to particulate matter (PM), black carbon (BC), benzene, lead and cadmium (Miri *et al.*, 2019).

A relevant risk factor for mortality and morbidity worldwide is air pollution; in fact it is widely reported that atmospheric pollutants negatively affect respiratory system and cardiovascular system (Hamanaka and Mutlu, 2018). Systemic inflammation and oxidative stress have been suggested to be two main mechanisms underlying adverse health effects of air pollution. Finally, pollutants have been correlated with shorter telomeres (Zhao *et al.*, 2018).

Exposure to particulate matter has also been associated with problematic newborn births and often with poor baby health. Women exposed to particulate pollution during pregnancy have encountered newborn incomplete neurodevelopment, respiratory and cardiometabolic disorders and diseases associated with shorter telomeres (Chiu *et al.*, 2017; Korten, Ramsey and Latzin, 2017). Oxidative stress (OS) is certainly one of the main systemic toxic effects induced on the fetus when polluting particles are translocated into the placenta. OS can be induced by the generation of reactive oxygen species (ROS), by an impaired oxygen-starved mitochondrial functioning and by inflammatory activation. It is important to remember that the fetus is particularly vulnerable to oxidants due to its immature immune defenses (Jo *et al.*, 2020). Telomeres have been shown to be highly sensitive to damage caused by OS (Kawanishi and Oikawa, 2004; Houben *et al.*, 2008). ROS, particularly hydroxyl radicals, produce single-stranded DNA breaks and telomeric DNA has been reported to be deficient in repairing these damages (Petersen, Saretzki and Von Zglinicki, 1998). Telomere length has also been reported to decrease at a faster rate during oxidative stress (Von Zglinicki, 2002).

Other elements that can compromise the length of the telomeres are smoking and obesity, risk factors for many diseases related to age and cancer (Shammas, 2011). A study carried out on a sample of women of heterogeneous age, demonstrated the presence of shorter telomeres in

obese women and dose-dependent shortening in smokers compared to nonsmokers (Figure 9) (Valdes *et al.*, 2005).

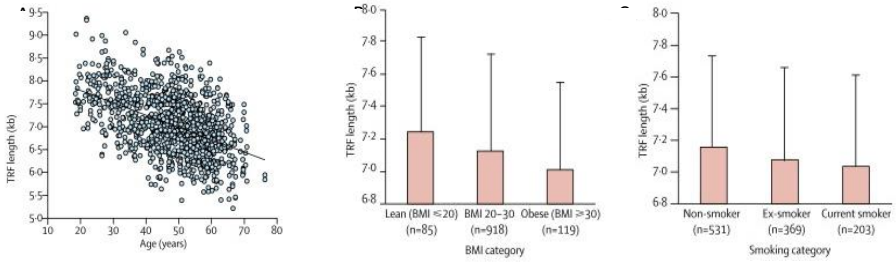

Figure 9. Relation between telomere length and (A) age, (B) BMI and (C) smoking history (from (from Valdes *et al.*, 2005).

The correlation of telomere length with environmental stimuli and psychological stress has also been demonstrated in yeast, where a shortening of telomeres has been observed following exposure to multiple doses of different types of stress (caffeine, high temperatures) (Romano *et al.*, 2013).

In conclusion, there is a growing need to know and evaluate the risks associated with exposure to mutagenic agents present or manipulated in the workplace or at home, in the air, water, soil or foods, and also risks related to the lifestyle led by each of us.

2.2.2. The telomeric protein TRF2 - Telomeric Repeat Binding Factor 2

2.2.2.1. Structure and function of TRF2

TRF2 is an important multimeric protein of the Shelterin complex. The gene is located on chromosome 16q22.1, has a length of 30 kb and is widely expressed in many human tissues. TRF2 comprises 4 functional domains (Figure 10) (Feuerhahn *et al.*, 2015):

- The basic N-terminal region, rich in glycine and arginine residues, is a flexible hinge domain involved in protein–protein interactions and is essential for the basic protection function of TRF2 (Van Steensel, Smogorzewska and De Lange, 1998); The basic domain of TRF2 can interact with the subunits of the origin recognition complex 1 domain to promote the formation of telomeric heterochromatin and participate in the regulation of DNA damage response (DDR) (Deng *et al.*, 2010). Finally, through electrostatic bonding, it improves the affinity of TRF2 to DNA and protects the D-loop from the action of endonucleases;
- The dimerization domain, also known as the TRF homology (TRFH) domain, is involved in the formation of homodimers and it recognizes motif-specific (Y / F) XL. This domain is important in maintaining topological structure of telomere DNA, inhibiting the activation of the ataxia telangiectasia-mutated (ATM) kinase checkpoint and preventing telomere non-homologous end joining (NHEJ);
- The orientation sequence (nuclear localization signal), or flexible hinge domain, contains sites of interaction of TRF2 with other shelterin proteins, such as RAP1 and TIN2;
- The C-terminal domain (Broccoli *et al.*, 1997) (Myb/homeodomain-like telobox DNA-binding domain) is mainly responsible for the specific recognition and binding of the DNA repeat sequence TTAGGG (Figure 10) (Bilaud *et al.*, 1997; Court *et al.*, 2005; Hanaoka, Nagadoi and Nishimura, 2009).

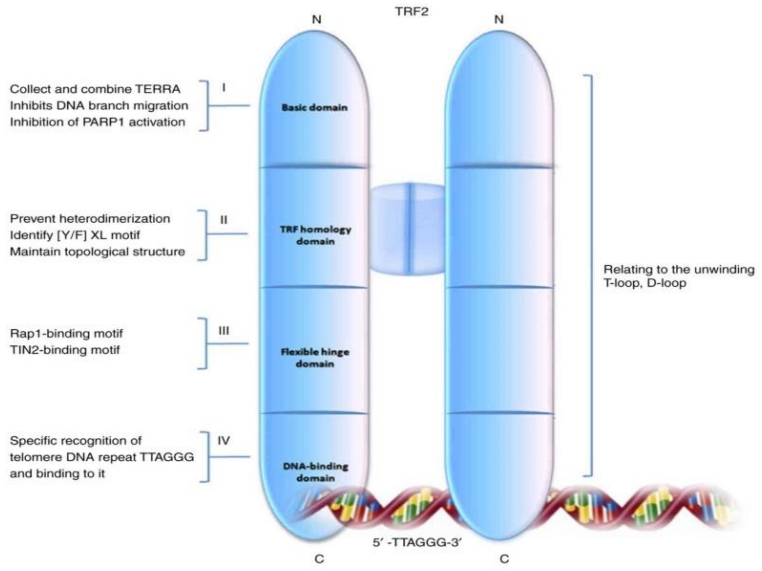

Figure 10. Structure and main functions of TRF2 (from Wang and Xiaoying, 2021).

TRF2 is a key factor in regulating telomere integrity. TRF2 dysfunctions cause telomere deprotection and trigger the activity of mutated ataxia telangiectasia (ATM) kinase (Karlseder *et al.*, 2004; Celli and de Lange, 2005; Denchi and De Lange, 2007). The subsequent localization of DNA damage response (DDR) components such as phosphorylated H2AX (γH2AX) and 53BP1 at the extremities of the chromosome, causes the formation of the so-called "foci induced by telomere dysfunction" (TIF) (Takai, Smogorzewska and De Lange, 2003). Furthermore, loss of TRF2 induces the formation of end-to-end chromosome fusions, mediated by the Ku70/80 (Celli, Denchi and de Lange, 2006) and DNA ligase IV-dependent (Smogorzewska *et al.*, 2002) classical non-homologous end-joining pathway (c-NHEJ). The fused chromosomes eventually result in strong proliferative defects and an increased risk of genome instability.

The model proposed for restricting the accessibility of DDR factors to telomeres involves remodeling the linear chromosome ends into DNA loops (Stansel, De Lange and Griffith, 2001) by preferentially binding to double-stranded telomeric DNA duplex containing a single-stranded 3'TTAGGG protrusion. Once tied, it migrates to the junction of the T-loop, where the single-stranded protrusion invades the region upstream

of the double-stranded. Studies *in vitro* and *in vivo* have shown that TRF2 knockout in somatic cells does not allow t-loop formation, which coincides with telomere deprotection, chromosome end-to-end fusions, loss of telomeric DNA and, consequently, early cell death (Doksani *et al.*, 2013; Ruis *et al.*, 2021). In addition, it has been shown that deprotection of telomeres by removal of TRF2 can confer an altered chromatin environment involving modification of telomeric histones (Dimitrova *et al.*, 2008; Wu and de Lange, 2008; Peuscher and Jacobs, 2011; Galati *et al.*, 2012; Fradet-Turcotte *et al.*, 2013).

2.2.2.2. Role of TRF2 in cancer

TRF2 has been found overexpressed in various malignant tumors (lung, liver, gastric and BC), both in cancer cells and in vascular cells and this is typically associated with poor prognosis (Cherfils-Vicini *et al.*, 2014; Benhamou *et al.*, 2016; Zizza *et al.*, 2019).

This suggests that it contributes to carcinogenesis (Blasco, 2005) and it is regulated by the Wnt/β-catenin pathway, WT1 and p53 pathways. In support of this, increased TRF2 dosage in a variety of tumor cells increased their tumorigenicity, while TRF2 depletion reduced tumor growth (Muñoz *et al.*, 2005; Biroccio *et al.*, 2006, 2013; Bai *et al.*, 2014). How TRF2 interacts with the tumorigenesis process is a hotly debated topic, but it is thought that overexpression of TRF2 may suppress the ATM-dependent DNA damage response triggered by short telomeres, thus allowing the accumulation of chromosomal aberrations and leading to continued cell growth. Moreover, this increased chromosomal instability can promote tumorigenesis in the presence of normal telomerase levels (Muñoz, Blanco and Blasco, 2006).

Furthermore, the role of TRF2 in cancer is not based only on the protection of telomeres, but also on its ability to modulate gene expression, in fact it has been demonstrated that TRF2 occupies a series of interstitial regions throughout the human genome (interstitial

telomeric sequences (ITS)) and can act as transcriptional activator. It is involved in various steps in tumor formation, progression and metastasis (Zizza *et al.*, 2019). In particular, it has been shown that the overexpression of TRF2 affects the early stages of tumorigenesis as it can lead to neoangiogenesis and create a powerful immunosuppressive microenvironment (Biroccio *et al.*, 2013).

By altering the expression of heparan sulfate proteoglycans, TRF2 recruits and activates myeloid-derived suppressive cells (MDSCs) via the TLR2 pathway. In this way, a powerful inhibition of NK cell immunosurveillance is triggered, with a strong decrease in the production of IFNγ (Figure 11) (Cherfils-Vicini *et al.*, 2019).

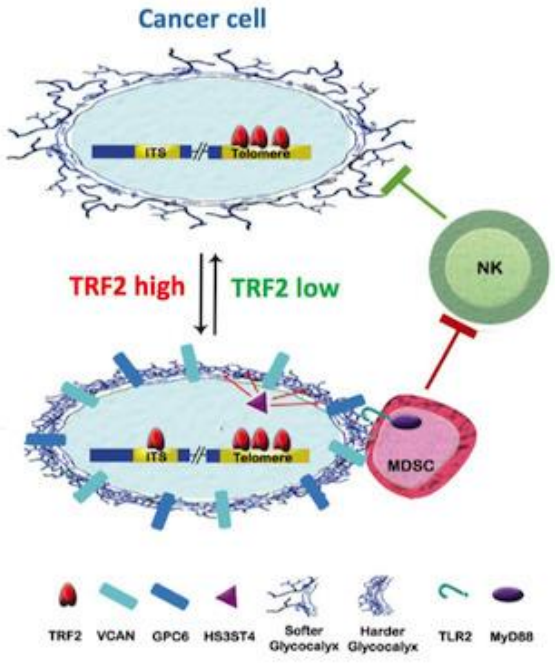

Figure 11. Extratelomeric role of TRF2 in tumor cells. It alters the expression of the glycocalyx gene, recruits myeloid-derived suppressor cells (MDSCs), and a potent inhibition of NK cell immune surveillance is triggered (from Cherfils-Vicini *et al.*, 2019).

In light of these data, TRF2-targeted tumor therapy shows broad application perspectives. Inhibition of TRF2 could activate ATM-dependent DDR pathways and induce apoptosis or cellular senescence (Pal *et al.*, 2015). When RNA interference was used to knock down the expression level of TRF2 in colorectal cancer and renal epithelial

carcinoma cell lines, tumor cell proliferation and clonal formation were significantly inhibited and apoptosis was significantly induced (Dong *et al.*, 2009; Bidzinska, Baginski and Skladanowski, 2014). Furthermore, previous studies (Horikawa, Fujita and Harris, 2011; Yang *et al.*, 2015) suggest that TRF2-targeted therapy may be more effective than telomerase inhibition for the treatment of some types of tumors. There are several reasons that support this hypothesis, first, telomerase inhibitors were not effective on ALT tumor cells; secondly, in tumors showing increased expression of TRF2, the therapeutic effect of telomerase inhibitors was not noticeable (Horikawa, Fujita and Harris, 2011) and finally, the reduction in the level of TRF2 expression shortened the 3 'overhangs of the telomeres, leading to fusion chromosomal and premature senescence of cancer cells.

To date, it is known that TRF2 plays an important role in the tumor formation, but very little is known about the role of TRF2 in mammary carcinogenesis. Nijjar et al showed that cultures of immortally transformed and tumor-derived human breast cells have high levels of TRF2 protein relative to their controls, suggesting its involvement in BC progression (Nijjar et al., 2005). TRF2 could act like a powerful oncogene, but the mechanism through which it acts remains to be determined.

In conclusion, modulate expression levels of TRF2 could prove to be a reliable strategy for the treatment of some types of cancers.

2.2.2.3. The link between TRF2 and the environment in tumorigenesis

Chromosomal stability is highly dependent on adequate telomere length, and an increase or decrease in the level of TRF2 expression can cause changes in telomere length. When the critical telomere length is reached, the genome is subject to mutations strongly influenced by a variety of environmental factors (Mondello, Smirnova and Giulotto, 2010), which can promote the proliferation of immortal tumor cells (Counter *et al.*, 1992; Sabatier *et al.*, 2005; Bailey and Murnane, 2006; Hayashi *et al.*, 2015). As these cells grow and proliferate, the genetic

mutations gradually accumulate and lead to the development of a variety of cancers.

In addition, when some environmental and pathological factors (like ionizing radiation, benzene and toluene, paints and pesticides, waste) cause TRF2 dysfunctions, the physiological balance of cells is severely disrupted, telomeres lose protein protection, telomere caps are eliminated, DDR is activated, the cell cycle is stopped and DNA is abnormally repaired (Wright, Pereira-Smith and Shay, 1989; O'Hagan *et al.*, 2002; Feldser and Greider, 2007; Fumagalli *et al.*, 2012). Due to the blockage of the cellular checkpoint, cells undergo senescence and apoptosis. However, when mutations, for example in the protein p53, which is common in most malignancies, DDR-induced apoptosis is bypassed mechanism and the telomeric crisis is activated (Counter *et al.*, 1992).

During telomere crisis, chromosomes recombine to generate large-scale mutant cells, called precancerous cells. Finally, the mechanisms known to extend telomeres are activated, so as to gradually stabilize chromosomes and form immortal cells with heterogeneous characteristics (Wang and Xiaoying, 2021).

In summary, the telomeric functions and the ability of the environmental factors to promote the onset of tumors seems to be closely related. Furthermore, both TRF2 alterations and some environmental mutagens act on many proteins linked to the signaling pathway associated with cell proliferation, stimulate peripheral angiogenesis, inhibit the immune system and the ability of the microenvironment to counteract tumor proliferation and maintain the stem characteristics of cancer cells (Figure 12).

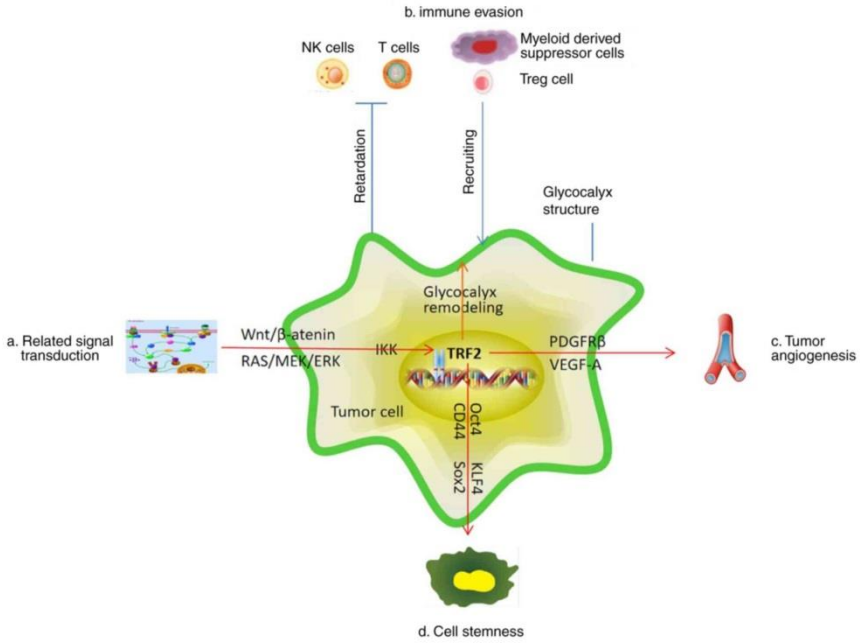

Figure 12. Summary diagram of the tumor-promoting effect of TRF2 (from Wang and Xiaoying, 2021).

3. AIM OF THE THESIS

Over the years many studies have shown how exposure to environmental factors, including atmospheric pollution, electromagnetic radiation or carcinogenic substances such as arsenic, can induce oxidative stress causing DNA damage, genomic instability and shortening of telomeres. These environmental factors are all elements that cause an increased risk of incidence of various types of tumors.

The aim of this work was to simulate the effect of environmental factors to study their molecular mechanisms of action, still unknown, during tumorigenesis and metastasis. To this end, the work is focused on the regulation of a protein that plays a key role in telomeric integrity and genomic instability, the TRF2 protein. TRF2 is overexpressed in several human malignancies, including BC, which appears to be a leading cause of cancer mortality in women in developed countries, mainly due to distant metastasis formation. Furthermore, among the molecular subtypes, negative triple BCs (TNBCs) are characterized by a more aggressive clinical course and their treatment cannot be limited to conventional chemotherapy, but it requires the identification of new molecular targets, such as TRF2.

In this tumor subtype, the key role of TRF2 during the metastasis process, both *in vitro* and *in vivo*, was investigated using methodologies that simulate the tumor microenvironment.

The interaction between TRF2, some components of the cytoskeleton and various components of the nuclear lamina during cell migration has been also examined in order to identify the mechanisms that delineate the role of TRF2 in cellular polarization, preparatory to the metastasis process. Finally, the clinical relevance of the results obtained was assessed, thanks to the analyzes conducted on patients at Regina Elena National Cancer Institute.

4. ARTICLE

"TRF2 interaction with the inner nuclear membrane is required for cell polarization and metastasis in triple negative breast cancer"

4.1. ABSTRACT

The Telomere repeat-binding factor 2 (TRF2) contributes to cancer progression by both telomere-dependent and independent mechanisms including immune escape and angiogenesis. Here, we describe a novel cell-intrinsic mechanism by which TRF2 promotes a pro-migratory phenotype in TNBC. We found that TRF2, by interacting with the nuclear envelope, ensures the proper establishment of cell polarity and directional cell migration. Using a spontaneous model of TNBC metastasis combined with intravital imaging, we demonstrated that TRF2 expression promotes cell migration at the primary tumor site and is required for the early steps of the metastatic cascade in vivo. In human BCs, aberrantly elevated TRF2 expression positively correlates with cancer progression, metastasis and poor prognosis, identifying TRF2 as a potential drug target for the development of new TNBC treatments.

4.2. INTRODUCTION

Human telomeric DNA is specifically bound by a multi-protein complex named Shelterin that prevents natural chromosome ends from being recognized as DNA breaks by cell machinery, thereby suppressing DNA repair processes at chromosome ends (De Lange, 2018).

The Telomeric Binding Factor (TRF2) is a central member of Shelterin that acts as a suppressor of ATM-mediated DNA damage response and

non-homologous end joining (NHEJ) repair pathway at telomeres (De Lange, 2018). TRF2 is highly expressed in various human cancers and contributes to tumorigenesis in mice through telomere-dependent mechanisms (Nakanishi *et al.*, 2003; Blanco *et al.*, 2007; Diehl *et al.*, 2011; Pal *et al.*, 2015). However, beyond the well-known role in telomere maintenance, recent works demonstrated that TRF2 exerts unexpected extra-telomeric functions through its ability to bind to interstitial telomeric sequences (ITS) dispersed throughout the human genome (Simonet *et al.*, 2011; Yang *et al.*, 2011). In particular our previous studies revealed a positive correlation between TRF2 expression and the establishment of a pro-tumorigenic microenvironment that promotes cancer progression. We demonstrated that TRF2 impacts on glycocalyx structure by modulating a network of genes (HS3ST4, GPC6, VCAN, SULF2) involved in the biosynthesis and post-synthetic modification of heparan sulphate proteoglycans (Biroccio *et al.*, 2013; Cherfils-Vicini *et al.*, 2019; Zizza *et al.*, 2019). These changes in glycocalyx prevent, on one hand, Natural Killer (NK) cell recruitment/activation at the tumor site and, on the other hand, increase VEGF-A secretion with a consequent impact on tumor neoangiogenesis (Biroccio *et al.*, 2013; Cherfils-Vicini *et al.*, 2019; Zizza *et al.*, 2019). Till now TRF2 extra-telomeric functions have been ascribed to its ability to bind to ITS and consequently regulate gene expression. However, TRF2 has been reported to serve as molecular platform for telomeric association of accessories factors and interact through its TRFH domain with different proteins sharing a specific aminoacidic motif ([Y/F]XL). Thus TRF2 acts as a protein hub for different signaling pathways (Chen *et al.*, 2008; Di Maro *et al.*, 2014; Higa *et al.*, 2017; Kim *et al.*, 2017). Based on this set of observations, we posit that increased TRF2 abundance in tumor cells might alter TRF2 interactome and foster aberrant signaling pathways toward cancer progression.

Here, we found that TRF2 interaction with various components of the nuclear envelope including Lamin B1, Emerin, SUN1 and SUN2 is functional to the establishment of cell polarity and to directional cell

migration in TNBC models. Accordingly, loss of TRF2 strongly reduces spontaneous metastasis formation in vivo by perturbing local migration/ invasion at the primary tumor site. We propose that TRF2 directly promotes intracellular pathways that result in a more invasive phenotype and increase TNBC metastatic potential.

4.3. RESULTS

4.3.1. TRF2 is required for directional migration in TNBC cells

To investigate the role of TRF2 in the regulation of cell-intrinsic properties of aggressive cancer cells, we generated TRF2 gain and loss of function models of TNBC cells by viral transduction. Stable over-expression (pTRF2) and knockdown of TRF2, obtained by using two independent shRNAs (shTRF2 N1; shTRF2 N2), were confirmed by Western blotting analysis in MDA-MB-231 and MDA-MB-436 cell lines (Figure 13).

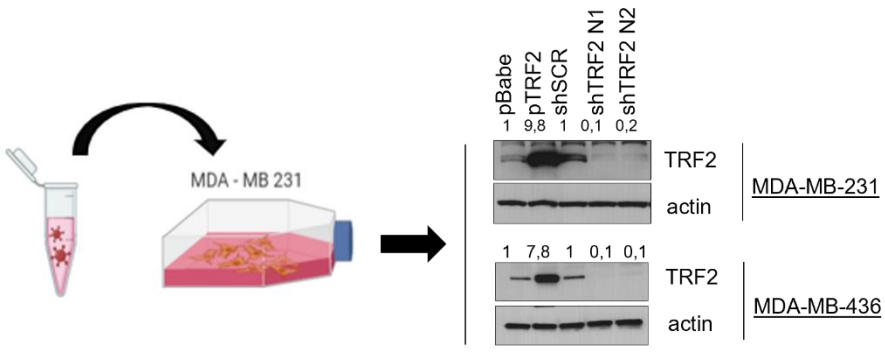

Figure 13. Stable TRF2 over-expressing (pTRF2) or interfered (shTRF2 N1, shTRF2 N2) MDA-MB-231 and MDA-MB-436 cells and their control counterparts (pBabe/shSCR) were subjected to Western blotting for TRF2 expression analysis. Discrete values of TRF2 quantitative densitometric analysis are reported on the top of each blot; controls (pBabe/shSCR) were set to 1.

Early passages, TRF2 over-expressing or interfered cells were subjected to 3D spheroids invasion assay. Under these conditions, a tumor spheroid embedded in the extracellular matrix (ECM) invades isotropically in a multidirectional manner. Measurements of spheroids invasive area over time revealed that TRF2-over-expressing spheroids displayed a significant increase of surface area compared to their respective controls (Figure 14). Conversely, silencing of TRF2 significantly impaired 3D spheroids invasion (Figure 14). By comparing cell lines with the highest (pTRF2) and the lowest TRF2 levels (shTRF2 N1, shTRF2 N2), we observed a difference of about 50% in the spheroid surface area at day 4 in MDA-MB-231 and at day 6 in MDA-MB-436, respectively (Figure 14).

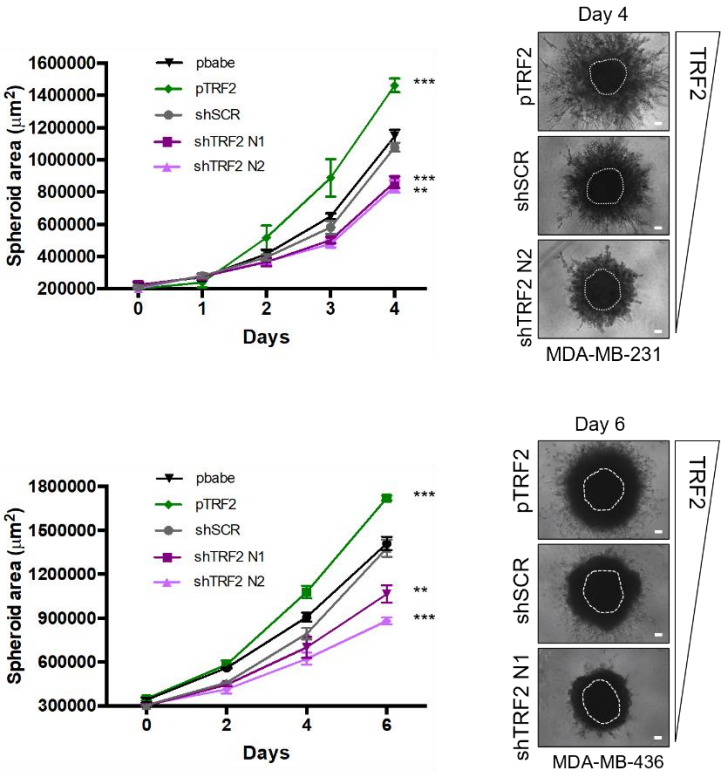

Figure 14. For 3D spheroid invasion assay, stable cell lines were plated in a 96 well plate with a specialized ECMR to drive spheroid formation of the cells. After 3 days (day 0) spheroids were embedded in Invasion MatrixR and 3D invasion was visualized microscopically at indicated time points. Invasive activity into ECM was expressed as total spheroid area. Data are the mean ± SD (n = 3 independent experiments). Two tailed t student test was used to calculate statistical significance. *P<0.05, **P<0.01, ***P<0.001. Right panel: phase contrast images of representative spheroids for the indicated experimental conditions at day 4-6 are shown. Dashed circle indicates the size of spheroids at day 0. Scale bars, 100µm.

Consistently, a significant reduction of 3D spheroids invasion was also seen in MDA-MB-231 upon transient TRF2 knockdown by siRNAs or through the expression of an inducible TRF2 knockout system based on CRISPR-Cas9 technology (Okamoto *et al.*, 2013) (Figure 15), further confirming that TRF2 expression is required for effective 3D migration in the surrounding ECM.

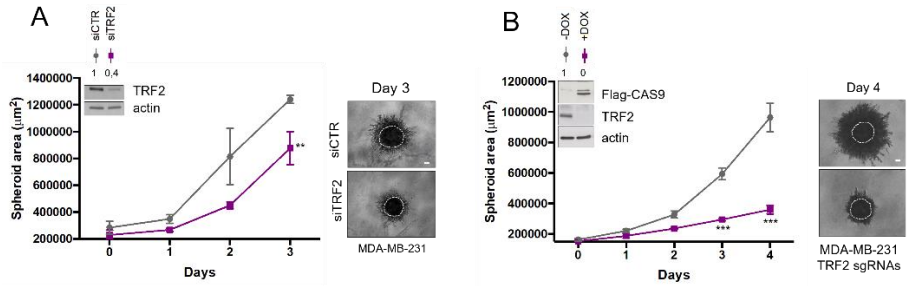

Figure 15. A. Left panel: MDA-MB-231 cells were transiently transfected with TRF2 specific siRNA or with a non-targeting control siRNA and subjected to Western blotting for TRF2 expression analysis and to 3D spheroid invasion assay as described in Figure 1B. For Western blotting, discrete values of quantitative TRF2 densitometric analysis are reported on the top of each blot; si-control was set to 1. For 3D spheroid invasion assay, data are the mean of spheroids area ± SD (n = 3 independent experiments). Right panel: phase contrast images of representative spheroids at day 3 are shown. Dashed circle indicates the size of spheroids at day 0. Scale bars, 100µm. B. Left panel: Doxycycline-inducible CRISPR/CAS9 TRF2 knockout MDA-MB-231 cells were cultured in the absence (-) or in the presence (+) of doxycycline for 3 days and subjected to Western Blotting analysis with the indicated antibodies and to 3D spheroid invasion assay as described in Figure 1B. For Western blotting, discrete values of TRF2 quantitative densitometric analysis are reported on the top of each blot; - doxy was set to 1. For 3D spheroid invasion assay data are the mean of spheroids area ± SD (n = 3 independent experiments). Right panel: phase contrast images of representative spheroids at day 6 are shown. Dashed circle indicates the size of spheroids at day 0. Scale bars, 100µm.

Given the well-established role of TRF2 in protecting chromosome ends, global and telomeric DNA damage response (DDR) were tested in our experimental models. We found that transient silencing of TRF2 and inducible TRF2 knockout caused the activation of a global DNA damage as shown by Western blotting of ATM-mediated response markers (Figure 16 A,B). In line with this, transient TRF2 silencing is able to significantly induce telomeric DNA damage revealed by analysis of Telomere-Dysfunction Induced Foci (TIF) (Figure 16 C,D). Interestingly, in agreement with published data (Biroccio *et al.*, 2013; Salvati *et al.*, 2014; Zizza *et al.*, 2019), global and telomeric DNA

damage signaling were attenuated upon stable modulation of TRF2 (Figure 16 E-G).

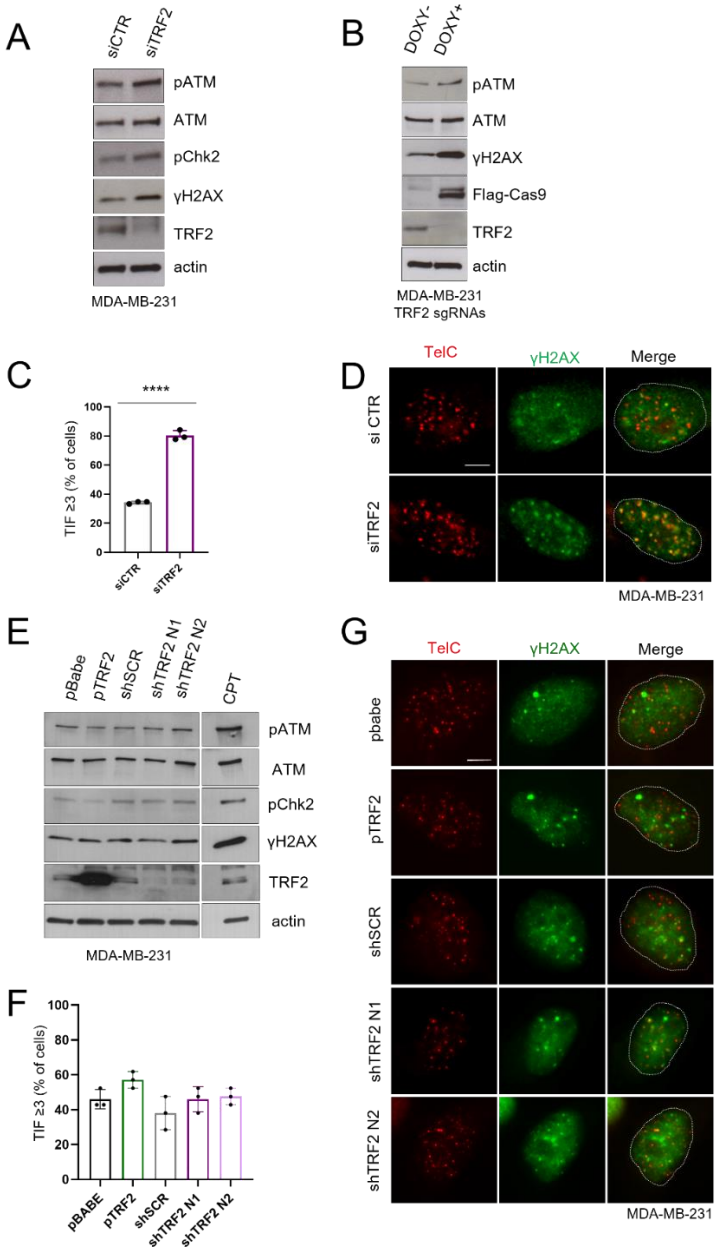

Figure 16. A. Global DNA damage analysis upon RNAi-mediated silencing of TRF2. Indicated DNA damage markers were analysed by Western blotting. B. Global DNA damage activation analysis upon inducible CRISPR/Cas9 TRF2 KO. Indicated DNA damage markers were analysed by Western blotting. C. Telomeric DNA damage analysis by telomeric FISH combined with γH2AX immunofluorescence in indicated samples. Data are the mean of cells (%) with ≥3 colocalizations (TIF) per nucleus ± SD (N = 3 independent experiments, at least 60 nuclei analyzed per experimental condition). D. Representative images of C. Scale bar, 5μm. E. Global DNA damage activation analysis of stable TRF2 over-expressing (pTRF2) or interfered (shTRF2 N1, shTRF2 N2) MDA-MB-231 cells and their control counterparts (pBabe/shSCR). Indicated DNA damage markers were analysed by Western blotting. Camptothecin treatment (0.5 μM, 24hrs) was used as positive control. F. Telomeric DNA damage analysis by telomeric FISH combined with γH2AX immunofluorescence in indicated samples. Data are the mean of cells (%) with ≥3 colocalizations (TIF) per nucleus ± SD (N = 3 independent experiments, at least 60 nuclei analyzed per experimental condition). G. Representative images of C. Scale bar, 5μm.

In line with unperturbed DNA damage, these cells display no changes in cell proliferation rate nor induction of apoptosis end/or senescence, allowing us to study additional mechanisms by which TRF2 might impact on cell migration.

Next, to further characterize the impact of TRF2 on migratory behavior in TNBC cells, we performed a battery of 2D and 1D single cell migration assays. To this end, we monitored MDA-MB-231 cell migration by time-lapse microscopy in stably depleted or over-expressing TRF2 cells that were seeded on uniformly fibronectin-coated plates (2D random migration) or fibronectin micropatterned lines (1D migration) (Figure 17 A,B). Automated cell tracking analysis showed that alterations of TRF2 level had no significant impact on the random locomotion of cells plated on flat surfaces (2D migration) (Figure 17 C,D); indeed, despite an increase in cell velocity and persistence in TRF2 depleted cells, we detected no significant variations in the effective walking distance (Figure 17 C). In the 1D model system, where the cells are forced to polarize and move on linear patterns that mimic the ECM fibres of a constrained 3D environment (Rizzo *et al.*, 2017), we found, instead, that TRF2 knockdown significantly reduced cell velocity, persistence and effective travelled distance (Figure 17 E). Conversely, TRF2 over-expressing cells were significantly faster, more persistent and travelled a greater effective distance (Figure 17 F).

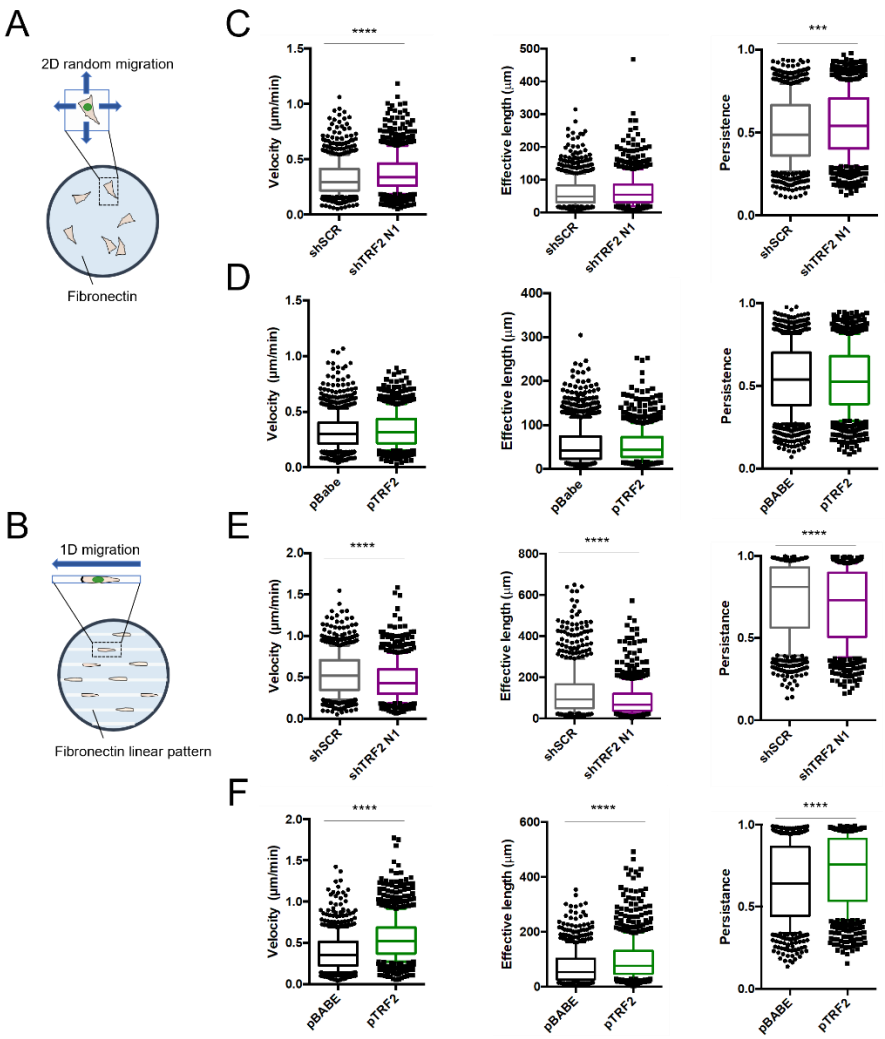

Figure 17. A. Schematic representation of cells on fibronectin coated plates for random migration analysis (2D migration). B. Schematic representation of cells on micropatterned lines, showing a polarized migratory morphology for 1D migration analysis. C. Box-and-whisker plots (10-90 percentile) representing velocity, persistence time and effective length parameters of MDA-MB-231 cells stably depleted for TRF2 (shTRF2 N1) random migrating on the plate. D. Box-and-whisker plots (10-90 percentile) representing velocity, persistence time and effective length parameters of MDA-MB-231 cells stably over-expressing TRF2 random migrating on the plate. E. Box-and-whisker plots (10-90 percentile) representing velocity, persistence time and effective length parameters of MDA-MB-231 cells stably depleted for TRF2 (shTRF2 N1) migrating on micropatterned lines. F. Box-and-whisker plots (10-90 percentile) representing velocity, persistence time and effective length parameters of MDA-MB-231 cells stably over-expressing TRF2 migrating on micropatterned lines. For C-D and E-F, two independent experiments were performed. At least 600 cells were analyzed. Kolmogorov-Smirnov test was used to calculate statistical significance. *P<0.05, **P<0.01, ***P<0.001.

Consistent with these results, in Boyden chamber Transwell assay, where the direction of migration is imposed by the serum gradient, we observed an increased number and a reduced number of migrated cells, respectively in TRF2 over-expressing and TRF2 depleted cells (Figure 18).

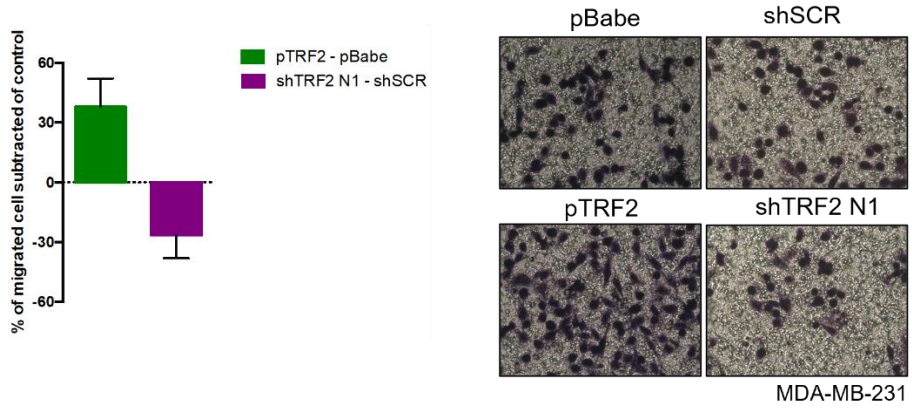

Figure 18. Left panel: stable MDA-MB-231 cell lines over-expressing (pTRF2) or interfered for TRF2 (shTRF2 N1) and their control counterparts (pBabe/shSCR) were subjected to transwell migration assay. Data are the mean ± SD of migrated cells (%) subtracted of control (pTRF2-pBabe; shTRF2 N1-shSCR) (n = 3 independent experiments, fifteen fields analyzed for each experiment); controls set to 100%. Right panel: representative images of crystal violet dye staining of the lower chambers.Scale bar, 200μm For A, B, C, D, two-tailed t student test was used to calculate statistical significance. *P<0.05, **P<0.01, ***P<0.001.

Altogether these data indicate that the TRF2 is not essential for cell motility per se, but specifically influence the ability of TNBC cell to invade and move directionally.

TRF2 alters nuclear structure and interacts with inner nuclear membrane components.

Cell migration is a highly orchestrated process that requires the coordination of cytoskeletal and nuclear dynamics, adhesion to the substratum and signal transduction (Nastały *et al.*, 2020).

To dissect cellular mechanisms underlying migration defects in TRF2 knockdown cells, we first examined the actin cytoskeleton during cell spreading. TRF2-interfered or over-expressing MDA-MB-231 cells were plated on fibronectin-coated slides, fixed at different time points, and subjected to Phalloidin staining. We detected no impact on cell spreading as shown by cell area measurements at 1,5 and 5 hrs after cell seeding and no relevant difference in the organization of actin cytoskeleton after modulation of TRF2 expression. Similarly, the analysis of Vinculin staining revealed that TRF2 expression had no significant impact on focal adhesion number or area, nor it affected the

ability of cells to adhere to fibronectin. Next, based on recent evidences pointing to a more active role of the nucleus during cell migration (Chang, Antoku and Gundersen, 2016; Tavera-Mendoza and Brown, 2017), we analyzed nuclear morphology in MDA-MB-231 cells stably depleted for TRF2. Lamin A/C nuclear staining revealed that shTRF2 cells display a modified nuclear morphology characterized by an increased circularity index compared to control cells (Figure 19).

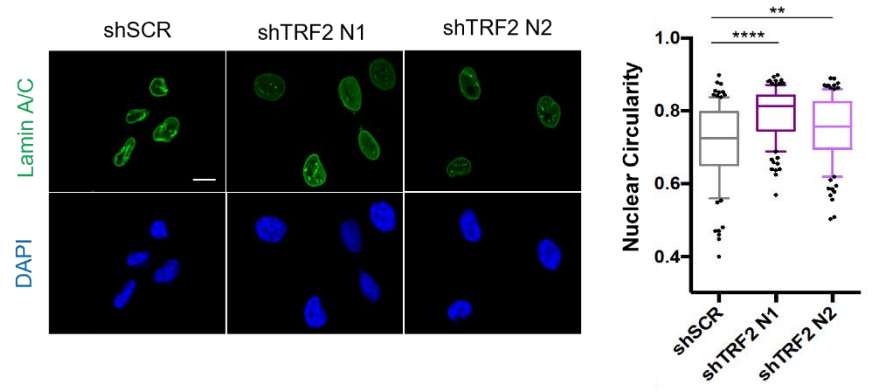

Figure 19. Left panel: representative images of nuclear morphology of TRF2-depleted MDA-MB-231 cells visualized with immunofluorescence of Lamin A/C and DAPI (scale bar, 10 µm). Righ panel: Box-and-whisker plots (10-90 percentile) of nuclear circularity index (n=100).

A similar alteration was induced by transient TRF2 knockdown by siRNAs. Conversely, stable TRF2 overexpression caused a reduction of nuclear circularity index.

Alterations of nuclear envelope structure can impact the mechanical properties of the nucleus and of the entire cell. In keeping with this concept, atomic force microscopy (AFM) analysis revealed that TRF2 knockdown cells had a significantly reduced Young's modulus, indicative of decreased stiffness, as compared to control, suggesting that TRF2 expression alters nuclear and cell mechanics.

The analysis of the expression and localization of major determinants of nuclear morphology and stiffness (Lamins, Emerin, LINC complex) in TRF2-depleted and over-expressing cells, did not reveal any significant alterations. However, it is known that telomeres are tethered

to the nuclear envelope for proper meiotic pairing and recombination of homologous chromosomes during meiosis in yeast and mammals, but also during post-mitotic nuclear assembly in mammalian cells (Takai *et al.*, 2010; Meijering, Dzyubachyk and Smal, 2012; Fedchenko and Reifenrath, 2014; Kim *et al.*, 2017). Based on this consideration, we interrogated the protein-protein interaction software (STRING) to explore shelterin-nuclear inner nuclear membrane proteins network. In line with previous works (Doyle *et al.*, 2009; Takai *et al.*, 2010), this analysis revealed a close association of telomeric proteins with various components of the nuclear lamina and inner nuclear membrane (Figure 20).

Importantly, in co-immunoprecipitation experiments, we found that endogenous TRF2 interacted with nuclear Lamin B1 and the inner nuclear membrane proteins Emerin, SUN1 and SUN2 (Figure 20).

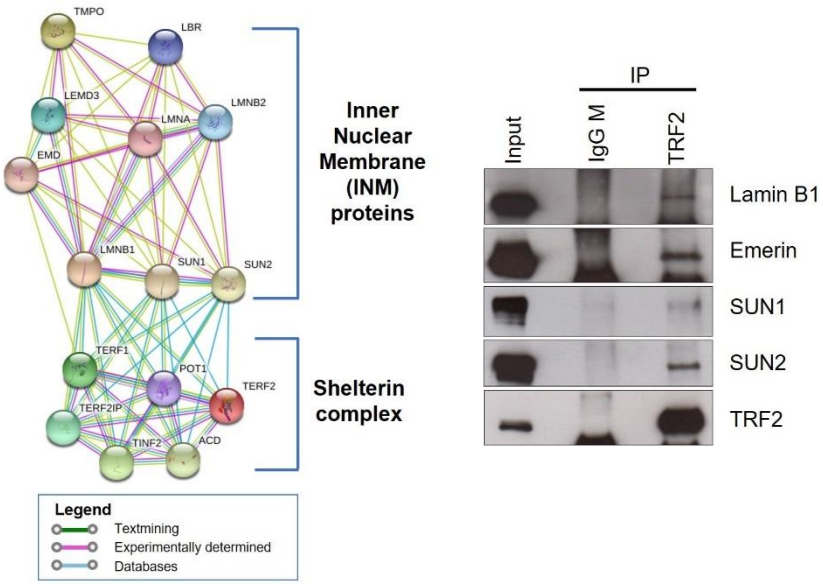

Figure 20. Protein-protein interaction map (STRING) to explore Shelterin-nuclear inner nuclear membrane proteins network. Co-immunoprecipitation experiment with anti-TRF2 antibody in MDA-MB-231 cells. Mouse immunoglobulines (IgG M) were used as negative control. Immunoblots were probed with the indicated antibodies.

Consistently, Proximity Ligation Assay (PLA), showed a direct interaction of TRF2 with Lamin B1 or Emerin at distinct nuclear sites of interphase cells (Figure 21).

Specifically, the number of interaction sites per nucleus doubled in TRF2 over-expressing cells and significantly decreased in TRF2 stably interfered cells or in cells transiently silenced for Lamin B1/Emerin (Figure 21).

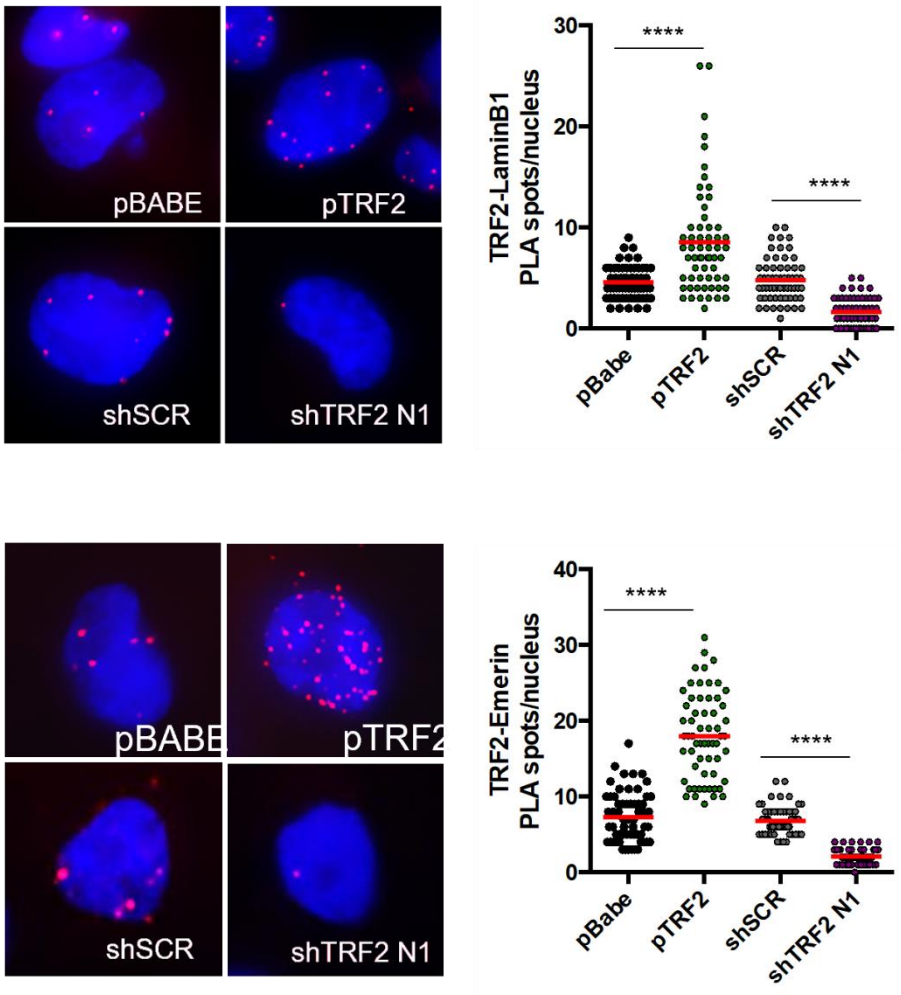

Figure 21. Proximity ligation assay to visualize interaction of TRF2 with Lamin B1 and Emerin in MDA-MB-231 cells stable overexpressing or silenced for TRF2. Left panel: representative images. Right panel: quantification of PLA spots per nucleus (n=60 cells), red lines represent mean values.

Next, to identify the domain/s of TRF2 responsible for its interaction with inner nuclear membrane proteins, we performed pull down

experiments by using a recombinant TRF2 full length protein or different fragments of TRF2 fused to GST as illustrated in Figure 22 A. Confirming immunoprecipitation experiments, Lamin B1, Emerin, SUN1 and SUN2 specifically bound to TRF2 WT protein but not to GST- control (Figure 22 B,C). Among the recombinant TRF2 fragments, only the GST-Basic domain retained the ability to bind with high affinity to the inner nuclear membrane proteins (Figure 22 B,C). These results clearly showed that the interaction of TRF2 with Lamin B1, Emerin, SUN1 and SUN2 is mediated by a Basic domain of TRF2.

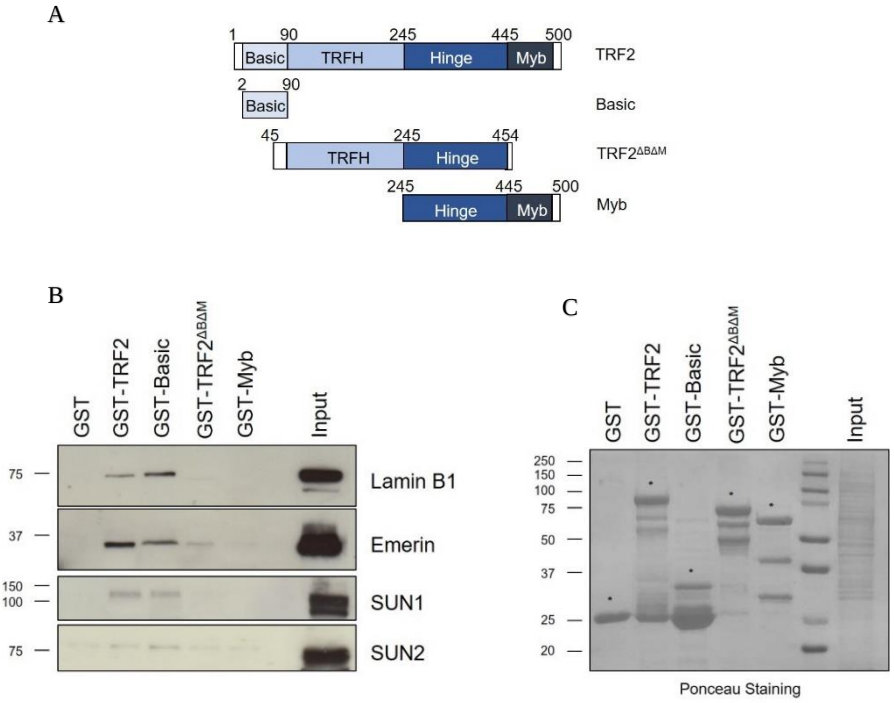

Figure 22. A. Schematic representation of TRF2 and its deletion mutants used in this study. B-C. The various GST-TRF2 proteins or GST alone were affinity-purified and incubated with lysates prepared from MDA-MB-231 cells, followed by Western blotting with indicated antibody (Lamin B1, Emerin, SUN1, SUN2) (B). The purified GST fusion proteins (indicated by the asterisks) were visualized by ponceau staining (C). Molecular mass markers are expressed in kilodaltons (KDa). Kolmogorov-Smirnov test was used to calculate statistical significance. *P<0.05, **P<0.01, ***P<0.001, ****P<0.0001.

4.3.2. TRF2 contributes to the establishment of cell polarity

Recent evidence showed that mutations or alterations of nuclear lamins and other components of the nuclear envelope can result in defective nucleus-cytoplasmic connections. This, in turn, leads to altered nuclear positioning and improper establishment of cell polarity, a fundamental step in determining the direction of cell motion (Khatau *et al.*, 2012; Devreotes and Horwitz, 2015; Fruleux and Hawkins, 2016). We therefore investigated whether migration defects induced by TRF2 knockdown were the result of impaired cell polarization. We took advantage of a starved confluent monolayer of MDA-MB-436 cells stimulated to migrate by a scratch-wound followed by treatment with the serum factor lysophosphatidic acid (LPA) (Tomita and Cooper, 2006). This agent triggers the synchronized polarization of previous starved MDA-MB-436 cells. Importantly, by measuring pericentrin orientation angle at different time points after LPA treatment, we found that TRF2 knockdown induced a significant delay in cell polarization in MDA-MB-436 (Figure 23). On the contrary, TRF2 over-expressing cells polarized more rapidly compared to their respective control (Figure 23).

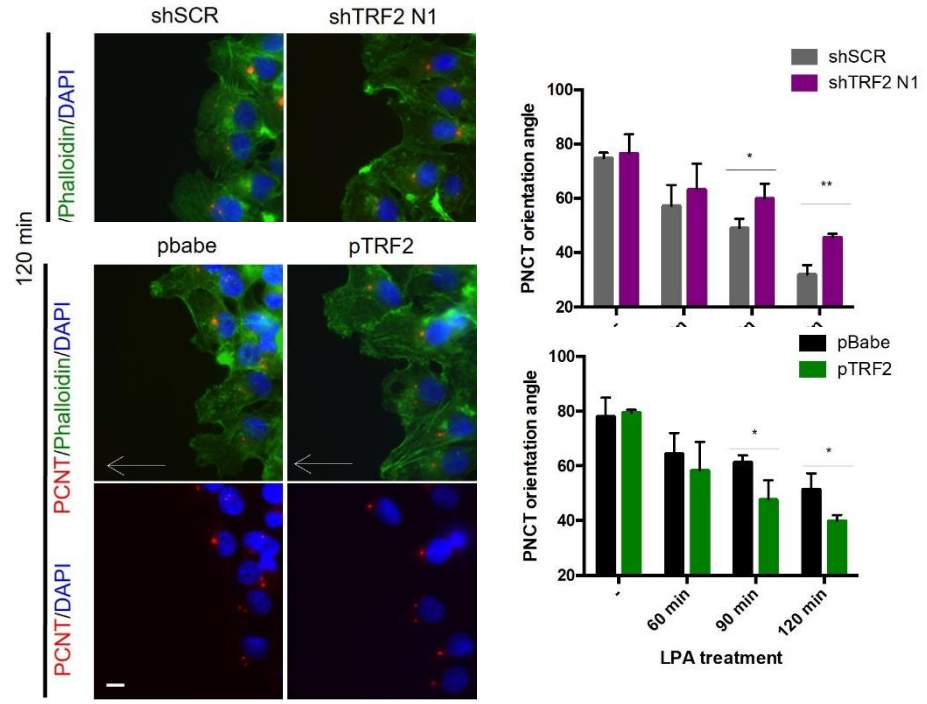

Figure 23. Starved confluent monolayers of stable TRF2 interfered (shTRF2 N1) and over-expressing (pTRF2) MDA-MB-436 cells and their respective control (shSCR, pBABE) were scratch-wounded and stimulated by Lysophosphatidic acid (LPA) (10µM). Cells fixed at different times upon LPA treatment, were stained with a centrosome marker (pericentrin), Phalloidin and DAPI. Representative images at 120 min are shown. An example of measurement of pericentrin orientation angle is shown in shTRF2 representative image. For each cell, a first line was drawn from the center of the nucleus to the wound edge and a second line was drawn from the center of the nucleus to the center of the centrosome. The angle formed between the lines was measured. Scale bars, 10µm.

To test whether TRF2 interaction with inner nuclear membrane components is functional to the establishment of cell polarity in TNBC cells, MDA-MB-436 cells stable over-expressing a deletion mutant of TRF2 lacking the Basic domain (pTRF2_ΔB) were generated and compared to TRF2 full length over-expressing cells in polarity assay (Figure 24 A,B,C). The over-expression of TRF2_ΔB did not recapitulate the effect induced by TRF2 WT form showing no effect on cell polarity (Figure 24 B,C). In line with this, over-expression of TRF2_ΔB had no impact on 3D migration of MDA-MB-231 spheroids (Figure 24 D,E), indicating that the interaction of the Basic domain with inner nuclear membrane components mediates the pro-migratory effect of TRF2.

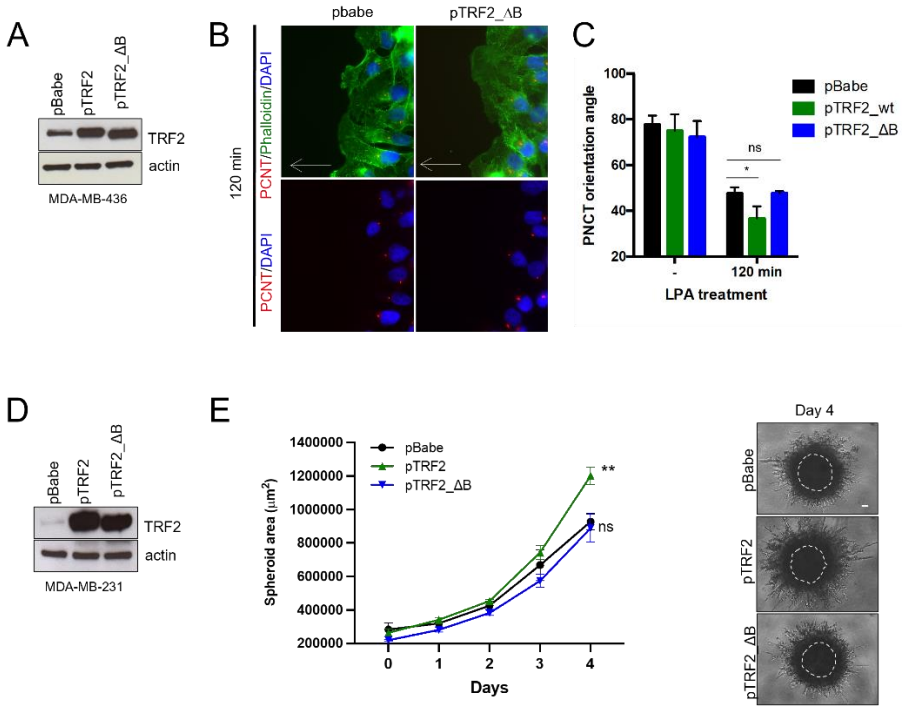

Figure 24. A. MDA-MB-436 cells stable overexpressing TRF2 WT (pTRF2) or TRF2_ΔB (pTRF2_ΔB) deletion mutant and their control (pBabe) were subjected to Western blotting for TRF2 expression analysis. B. Stable MDA-MB-436 cell models were processed as previously described. Representative images of at 120 min are shown. C. Quantification of centrosome orientation angle in untreated or LPA treated cells for indicated experimental conditions at 120 min. D. MDA-MB-231 cells stable overexpressing TRF2 WT (pTRF2) or TRF2_ΔB (pTRF2_ΔB) deletion mutant and their control (pBabe) were subjected to Western blotting for TRF2 expression analysis. E. Stable MDA-MB-231 cell models were subjected to 3D spheroid invasion assay. Left panel: quantification of spheroids area (n=3 independent experiments). Righ panel: phase contrast images of representative spheroids at day 4 are shown. Dashed circle indicates the size of spheroids at day 0. Scale bars, 100μm. Data are the mean ± SD (n=3 independent experiments, at least 50 cells analysed in each experiment n Δ150). Two-tailed t student test was used to calculate statistical significance. *P<0.05, **P<0.01, ***P<0.001, ****P<0.0001.

4.3.3. TRF2 expression is required for spontaneous metastasis formation in vivo

Cell polarization and migration defects induced by TRF2 knockdown in vitro might affect cancer cell migration from primary tumor to distal sites of the body to give rise to secondary tumors, a multistep process known as metastasis.

To investigate this possibility, we generated a spontaneous model of TNBC metastasis that reproduces the entire cascade from primary tumor formation to metastases appearance (Figure 25). Luminescent shSCR and shTRF2 N1 MDA-MB-231 were orthotopically injected

into the mammary fat pad of immune-compromised mice to allow primary tumor formation. Subsequently, primary tumors were resected and the formation of spontaneous lung metastases was monitored by bioluminescence imaging (Figure 25).

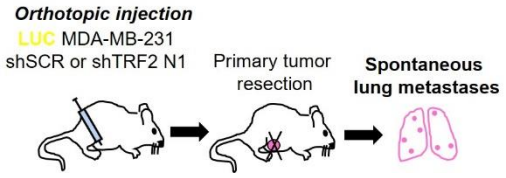

Figure 25. Schematic representation of spontaneous metastasis experiment. Luminescent MDA-MB-231 shSCR and shTRF2 N1 were injected in the mammary gland of female NSG mice. Primary tumor was resected at day 19 and spontaneous lung metastases formation was monitored.

Under these experimental conditions, we did not observe any significant change in primary tumor growth as shown by quantitative bioluminescence imaging. Moreover, immunohistochemistry (IHC) analysis of the xenografts indicates that primary tumors derived from TRF2 knockdown cells did not display any relevant changes in DNA damage activation (γH2AX staining), cell proliferation (Ki67 staining), and apoptosis induction (TUNEL assay) as compared to primary tumors derived from shSCR cells (Figure 26).

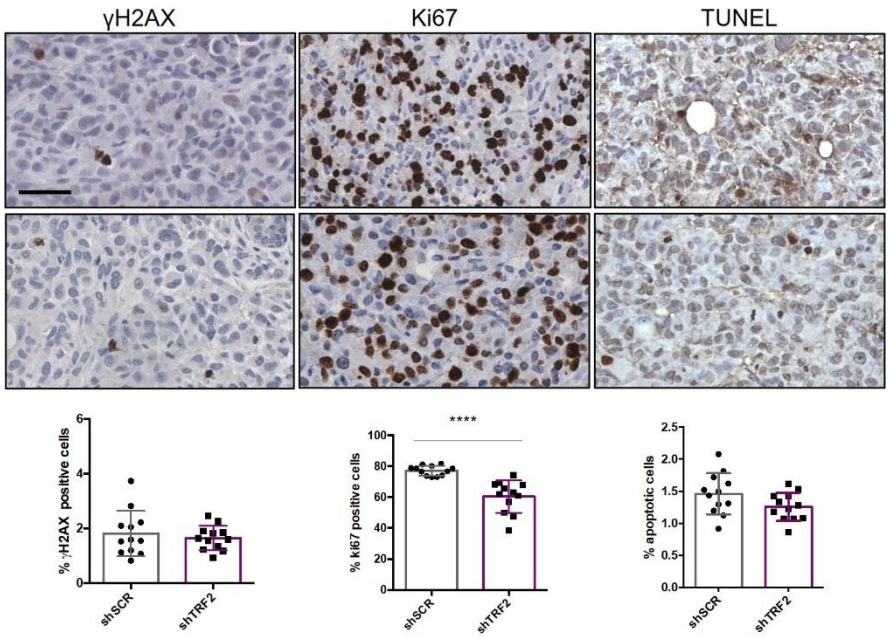

Figure 26. Immunoistochemical analysis of primary tumors derived from orthotopic injection of LUC shSCR or shTRF2 N1 MDA-MB-231 cell lines. Analyzed markers are indicated (γH2AX, Ki67, TUNEL ASSAY). Representative images are shown. Scale bars, 30μm. Data are the percentage of positive cells ± SD. Twelve fields derived from three animals for condition were analyzed.

Quantitative bioluminescence imaging at day 10 post-resection, when all control mice showed detectable lung metastases signal, revealed that TRF2 knockdown drastically reduced spontaneous metastases formation (Figure 27). Notably, one mouse from shTRF2 group resulted completely negative for lung metastasis (Figure 27).

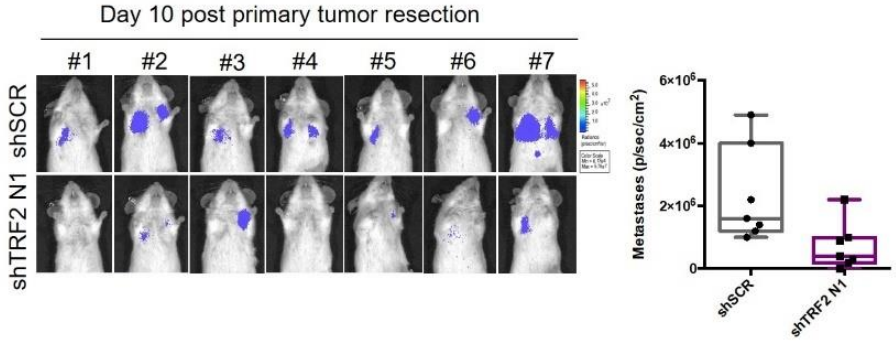

Figure 27. Left panel, representative images of all mice ten days post primary tumor resection. Right panel, Box-and-whisker plot representing lung metastases bioluminescence intensity; shSCR (N=7), shTRF2 (N=7). Two-tailed t student test was used to calculate p value.

For ethical reasons, mice were sacrificed at day 20 and lungs were subjected to ex vivo analyses. Hematoxylin and eosin staining of lung sections revealed a significant reduction in the number and size of metastatic foci in mice injected with shTRF2 N1 cells (Figure 28).

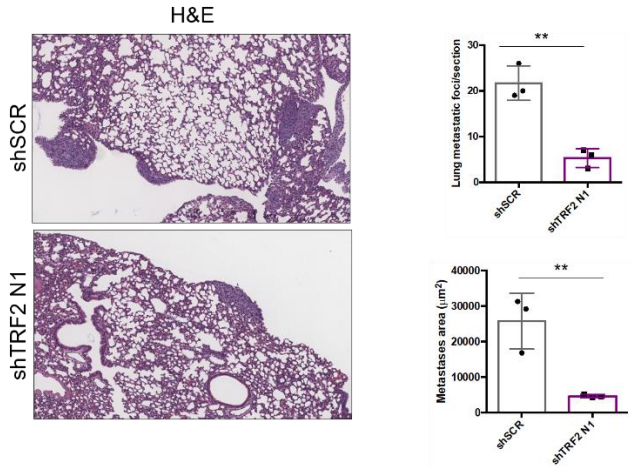

Figure 28. Left panel, representative images of hematoxylin&eosin staining of lung sections from spontaneous metastasis experiment. Scale bars, 200 μm. Right panel, quantification of the number or area of metastatic foci.

Consistently, by performing AE1/AE3 cytokeratin staining to detect the presence of metastatic deposits we observed a reduction in the number of both single BC cells and metastatic foci in the lungs of the mice injected with shTRF2 N1 cells (Figure 29).

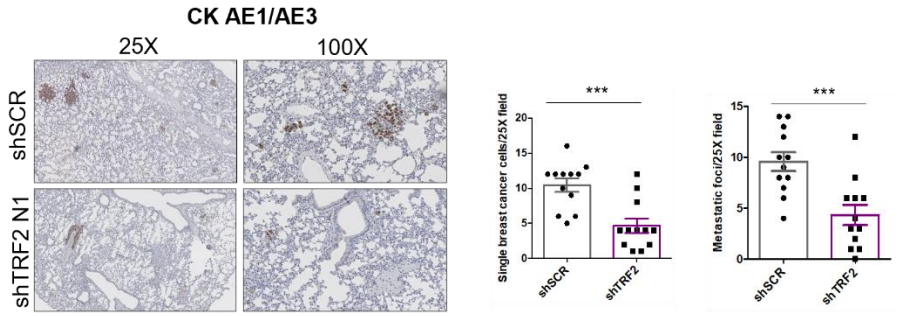

Figure 29. Representative images of Cytokeratin AE1/AE3 immunostained sections of lungs from spontaneous metastasis experiment. Scale bars, 100 μm. Quantification of the number of single BC cells and metastatic foci per 25X field.

Importantly, the reduction of spontaneous metastasis formation was confirmed after orthotopically injection of MDA-MB-436 TNBC cell line. This result indicates that the pro-metastatic effect of TRF2 is a general phenomenon in TNBC.

We, then, used high-resolution time-lapse intravital imaging to assess whether cell migration defects at the primary tumor site may proceed the reduced metastasis. Our shSCR and shTRF2 N1 MDA-MB-231 lines stably expressing a nuclear fluorescent protein (H2B-Dendra2) were injected into the mammary fat pad of NSG mice. Upon tumor formation, migration of tumor cells was imaged by surgically exposing the tumor and placing it on the imaging stage. Series of time-lapse z-stack images of the tumor were acquired every 30 min for at least 6 hours. Cell tracking analysis revealed that, in line with our in vitro data, shTRF2 cells in the in vivo setting show reduced cell velocity, displacement and persistence compared to their control counterparts. These findings indicate that TRF2 knockdown impairs the local invasion of primary tumor cells in the surrounding ECM, thus delaying the early step of the metastatic process.

To exclude a possible involvement of TRF2 in the late phases of the metastatic cascade (extravasation and colonization of ectopic sites), we injected luminescent shSCR and shTRF2 N1 MDA-MB-231 cells directly into the lateral tail vein of severely immune-compromised mice and monitored lung colonization by quantitative bioluminescence imaging (Figure 30 A). Under these experimental conditions, we observe no difference in lung metastasis formation in mice injected with shTRF2 N1 cells compared to control animals (Figure 30 B), as confirmed by hematoxylin and eosin analysis of the number and area of metastases and by AE1/AE3 cytokeratin staining on ex vivo lung sections (Figure 30 C,D).

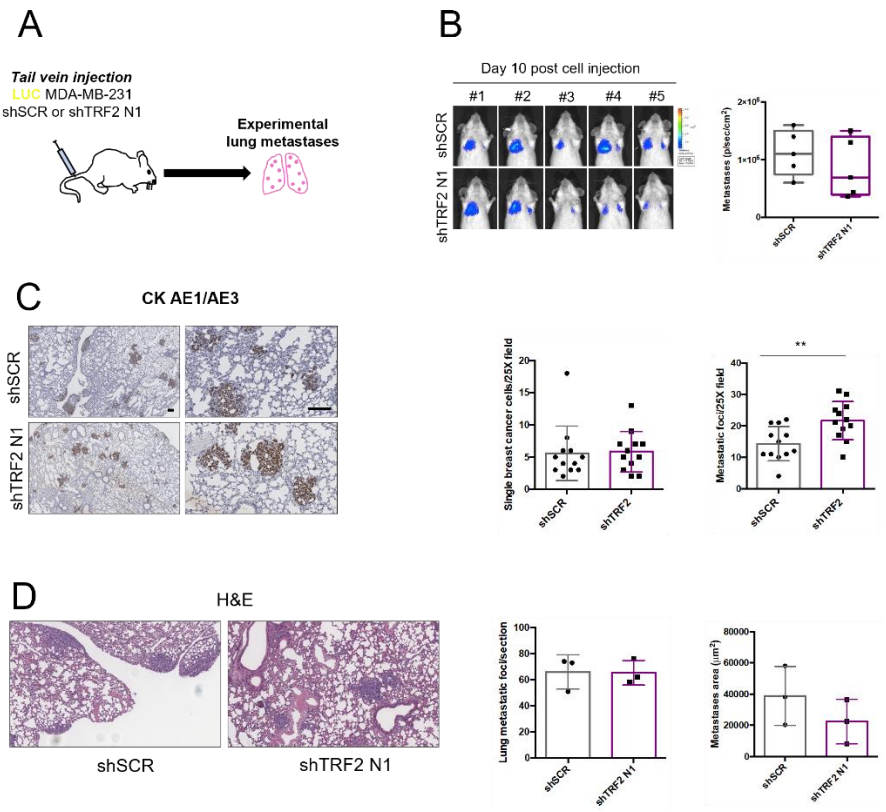

Figure 30. A. Schematic representation of experimental metastasis experiment. Luminescent MDA-MB-231 shSCR and shTRF2 N1 were injected in the tail vein of NSG mice and colonization of the lungs was monitored by bioluminescence imaging followed by ex vivo analyses. B. Left panel, representative images of all mice ten days post cell injection. Right panel, Box-and-whisker plots representing lung metastases bioluminescence intensity; shSCR (N=5), shTRF2 (N=5). C. Representative images of Citokeratin AE1/AE3 immunostained sections of lungs from experimental metastasis experiment. Scale bars, 100 µm. D. Quantification of the number of single BC cells and metastatic foci per 25X field. E. Left panel, representative images of hematoxylin&eosin staining of lung sections from experimental metastasis experiment. Scale bars, 200 µm. Right panel, quantification of the number or area of metastatic foci per section. t student was used to calculate statistical significance. *P<0.05, **P<0.01, ***P<0.001, ****P<0.0001.

Finally, we measured TRF2 levels by IHC analysis on primary tumors and lung metastases from both orthotopic and intravascular injection models. As expected primary tumors derived from TRF2 knockdown cells maintained reduced TRF2 levels (Figure 31). Surprisingly, we found that spontaneous metastases derived from shTRF2 N1 primary tumors expressed high levels of TRF2 as those derived from primary control tumors (Figure 31). On the contrary, TRF2 silencing was maintained in lung metastases resulting from colonization of intra-vein injected shTRF2 N1 cells (Figure 31). Altogether these data demonstrate that TRF2 expression is required for the early steps of the metastatic cascade in TNBC.

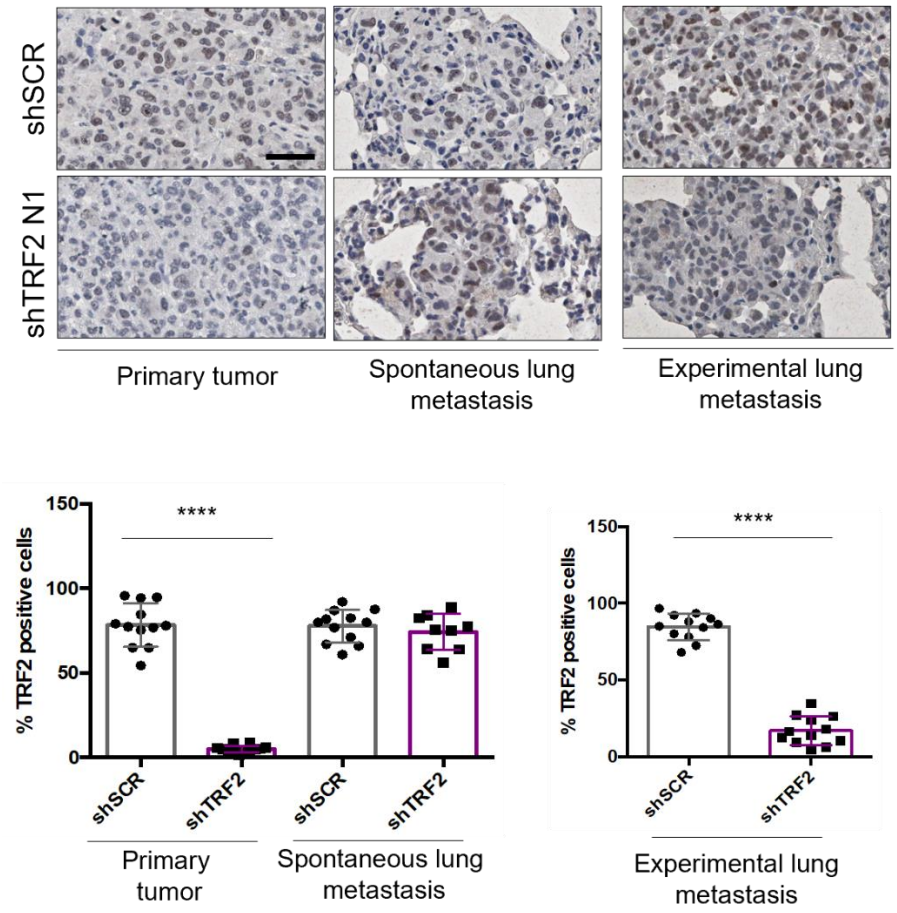

Figure 31. Representative images of TRF2 immunostained sections of primary tumor, spontaneous and experimental lung metastases. Scale bars, 30μm. Quantification of the percentage of TRF2 positive cells in primary tumors and lung metastasis sections. Twelve fields derived from three animals for condition were analyzed. t student was used to calculate statistical significance. *P<0.05, **P<0.01, ***P<0.001, ****P<0.0001.

4.3.4. TRF2 expression correlates with breast cancer progression and is required for metastasis formation in human patients

To test the clinical relevance of our findings, we investigated the correlation between TRF2 expression and BC formation and progression in human patients. Human samples of normal breast tissue (N=41), benign lesions (N=51) or malignant tumors (N=55) surgically treated at Regina Elena National Cancer Institute were analyzed for TRF2 protein expression by IHC analysis (Figure 32). Interestingly,

TRF2 Immunoreactive score (IRS), obtained by multiplying the TRF2 positive cells proportion score for the TRF2 staining intensity score, progressively increases from normal tissue to benign lesions and becomes even higher in malignant tumors (Figure 32).

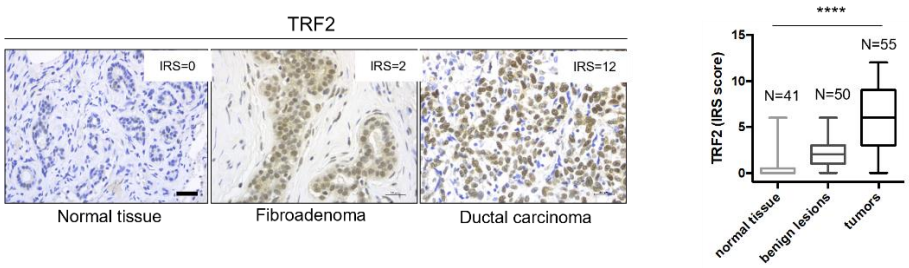

Figure 32. Representative images of immunohistochemistry evaluation of TRF2 expression in Normal breast tissue, Fibroadenoma (benign lesion) and Ductal carcinoma (malign tumor). Scale bars, 30μm. Quantification of TRF2 expression (Immunoreactive score) in Normal breast tissue (N=41), benign lesions (N=51) and malign tumors (N=55) surgically treated in IRCCS-Regina Elena National Cancer Institute. Statistical significance was calculated by one-way ANOVA (****P<0.0001).

To establish whether TRF2 expression varied among the different subtypes of malignant tumors, we used a larger cohort of BC patients (N=1026) from The Cancer Genome Atlas (TCGA) dataset. TRF2 mRNA expression progressively increases with the increasing aggressiveness of tumor subtypes, reaching the highest level in the basal subtype. According to this, TRF2 expression is higher in breast tumors negative for estrogen, progesterone and HER2 receptors (Triple Negative), characterized by the most aggressive clinical course, early relapse and poor outcome30. Moreover, TRF2 expression is higher in stage II-III-IV as compared to stage I BC patients.

To address whether TRF2 expression is important for BC metastasis in human patients, we performed an analysis of TRF2 expression on primary TNBC and their matched metastatic lesions from a cohort of patients surgically treated in our institute (N=30). We found a significant increase of TRF2 expression in metastatic lesions compared to primary tumors regardless the site of metastasis (local recurrence or

different distant organs) and independently from the route of spread (blood or lymphatic system) (Figure 33).

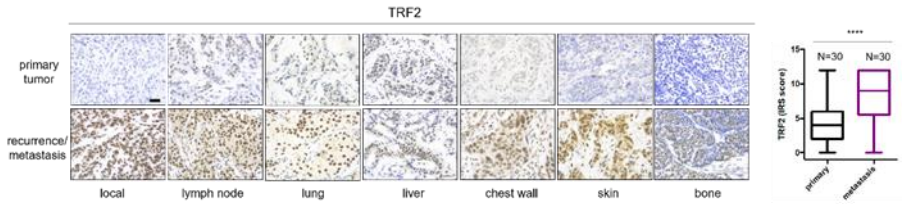

Figure 33. Representative images of immunohistochemistry evaluation of TRF2 expression in primary TNBC and their matched metastatic lesions (local recurrence and different distant organs). Scale bars, 30μm. Quantification of TRF2 expression (Immunoreactive score) in primary TNBC and their autologue metastatic lesions from patients surgically treated in IRCCS-Regina Elena National Cancer Institute (N=30). Statistical significance was calculated by Wilcoxon matched-pairs rank test (****P<0.0001).

These results indicate that TRF2 plays a critical role in promoting metastatic process in human TNBC patients. Finally, by stratifying patients from TCGA dataset on the basis of the TRF2 mRNA expression (TRF2 low 314/599; TRF2 high 285/599), we found that high levels of TRF2 correlate with a worse clinical outcome of BC patients also by excluding stage IV patients.

Altogether these data support the concept that TRF2 expression positively correlates with BC aggressiveness, metastasis formation and poor clinical outcome of BC patients.

4.4. DISCUSSION

BC is the leading cause of cancer-related mortality in women in developed countries. Among molecular subtypes, basal-like TNBC, defined by lack of expression of estrogen receptor (ER), progesterone receptor (PR), and human epidermal growth factor receptor-2 (HER2) is characterized by the most aggressive clinical course due to cancer recurrence as distant metastasis (Ding *et al.*, 2007). However, the

molecular mechanisms underlying this aggressive behavior are not fully elucidated and robust prognostic and predictive biomarkers that could improve clinical outcome of these patients are still lacking.

Here, we identified the Telomere repeat-binding factor 2 (TRF2) as a marker of aggressiveness and metastasis in TNBC. Our data in mouse models and human patients showed that TRF2 is overexpressed in the metastatic lesions, compared to the primary tumors, regardless the dissemination site. Interestingly, multiple experimental approaches allowed us to demonstrate that TRF2 affects the initial local invasion of cancer cells at the primary tumor site, one of the key steps of the metastatic cascade. Indeed, TRF2 knockdown significantly reduced the appearance of spontaneous metastases induced by orthotopic injection of TNBC cells while no effect was observed by direct intra-vein injection of the same cells excluding a possible role of TRF2 in the extravasation and colonization steps. Importantly, high-resolution time lapse intravital imaging by monitoring single cell migration exactly at the primary tumor site allowed us to confirm that reduced metastasis is directly linked to reduced velocity, displacement and persistence of TRF2 depleted cells in their in vivo setting.

This work goes an important step further, investigating the impact of TRF2 on cell migration in vitro and dissecting the molecular mechanisms behind it.

A battery of single cell migration assays upon modulation of TRF2 expression revealed that lack of TRF2 does not impair cell motility per se, but prevents TNBC cells from performing directional and productive linear migration. Indeed, we found a significant effect of TRF2 on 1D and 3D migration, where the cells are forced to polarize and directionally migrate in a constrained environment. Although previous reports showed that TRF2 expression can impinge on migration of endothelial cells and renal cell carcinoma cells in wound healing assays (Pal *et al.*, 2015; Wang *et al.*, 2018), our work provides for the first time a comprehensive characterization of the migratory behavior induced by over-expression/depletion of TRF2 in TNBC models.

The effects observed on 1D and 3D migration analyses directed us to investigate the contribution of the nuclear morphology and dynamics. We first observed that TRF2 depletion modified nuclear shape by increasing nuclear circularity index. This is in agreement with recent works showing that high nuclear circularity correlates with a less invasive phenotype in BC. Indeed, nuclei of normal human breast epithelial cells (MCF-10A) have a more circular and regular shape compared to invasive BC cell lines (MDA-MB-231, MDA-MB- 157) (Crabbe *et al.*, 2012). Linked to alteration of nuclear structure, we found that TRF2 impacts on cell mechanic properties. In particular, measure of the Young's modulus placing the AFM cantilever over the nucleus, revealed that TRF2 knockdown cells have a decreased stiffness, as compared to control cells. Although many studies have shown that more invasive cells are softer than their counterparts, a correlation between cell stiffness and cell motility remains controversial. Indeed, this correlation appears valid in studies where normal tissues were compared to tumors in different progression stages. However, it is significantly less strong in experiments where changes in migration ability are induced by pharmacological agents or genetic modifications (Wood *et al.*, 2014), as in our case. Moreover, in line with our findings, a lower cell stiffness induced by stable silencing of ATR correlates with reduced cell migration and tumor cells dissemination in vivo (Folker *et al.*, 2011).

More detailed investigation into nuclear morphology alterations and cell stiffness, enable us to rule out significant changes in the expression or localization of main nuclear envelope components. Interestingly, however, we found that, in addition to the recently demonstrated interaction with Lamin B1 (Chang *et al.*, 2013), TRF2 binds also to other, previously unreported, nuclear envelope proteins such as Emerin and two members of the LINC complex (SUN1 and SUN2), strengthening the existence of a close association of TRF2 with the inner nuclear envelope. Importantly, we provided new insights in this direction by identifying the Basic domain as the main region of TRF2 responsible of this association. TRF2 Basic domain is reported to act as

a branched DNA binding domain involved in the stabilization of the telomeric t-loop three-way junction (Östlund *et al.*, 2019). However, its ability to bind core histones (H3/H4, H2A/H2B) regardless of the presence of DNA (L. Yin *et al.*, 2020), indicates that the TRF2 Basic domain can directly mediate protein-protein interactions.

Next, we investigated whether TRF2-nuclear envelope interaction is functional to the establishment of cell polarity. We found that TRF2 expression impacts on centrosome orientation during cell polarization process, a fundamental step in determining the direction of migration. This is in line with nuclear positioning and cell polarization defects observed in laminopathies or upon alteration of Lamin A, Emerin or LINC complex in fibroblasts or myoblasts (Khatau *et al.*, 2012; El Maï *et al.*, 2014; Fruleux and Hawkins, 2016; Gadad *et al.*, 2021). Importantly, overexpression of deletion mutant of TRF2 lacking the Basic domain did not recapitulate effects induced by TRF2 WT overexpression on cell polarization and 3D migration, indicating that TRF2 interaction with the inner nuclear membrane is required to drive the pro-migratory phenotype. Based on these data TRF2 becomes part of the mechano-transduction machinery of the cells, participating to the communication between the cytoplasm and nuclear interior finally ensuring productive migration of TNBC cells.

Finally, we addressed clinical relevance of our findings by identifying a positive correlation between TRF2 expression and BC progression in human patients by integrating analyses from TCGA dataset and from a cohort of patients surgically treated at Regina Elena National Cancer Institute. We found that TRF2 protein expression increases during the progression from normal tissue to benign lesion up to malignant lesion. Moreover, TRF2 mRNA level is higher in TNBCs and positively correlates with stage progression and a worse clinical outcome in BC patients (TCGA).

Collectively, our data demonstrated that TRF2, along with the regulation of cell-extrinsic pathways (tumor immunosurveillance and angiogenesis), has a direct effect on cancer cell intrinsic features such as cell migration and metastasis. Interestingly, our work unravels, on

one hand, new insights on TRF2 biology and, on the other hand, identifies TRF2 as a marker of metastasis and prognosis in TNBC that could represent a pertinent drug target for development of new treatments.

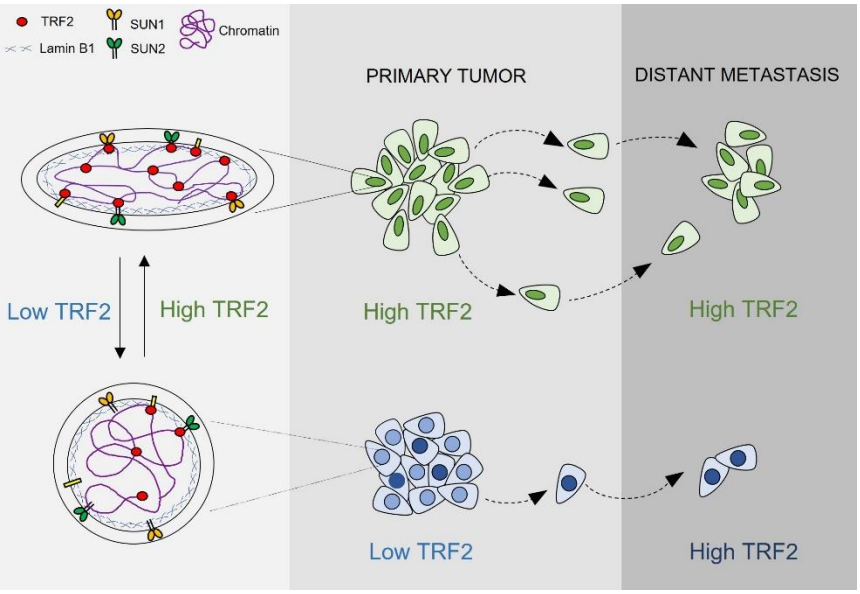

Figure 34. Model for TRF2 regulation of BC metastasis. TRF2 by interacting with nuclear envelope components regulates nuclear shape and cell stiffness, thus allowing proper establishment of cell polarity and directional migration of cancer cells from primary tumor to distant site of the body giving rise to spontaneous metastasis. Knockdown of TRF2 increases nuclear circularity, reduces cell stiffness, impairs cell polarity and directional cell migration, finally leading to reduced metastasis formation. TRF2 expression results higher in metastatic lesion as compared to matched primary tumor.

4.5. MATERIALS AND METHODS

Cell lines, culture conditions, transfections and infections

TNBC cell line MDA-MB-231 was kindly provided by Dr. Patrizio Giacomini, IRCCS – Regina Elena National Cancer Institute. MDA-MB-436 cell line was obtained by Dr. Vincenzo Cerullo, University of Naples Federico II, Italy. Both the cell lines were grown in high glucose Dulbecco modified eagle medium (DMEM; Invitrogen, Carlsbad, CA,

USA) supplemented with L-glutamine, Penicillin/streptomycin and 10% fetal bovine serum (FBS, Hyclone).

Stable cell lines were generated as previously described (Zizza *et al.*, 2019). Briefly, TRF2-overexpressing cells (pBabe-puro-mycTRF2, pBabe-puro-mycTRF2ΔB) and the control counterpart (pBabe-puro-Empty) (Luo *et al.*, 2016) were obtained by infecting the cells with amphotropic retroviruses generated into Phoenix packaging cells transfected with retroviral vectors, using the JetPEI reagent (Polyplus, New York, NY, USA), according to the manufacturer's instructions.

For stable silencing of TRF2 gene, cells were infected with lentiviral particles produced into HEK293T cells transfected with the packaging pCMVR8.74 and the envelope pMD2.G vectors in combination with the vectors encoding either for a scramble short hairpin sequence (shSCR; N2040 targeting Escherichia coli DNA polymerase) or for one of the two short hairpin sequences directed against TRF2 (shTRF2_N1: N2571 TRCN0000004811 or shTRF2_N2: N2573 TRCN0000004813 which were a gift from Prof. Stefan Schoeftner, University of Trieste). Early passages of stably infected cells were used for all experiments.

For in vitro single cell migration analysis, MDA-MB-231 stably TRF2 over-expressing /depleted cell lines were transduced with H2B-GFP retroviral vector (pBABE-H2BGFP) for nuclear staining and positive cells were selected by FACS sorting to reach a homogeneous cell population.

For intravital imaging analysis, MDA-MB-231 stably depleted for TRF2 and expressing H2B-Dendra2 were generated by transfection with a specific vector (pMiniTol-EF1a-H2B-Dendra2) in combination with trasposase vector (pCS3-Trasposase), followed by FACS sorting.

For generation of spontaneous and IV metastasis models, MDA-MB-231 stably depleted for TRF2 were infected with lentiviral luciferase vector pRRLSIN.cPPT.RFPL4b (Addgene) that allows stable expression of luciferase for in vivo monitoring of metastases.

Supplementary cell lines, transfections and infections

For transient RNA interference experiments, siTRF2 (TRF2 Modified siRNA GEHCI-000246 GCAGAAGUGGACUGUAGAAUU, Dharmacon Inc., Chicago, USA) and siCTR (Control siRNA-A4, sc-37007, Santa Cruz Biotechnology; CA, USA Lot D1421) were transfected into cells with Interferin (Polyplus) according to the manufacturer's instructions.

Generation of inducible CRISPR KO MDA-MB-231 cell line was performed as described in Kim et al (Kim *et al.*, 2017) thanks to vectors kindly provided by Zhou Songyang. Briefly, MDA-MB-231 cells stably expressing doxycycline-inducible Cas9 were generated by lentiviral transduction. A single clone with efficient Cas9 induction was selected. Vectors expressing dual shRNAs were introduced in the Cas9-inducible clone by lentiviral transduction followed by selection with specific antibiotics. For Induction of Cas9 and efficient knockout of TRF2, 5 days of incubation in 1 μgml−1 of doxycycline was used.

Cell senescence

Senescence was evaluated by β-galactosidase staining kit (Cell Signaling Technology) according to the manufacturer's instructions.

Growth curve

Cells ($5x10^4$) were plated in each well of a 6-well plate and cell proliferation was monitored through 6 days using an Incucyte Live-Cell Imager (PHCBi Panasonic). Confluence of the cultures was measured using Incucyte software.

Adhesion Assay

24-well plates were coated with BSA 1% or fibronectin 0,5% (Sigma Aldrich) at 37 °C overnight and blocked with BSA 1% for 1 hour. Cells were washed with PBS and 2x105 cells, resuspended in PBS, were

plated on each coated well and incubated at 37°C. Nonadherent cells were removed by washing with PBS. Cells were fixed in 4% formaldehyde (PFA) for 15 minutes, washed 3 times with PBS and stained with crystal violet solution (0.5% in 20% methanol) for 30 minutes. Cells were measured in a spectrophotometer at 570 nm after solubilization in acetic acid.

Protein Extracts and Western Blotting

Total cell lysates were prepared using a lysis buffer (50 mmol/L Tris-HCl (pH 7.5) 250 mmol/L NaCl, 5 mmol/L EDTA, 0,1% Triton) with the addition of protease and phosphatase inhibitors. They were then boiled with Laemmli buffer and 25 μg were resolved using precast Mini-PROTEAN® gels (Biorad), transferred to a nitrocellulose membrane and probed as with primary (overnight at 4 ° C) and secondary antibodies (1 h at temperature environment) and acquired through the imaging system. Image intensity measurements were made using ImageJ (Kidiyoor *et al.*, 2020). Primary antibodies are listed in Table 1.

Immunoprecipitation (IP)

Nuclear cell extracts were obtained by a sequential lysis with buffer A (10 mM Hepes pH 7.9, 10 mM KCl, 0.1 mM EDTA, 0.1 mM EGTA, 0.6% NP-40, 1 mM DTT and 1 mM PMSF) and buffer C (20 mM Hepes pH 7.9, 400 mM NaCl, 0.1 mM EDTA, 0.1 mM EGTA, 1 mM DTT and 1 mM PMSF), which resulted respectively in cytosolic and nuclear fraction isolation. Protein concentration was determined and 500 μg of nuclear fraction were used for each IP.

Magnetic beads A and G (Dynabeads, Thermo Fisher Scientific) were washed with PBS 0.02% Tween20 (Wash Buffer) and bound to 4 μg of specific antibody or mouse IgG as negative control (15 minutes of incubation at room temperature). Then antibody-beads complexes were

washed and incubated with nuclear extracts for 45 minutes at room temperature. Immunoprecipitates were washed, eluted from the magnetic beads, and boiled at 95°C for 5 minutes before SDS page.

Pull-down assay

Pull-down assay was performed as previously described (Pennarun *et al.*, 2021). Briefly, 700 μg of nuclear protein fraction were incubated with 30 μl of each recombinant TRF2-conjugated resin. As a negative control, nuclear protein fraction was incubated with GST-conjugated resin.

3D spheroids invasion assay

For 3D invasion assay, Cultrex 3D Spheroid Cell Invasion Assay kit (Trevigen) was used according to the manufacturer's instructions. Briefly, cells spheroids were generated by plating 2500 cells with a specialized ECMR in 96 well round bottom plates to drive spheroid formation. After 3 days spheroids were embedded in Invasion MatrixR and photographed every 24 hours at 4x magnification using a Nikon Eclipse TS100 microscope equipped with Infinity 1 digital camera. Invasive activity of each spheroid was quantified as the surface area of the invasive structure by using ImageJ.

Transwell migration assay

Cells were starved for 24 hours, then harvested in 5% BSA serum free medium, centrifuged and resuspended in serum free medium. Boyden Chamber consisting of transwell filter inserts with 8 μm size polycarbonate membrane (Corning-Costar,Lowell MA) placed in a 24-well plate were used. Cells (9x104) were placed in the upper chambers, while the lower chambers were filled with 10% FBS medium. After 6 hours, inserts were removed and inner side was wiped with cotton swaps. Migrated cells were stained using Diff-Quick kit (Merz-Dade,

Switzerland). After letting the inserts dry, pictures were acquired with 20X objective of Nikon Eclipse TS100 microscope equipped with Infinity 1 digital camera and cells per field were counted.

Single cell migration analyses

For random migration analysis, cells were seeded on 10 μg/ml fibronectin-coated 6 well plate and left to adhere in the incubator overnight. Cell nuclei were labeled for 20 minutes at 37°C with Hoechst 34580 (Sigma-Aldrich) at 5 μg/ml or with NucBlue live cell stain (Thermofisher) according to the manufacturer's instructions.
For 1D migration analysis, coverslips (25mm) were micropatterned with 10 μm-wide lines as previously described (Schmutz *et al.*, 2017) and coated with fibronectin (10 μg/ml). Cells expressing nuclear H2B-GFP were seeded on the coverslips and left to adhere in the incubator overnight.
Afterwards, the coverslips were mounted in 35 mm magnetic chambers (Chamlide) for imaging.
For both random and 1D analyses, cell migration was monitored with a 10X objective every 10 minutes for 24 hours by fluorescence and transmission light, using an inverted wide-field motorized microscope (Olympus Scan^R) in a humidity- and temperature controlled environmental chamber (37°C & 5% CO2 perfusion). Cell velocity, persistence and effective length were analyzed as previously described (Schmutz *et al.*, 2017).

AFM indentation method

A modified AFM tip (NovaScan, USA) attached with 10 μm diameter bead was used to indent the center of the cell, in correspondence of nucleus. The spring constant of the AFM tip cantilever is 0.03 N/m. AFM indentation loading rate is 0.5 Hz with a ramp size of 3 μm. AFM indention force was set at a threshold of 2 nN. The data points below

0.5 μm indentation depth were used to calculate Young's modulus, using the Hertz model shown below:

$$F = \frac{4}{3}\frac{E}{(1-\nu^2)}\sqrt{R\delta^3}$$

where F is the indentation force, E is the Young's modulus to be determined, ν is the Poisson's ratio, R is the radius of the spherical bead, and δ is indentation depth. The cell was assumed incompressible and a Poisson's ratio of 0.5 was used.

Immunofluorescence

Cells were seeded on gelatin coated slides and left in culture for 24 or 48 hours. After this time, cells were fixed in 3.7% formaldehyde for 15 minutes, followed by permeabilization with 0.25% Triton X-100 for 5 minutes at room temperature. Cells were blocked for 45 minutes in 3% BSA, 0.1% Tween-20 in 1x PBS and incubated with primary antibodies (as indicated in Table 1) diluted in blocking solution at room temperature for 2 hours. Cells were washed in 0.3% BSA, 0.1% Tween-20 in 1x PBS and incubated with secondary antibodies (Table 2) for 1 hour at room temperature. Slides were washed in 0.1% Tween-20 1XPBS, stained with DAPI (Sigma-Aldrich) and mounted with Mowiol (Millipore-Calbiochem). For the analysis of nuclear circularity images were acquired with a Zeiss LSM510 inverted confocal microscope (Carl Zeiss, Gottingen, Germany) and circularity index was calculated using an ImageJ plugin, Active contour (ABSnake).

Polarity Assay

Centrosome orientation assay was performed as described in Chang et al (Tomita and Cooper, 2006) with same minor adaptations. Briefly, cells were plated on gelatin coated slides. After 48 hours, when the cells were at 90% of confluence, were starved with serum-free medium.

48hrs later, confluent monolayers were wounded with a 10-µl micropipette tip, and incubated for 30 minutes at 37°C to allow them to recover. Next, cells were incubated with serum-free medium containing Lysophosphatidic acid (LPA) (10 µM), or without LPA as negative control, and maintained at 37°C for indicated times. Slides were then fixed and processed for immunofluorescence as described in immunofluorescence section (antibodies listed in Table 1). Images were acquired with Leica DMIRE deconvolution microscope equipped with a Leica DFC 350FX camera and elaborated by a Leica LAS X software (Leica, Solms, Germany). Images analysis has been performed using ImageJ 1.46r. For each cell, a first line was drawn from the center of the nucleus to the wound edge and a second line was drawn from the center of the nucleus to the center of the centrosome. The angle formed between the two lines was measured.

Proximity Ligation Assay (PLA)

Cells were seeded on gelatin coated slides. After 24 hours cells were fixed and permeabilized as described for Immunofluorescence, then they were processed according to protocol of Duolink® PLA Fluorescence (Sigma Aldrich). Images were acquired with Leica DMIRE deconvolution microscope equipped with a Leica DFC 350FX camera and elaborated by a Leica LAS X software (Leica, Solms, Germany). Number of the spots per cell were counted by visual inspection on the maximum projection resulting from multiple z-stack images.

Immunofluorescence combined with telomere DNA FISH

Cells were seeded on gelatin coated slides and left in culture for 24 hours. After this time, cells were fixed in 4% formaldehyde for 15 minutes, followed by permeabilization with 0.1% Triton X-100 for 7 minutes at room temperature. Cells were blocked for 1 hour with 3%

BSA in 1X PBS and incubated with primary antibody (as indicated in Supplementary Table 1) diluted in blocking solution at 4°C over night. The next day, after two washes of 5 minutes with 0.05% Triton X-100 in 1x PBS, cells were incubated with secondary antibody (Table 2) diluted in blocking solution for 1 hour room temperature. Slides were washed 2 times with 1x PBS for 7 minutes and Telomere DNA FISH was carried out as previously described (Petti *et al.*, 2019). Cells were subjected to consecutive fixations with 4% formaldehyde (PFA), then were dehydrated with increasing alcohols and allowed to dry at room temperature. Samples, to which the telomere probe solution was added, were denatured for 3 minutes at 80°C and incubated for 2 hours in humid chamber. After a series of washes with FISH solution (70% formamide, 10 mM Tris pH 7.2, 0.1% BSA), samples were incubated with DAPI, then dehydrated with 70%, 90%, and 100% ethanol and mounted with Mowiol. Nuclei showing at least three telomere-γH2AX colocalization events were considered for the quantification.

Cell spreading and focal adhesion analysis

For spreading assay (3x104) cells were seeded on fibronectin coated slides and fixed after 1,5 and 5 hours with 3.7% formaldehyde for 15 minutes. Cell permeabilization and staining were performed following the immunofluorescence protocol previously described. The analysis was carried out by measuring the area of the cells with ImageJ Software. For focal adhesion analysis (3x104) cells were seeded on fibronectin coated slides, fixed after 5 hours and subjected to immunofluorescence. For analysis, focal adhesion number/cell and focal adhesion area were measured using ImageJ Software.

FACS analyses

Cell cycle analysis was performed by flow cytometry using a FACSCelesta (BD Biosciences, San Jose, CA, USA). Briefly, adherent cells (2×105) were fixed and resuspended in a solution containing

propidium iodide at a concentration of 50 μg/ml and RNase at a final concentration of 75 kU/mL, incubated for 30 minutes in the dark.
Apoptosis was evaluated by annexin V versus PI assay, as described in (Biroccio *et al.*, 2002). Briefly, cells were harvested, suspended in annexin-binding buffer (1×106 cells/ml), incubated with fluorescein isothiocyanate-annexin V (annexin-FITC) and PI (Molecular Probes) for 15 minutes at room temperature in the dark, and then immediately analyzed by flow cytometry using a FACScan (BD Biosciences).
For each experiment, 20 000 events were collected using excitation/emission wavelengths of 488/525 and analyzed with CELLQuest and FACS Diva Software (BD Biosciences).

Spontaneous model of metastasis: orthotopic tumor implantation in mouse mammary fat pad

Female NSG mice (NOD.Cg-PrkdcSCIDIL-2R null) (Charles River Laboratories, Calco, Italy) were anesthetized with a combination of tiletamine–zolazepam (Telazol, Virbac, Carros, France) and xylazine (xylazine/ Rompun BAYER) given intramuscularly at 2 mg/kg, and a small incision of less than 3 mm is made externally and caudally to the nipple. With the aid of micro-dissecting forceps, the ventral most part of the fat pad is gently pulled out and exposed through the small incision.
LUC MDA-MB-231 or LUC MDA-MB-436 cells (1x106) were injected using an insulin syringe with a 27 gauge niddle. Successful injection is confirmed by the swelling of the tissue. The small incision is sealed using absorbable suture (PolySorbTM 5-0) (Konishi, Izumi and Shimizu, 2016). Finally, mice were medicated with an orally administration of 0.5 mg/kg of Metacam (meloxicam) to control post-operative pain and inflammation. Real time tumor growth was monitored weekly using the IVIS Lumina II CCD camera system (PerkinElmer). Mice were injected intraperitoneally with 150 mg/Kg D-Luciferin (PerkinElmer) and imaged 10 minutes after luciferin

injection. Imaging was performed at baseline and periodically (every 7-10 days) after tumor cell injection. Bioluminescence signals were determined by the number of photons and were acquired and analyzed using the Living image software version 4.3 (PerkinElmer). Primary tumors were surgically resected and fixed in formalin for IHC analysis. Mice were monitored periodically by Ivis imaging for metastases appearance until sacrifice when lungs were fixed in formalin and processed for IHC.

Experimental model of metastasis: intravenously injection of tumor cells

Female NSG mice (NOD.Cg-PrkdcSCIDIL-2R null) were injected in the tail vein with 2x105 LUC MDA-MB-231 cells in a volume of 200 μl PBS/ mouse. Real time lung metastases were monitored weekly using the IVIS Lumina II CCD camera system (PerkinElmer). Mice were injected intraperitoneally with 150 mg/Kg D-Luciferin (PerkinElmer) and imaged 10 minutes after luciferin injection. Bioluminescence signals were determined by the number of photons and were acquired and analyzed using the Living image software version 4.3 (PerkinElmer). Mice were sacrificed and lungs were fixed in formalin for IHC analysis.

Intravital imaging

All animal experiments were approved by the Animal Welfare Committee of the NKI, in accordance with national guidelines. All animals were maintained in the animal department of the NKI, housed in individually ventilated cage (IVC) systems under specific pathogen-free conditions and received food and water ad libitum. Tumor cells (1x106) were injected in the right inguinal mammary gland of female NOD-scid Il2rynullB2mnull mice knockout mice at 10-20 weeks of age. Mice bearing tumors of ~250 mm3 were used for intravital microscopy. Mice were sedated using isoflurane inhalation anaesthesia

(1.5% to 2% isoflurance/air mixture). The imaging site was surgically exposed, and the mouse was placed with its head in a facemask within a custom designed imaging box. The isoflurane was introduced through the facemask, and ventilate by an outlet on the other side of the box. The temperature of the imaging box and microscope were constantly adjusted to keep the mice between 36 and 37°C by a climate chamber that surrounds the whole stage of the microscope including the objectives. All images were acquired on an inverted Leica TCS SP8 multiphoton microscope. All images were collected in 12 bits with a 25X water immersion objective (HC FLUOTAR L N.A. 0.95 W VISIR 0.17 FWD 2.4. mm). All images were processes using ImageJ software and were smoothed (if necessary) and contracted linearly (if necessary). Images were corrected for XY and Z drift using custom-written software. Cell tracking analysis was performed using MTrackJ plugin for ImageJ (Chang *et al.*, 2019).

Tissue analyses (mouse)

Immunohistochemistry (IHC)

Formalin-fixed and paraffin embedded tissue blocks were sectioned (2μm) and subjected to deparaffinization, rehydration and antigen retrieval by PT Link (Dako Omnis), that allows the entire pretreatment process of tissue sections, low or high pH according to primary antibodies datasheet. Endogenous peroxidase was blocked for 10 minutes in Peroxidase-Blocking Solution (3% hydrogen peroxide in methanol, Dako Omnis) and then non-specific antibody binding was blocked for 20 minutes with Protein blocking buffer (Dako Omnis).
Sections were immunostained for 1 hour at room temperature with primary antibodies (Table 1) and then were covered with secondary antibody for 30 minutes at room temperature. The signal was developed by using DAB detection kit (Dako Omnis), then sections were counterstained with Harry's modified Hematoxylin. Finally, slides were washed, dehydrated with increasing alcohol and xylene and

mounted with Eukitt (Sigma Aldrich). Immunostaining results were recorded as percentage of positive cells.

Tunel Assay

Formalin-fixed and paraffin-embedded tissue blocks were sectioned, deparaffinized and rehydrated through a graded ethanol series. Detection of apoptotic cells by terminal deoxytransferase-mediated deoxy uridine nick end-labelling (TUNEL) assay was carried out utilizing In Situ Cell Death Detection POD Kit (Roche Molecular Biochemicals). Sections were stained according to the manufacturer's protocol for paraffin-embedded tissues. Immunostaining results were recorded as percentage of positive cells.

H&E Staining

Formalin-fixed and paraffin embedded tissue blocks were sectioned (3μm), deparaffinized and rehydrated through decreasing alcohol, finally washed in distilled water. Sections were stained by immersing slides in hematoxylin for 3 minutes, washed with running water for a few minutes to allow stain to develop and then with distilled water. Slides were counterstained with Eosin for 3 minutes, dehydrated with alcohol and xylene and mounted with Eukitt (Sigma Aldrich). Results were recorded as metastatic area (μm^2) or metastatic foci/section.

TRF2 Immunohistochemistry analysis in human BC patients

TRF2 immunostaining was performed in a series of 30 primary triple-negative breast carcinomas (BC) and their corresponding metachronous metastases, 55 invasive breast carcinomas with different molecular subtypes (10 LuminalA BC, 10 LuminalB/HER2 negative BC, 10 LuminalB/HER2 positive BC, 9 HER2 subtype BC, 16 triple-negative subtype BC) and 50 benign breast lesions with their adjacent normal tissue (evaluable in 41 cases), surgically treated at the Regina Elena

Cancer Institute (Rome, Italy) between 2001 and 2018. Formalin-fixed paraffin-embedded specimens were cut on SuperFrost Plus slides (Menzel-Gläser, Braunschweig, Germany). 3µm thick formalin-fixed paraffin-embedded sections were stained with a Bond Polymer Refine Detection on an automated autostainer (BondTM Max, Leica Biosystems, Milan, Italy) with anti-TRF2 antibody listed in Table1. Diaminobenzidine (DAB) was used as chromogenic substrate. Immunostaining was evaluated by 2 biologists (SB, ADB) and TRF2 was assessed as positive when tumor cells showed immunoreaction in at least 10% neoplastic cells. Immunostaining results were recorded as immunoreactive score (IRS) resulting from multiplication of TRF2 positive cell proportion score and TRF2 staining intensity score as described in Fedchenko et al (Fedchenko and Reifenrath, 2014).

TCGA dataset and bioinformatics analysis

Normalized TCGA-BRCA gene expression of tumor samples were obtained from Broad Institute TCGA Genome Data Analysis Center (http://gdac.broadinstitute.org/): Firehose stddata__2016_01_28. Broad Institute of MIT and Harvard. doi:10.7908/C11G0KM9

Statistical significance of gene modulation between different subgroup of samples was assessed by Wilcoxon test. ANOVA test was performed for comparison of more than two groups. Significance was defined at the $p<0.05$ level.

Overall survival (OS) were performed by using Kaplan-Meier analysis and the log-rank test was used to assess differences between curves. Patients with high and low signal intensity were defined by considering positive and negative z-score values, respectively.

The analyses were completely conducted with Matlab R2020b.

Statistical analysis

For all the presented data, statistical tests used and n values are reported in the relative Figure legend. P values were calculated with GraphPad

Prism 6. P values were indicated as followed *P≤0.05; **P≤0.01; ***P≤0.001. Where not reported p value is not statistically significant.

Study approval

All animal procedures were in compliance with the national and international directives (D.L. 4 March 2014, no. 26; directive 2010/63/EU of the European Parliament and of the council; Guide for the Care and Use of Laboratory Animals, United States National Research Council, 2011 Animal Research guidelines Reporting of In Vivo Experiments (ARRIVE) guidelines) and approved by the Italian Ministry of the health (authorization n. 607/2019-PR issued on date 07-08-2019).

Patients surgically treated at the Regina Elena National Cancer Institute received written informed consent and the study was reviewed and approved by the Local Ethic Committee of the same Institute (del. n. 1201/19 issued on date 19/03/2019).

Table 1: primary antibodies

Antibodies	Company	DILUTION WB	DILUTION IF	DILUTION IHC
Mouse anti-TRF2 (4A794)	Millipore, 05-521	1:1000	1:1500	1:500
Rabbit anti-γH2AX (BLR053F)	Bethyl Laboratories, A700-053			1:500
Mouse anti-γH2AX (JBW301)	Millipore, 05-636	1:1000	1:500	
Rabbit anti-ATM, D2E2	Cell Signaling Technology, 2873	1:1000		
Rabbit anti-pATM, S1981	Cell signaling Technology, 13050	1:1000		

Antibodies	Company	DILUTION WB	DILUTION IF	DILUTION IHC
Mouse anti-Ki67 (MIB-1)	Dako Omnis, GA626			Ready-to-use
Mouse anti-CK (AE1/AE3)	Dako Omnis, M3515			1:50
Mouse anti-Lamin A/C (636)	Santa Cruz Biotechnology, sc-7292	1:1000	1:500	
Rabbit anti-Lamin B1	Abcam, 6048	1:5000	1:500	
Mouse anti-Emerin (H-12)	Santa Cruz Biotechnology, sc-25284	1:1000	1:200	
Rabbit anti-SUN1	Novus Biologicals, NBP1-87396	1:1000	1:200	
Rabbit anti-SUN2 (EPR6557)	Abcam, ab124916	1:2000	1:200	
Mouse anti-β-Actin (AC-74)	Sigma Aldrich, A2228	1:10000		
Rabbit anti-PCNT	Abcam, 4448		1:500	
Vinculin (VIN-11-5)	Sigma Aldrich, V4505		1:100	

Table 2: Immunofluorescence secondary antibodies

Antibodies	Company
Goat anti-rabbit Alexafluor 488	Cell signaling Technology
Goat anti-mouse Alexafluor 488	Cell signaling Technology
Goat anti-rabbit Alexafluor 555	Cell signaling Technology
Goat anti-mouse Alexafluor 555	Cell signaling Technology
Alexa Fluor 488 phalloidin	Life Technologies

5. GENERAL CONCLUSIONS AND PERSPECTIVES

A clear relationship between human well-being and the state of the environment is now known. The pollution of air, water and soil matrices has negative repercussions on human health and is decisive in the development of diseases of all kinds, including oncological diseases in adults and children (Llopis-González *et al.*, 2015; Watson, Holman and Maguire-Eisen, 2016; Lewandowska *et al.*, 2019; J. Yin *et al.*, 2020).

Numerous carcinogenic substances are detectable in consumer goods such as clothing, cosmetics, cigarettes, pesticides, food and exhaust gases. Therefore, the organism is forced to continuously react to environmental conditions to preserve its health. For this reason, it is more than ever necessary to maintain a high level of prevention, with the aim of reducing the risk of developing pathologies, a risk based on the interaction between genetic and environmental factors. The former can be analyzed to identify any predisposing factors, the latter can be modified to reduce risks. In order to reach a level of prevention as high and specific as possible, it is necessary to investigate the mechanisms through which environmental factors act and the effects they can cause. For this purpose, this thesis aims to deepen the cause-effect relationship existing between environment and cancer, focusing on the modulation of TRF2, an important protein of telomere, which is also the target of multiple harmful environmental factors. In fact, over time, various studies have shown how telomere length, closely linked to tumor onset, is influenced by environmental factors and lifestyle.

Some of the preliminary data behind this thesis show a notable increase of TRF2 in several types of cancer, including BC. In the latter, the modulation of TRF2 expression has allowed to highlight new roles of the protein which, in fact, in addition to playing a role in tumor immunosurveillance and angiogenesis (Biroccio *et al.*, 2006, 2013; Cherfils-Vicini *et al.*, 2019; Zizza *et al.*, 2019), seems to have a direct effect on cell migration and metastasis. TRF2 expression has been

found to increase during progression from normal tissue to benign lesion to malignant lesion.

Therefore, the data obtained seem to have considerable clinical relevance as they identify a positive correlation between the expression of TRF2 and the progression of BC in patients.

Collectively, results reveal, on the one hand, new insights into the role of TRF2 and the downstream consequences of the action of harmful environmental factors, and on the other hand, they identify TRF2 as a marker of metastasis and prognosis in BC. TRF2 could therefore prove to be a valid pharmacological target, thus paving the way for the development of new treatments. In this regard, the therapeutic relevance and efficacy of some specific molecules capable of inhibiting the expression of TRF2 are already being analyzed, thus slowing down and hindering the process of metastatization.

6. REFERENCES

Akinyemiju, T. F. *et al.* (2015) 'Residential environment and breast cancer incidence and mortality: A systematic review and meta-analysis', *BMC Cancer*, 15(1). doi: 10.1186/s12885-015-1098-z.

Al-Mahmood, S. *et al.* (2018) 'Metastatic and triple-negative breast cancer: challenges and treatment options', *Drug Delivery and Translational Research*. doi: 10.1007/s13346-018-0551-3.

Alexandrov, L. B. *et al.* (2016) 'Mutational signatures associated with tobacco smoking in human cancer', *Science*, 354(6312). doi: 10.1126/science.aag0299.

Amorim, J. P. *et al.* (2016) 'The role of ATRX in the alternative lengthening of telomeres (ALT) phenotype', *Genes*. doi: 10.3390/genes7090066.

Anand, P. *et al.* (2008) 'Cancer is a preventable disease that requires major lifestyle changes', *Pharmaceutical Research*. doi: 10.1007/s11095-008-9661-9.

Bai, Y. *et al.* (2014) 'Molecular targeting of TRF2 suppresses the growth and tumorigenesis of glioblastoma stem cells', *GLIA*, 62(10). doi: 10.1002/glia.22708.

Bailey, S. M. and Murnane, J. P. (2006) 'Telomeres, chromosome instability and cancer', *Nucleic Acids Research*, 34(8). doi: 10.1093/nar/gkl303.

Bandaria, J. N. *et al.* (2016) 'Shelterin protects chromosome ends by compacting telomeric chromatin', *Cell*, 164(4). doi: 10.1016/j.cell.2016.01.036.

Baveye, P. and Laba, M. (2008) 'Aggregation and toxicology of titanium dioxide nanoparticles', *Environmental Health Perspectives*, 116(4), pp. 152–155. doi: 10.1289/ehp.10915.

Begus-Nahrmann, Y. *et al.* (2012) 'Transient telomere dysfunction

induces chromosomal instability and promotes carcinogenesis', *Journal of Clinical Investigation*, 122(6). doi: 10.1172/JCI61745.

Belpomme, D. *et al.* (2007) 'The multitude and diversity of environmental carcinogens', *Environmental Research*. doi: 10.1016/j.envres.2007.07.002.

Benarroch-Popivker, D. *et al.* (2016) 'TRF2-Mediated Control of Telomere DNA Topology as a Mechanism for Chromosome-End Protection', *Molecular Cell*, 61(2). doi: 10.1016/j.molcel.2015.12.009.

Benhamou, Y. *et al.* (2016) 'Telomeric repeat-binding factor 2: A marker for survival and anti-EGFR efficacy in oral carcinoma', *Oncotarget*, 7(28), pp. 44236–44251. doi: 10.18632/oncotarget.10005.

Bernardes de Jesus, B. and Blasco, M. A. (2013) 'Telomerase at the intersection of cancer and aging', *Trends in Genetics*. doi: 10.1016/j.tig.2013.06.007.

Bi, W. *et al.* (1992) 'Mortality and incidence of bladder cancer in benzidine-exposed workers in China', *American Journal of Industrial Medicine*, 21(4). doi: 10.1002/ajim.4700210404.

Bidzinska, J., Baginski, M. and Skladanowski, A. (2014) 'Novel Anticancer Strategy Aimed at Targeting Shelterin Complexes by the Induction of Structural Changes in Telomeric DNA: Hitting two Birds with one Stone', *Current Cancer Drug Targets*, 14(2). doi: 10.2174/1568009614666140120122535.

Bilaud, T. *et al.* (1997) 'Telomeric localization of TRF2, a novel human telobox protein', *Nature Genetics*. doi: 10.1038/ng1097-236.

Biroccio, A. *et al.* (2002) 'Glutathione influences c-Myc-induced apoptosis in M14 human melanoma cells', *Journal of Biological Chemistry*, 277(46), pp. 43763–43770.

Biroccio, A. *et al.* (2006) 'TRF2 inhibition triggers apoptosis and reduces tumourigenicity of human melanoma cells', *European Journal of Cancer*, 42(12). doi: 10.1016/j.ejca.2006.03.010.

Biroccio, A. *et al.* (2013) 'TRF2 inhibits a cell-extrinsic pathway through which natural killer cells eliminate cancer cells', *Nature Cell Biology*, 15(7), pp. 818–828.

Blackburn, E. H. and Collins, K. (2011) 'Telomerase: An RNP enzyme synthesizes DNA', *Cold Spring Harbor Perspectives in Biology*, 3(5). doi: 10.1101/cshperspect.a003558.

Blackburn, E. H., Epel, E. S. and Lin, J. (2015) 'Human telomere biology: A contributory and interactive factor in aging, disease risks, and protection', *Science*, 350(6265), pp. 1193–1198. doi: 10.1126/science.aab3389.

Blanco, R. *et al.* (2007) 'Telomerase abrogation dramatically accelerates TRF2-induced epithelial carcinogenesis', *Genes and Development*, 21(2), pp. 206–220. doi: 10.1101/gad.406207.

Blasco, M. A. (2005) 'Telomeres and human disease: Ageing, cancer and beyond', *Nature Reviews Genetics*, 6(8), pp. 611–622. doi: 10.1038/nrg1656.

Broccoli, D. *et al.* (1997) 'Human telomeres contain two distinct Myb-related proteins, TRF1 and TRF2', *Nature Genetics*. doi: 10.1038/ng1097-231.

Bryan, T. M. *et al.* (1995) 'Telomere elongation in immortal human cells without detectable telomerase activity', *EMBO Journal*, 14(17). doi: 10.1002/j.1460-2075.1995.tb00098.x.

Cayuela, M. L., Flores, J. M. and Blasco, M. A. (2005) 'The telomerase RNA component Terc is required for the tumour-promoting effects of Tert overexpression', *EMBO Reports*, 6(3). doi: 10.1038/sj.embor.7400359.

Celli, G. B., Denchi, E. L. and de Lange, T. (2006) 'Ku70 stimulates fusion of dysfunctional telomeres yet protects chromosome ends from homologous recombination', *Nature Cell Biology*, 8(8). doi: 10.1038/ncb1444.

Celli, G. B. and de Lange, T. (2005) 'DNA processing is not required for ATM-mediated telomere damage response after TRF2 deletion', *Nature Cell Biology*, 7(7), pp. 712–718. doi: 10.1038/ncb1275.

Cesare, A. J. and Griffith, J. D. (2004) 'Telomeric DNA in ALT Cells Is Characterized by Free Telomeric Circles and Heterogeneous t-Loops', *Molecular and Cellular Biology*, 24(22). doi: 10.1128/mcb.24.22.9948-9957.2004.

Chagpar, A. B. and Coccia, M. (2012) 'Breast cancer and socio-economic factors', *Working Paper of Public Health*, 1(1). doi: 10.4081/wpph.2012.6773.

Chakravarti, D., LaBella, K. A. and DePinho, R. A. (2021) 'Telomeres: history, health, and hallmarks of aging', *Cell*. doi: 10.1016/j.cell.2020.12.028.

Chan, S. R. W. L. and Blackburn, E. H. (2004) 'Telomeres and telomerase', *Philosophical Transactions of the Royal Society B: Biological Sciences*, 359(1441), pp. 109–121. doi: 10.1098/rstb.2003.1370.

Chang, W. *et al.* (2013) 'Emerin organizes actin flow for nuclear movement and centrosome orientation in migrating fibroblasts', *Molecular Biology of the Cell*, 24(24), pp. 3869–3880. doi: 10.1091/mbc.E13-06-0307.

Chang, W. *et al.* (2019) 'Imbalanced nucleocytoskeletal connections create common polarity defects in progeria and physiological aging', *Proceedings of the National Academy of Sciences of the United States of America*, 116(9), pp. 3578–3583. doi: 10.1073/pnas.1809683116.

Chang, W., Antoku, S. and Gundersen, G. G. (2016) 'Wound-healing assays to study mechanisms of nuclear movement in fibroblasts and myoblasts', *Methods in Molecular Biology*, 1411, pp. 255–267. doi: 10.1007/978-1-4939-3530-7_17.

Chen, Y. *et al.* (2008) 'A shared docking motif in TRF1 and TRF2 used for differential recruitment of telomeric proteins', *Science*, 319(5866),

pp. 1092–1096.

Chen, Y. *et al.* (2011) 'A conserved motif within RAP1 has diversified roles in telomere protection and regulation in different organisms', *Nature Structural and Molecular Biology*, 18(2). doi: 10.1038/nsmb.1974.

Chen, Y. (2019) 'The structural biology of the shelterin complex', *Biological Chemistry*. doi: 10.1515/hsz-2018-0368.

Cheng, I. *et al.* (2015) 'Contribution of the neighborhood environment and obesity to breast cancer survival: The California breast cancer survivorship consortium', *Cancer Epidemiology Biomarkers and Prevention*, 24(8). doi: 10.1158/1055-9965.EPI-15-0055.

Cherfils-Vicini, J. *et al.* (2014) 'A novel pathway links telomeres to NK-cell activity: Implications for immunotherapy', *OncoImmunology*, 3(1), pp. 2–4. doi: 10.4161/onci.27358.

Cherfils-Vicini, J. *et al.* (2019) ' Cancer cells induce immune escape via glycocalyx changes controlled by the telomeric protein TRF 2 ', *The EMBO Journal*, 38(11). doi: 10.15252/embj.2018100012.

Chiu, Y. H. *et al.* (2017) 'Prenatal particulate air pollution exposure and body composition in urban preschool children: Examining sensitive windows and sex-specific associations', *Environmental Research*, 158. doi: 10.1016/j.envres.2017.07.026.

Choi, J., Fauce, S. R. and Effros, R. B. (2008) 'Reduced telomerase activity in human T lymphocytes exposed to cortisol', *Brain, Behavior, and Immunity*, 22(4). doi: 10.1016/j.bbi.2007.12.004.

Claude, E. and Decottignies, A. (2020) 'Telomere maintenance mechanisms in cancer: telomerase, ALT or lack thereof', *Current Opinion in Genetics and Development*. doi: 10.1016/j.gde.2020.01.002.

Cohen, S. B. *et al.* (2007) 'Protein composition of catalytically active human telomerase from immortal cells', *Science*, 315(5820). doi: 10.1126/science.1138596.

Conlon, M. S. C. *et al.* (2020) 'Cigarette-smoking characteristics and interest in cessation in patients with head-and-neck cancer', *Current Oncology*, 27(5). doi: 10.3747/co.27.6019.

Coughlin, S. S. (2019) 'Social determinants of breast cancer risk, stage, and survival', *Breast Cancer Research and Treatment*. doi: 10.1007/s10549-019-05340-7.

Coughlin, S. S. and King, J. (2010) 'Breast and cervical cancer screening among women in metropolitan areas of the United States by county-level commuting time to work and use of public transportation, 2004 and 2006', *BMC Public Health*, 10. doi: 10.1186/1471-2458-10-146.

Counter, C. M. *et al.* (1992) 'Telomere shortening associated with chromosome instability is arrested in immortal cells which express telomerase activity', *EMBO Journal*, 11(5). doi: 10.1002/j.1460-2075.1992.tb05245.x.

Court, R. *et al.* (2005) 'How the human telomeric proteins TRF1 and TRF2 recognize telomeric DNA: A view from high-resolution crystal structures', *EMBO Reports*, 6(1). doi: 10.1038/sj.embor.7400314.

Coyle, Y. M. (2004) 'The effect of environment on breast cancer risk', *Breast Cancer Research and Treatment*, 84(3), pp. 273–288. doi: 10.1023/B:BREA.0000019964.33963.09.

Crabbe, L. *et al.* (2012) 'Human Telomeres Are Tethered to the Nuclear Envelope during Postmitotic Nuclear Assembly', *Cell Reports*, 2(6), pp. 1521–1529.

D'Adda Di Fagagna, F. *et al.* (2003) 'A DNA damage checkpoint response in telomere-initiated senescence', *Nature*, 426(6963), pp. 194–198. doi: 10.1038/nature02118.

Dai, X. *et al.* (2015) 'Breast cancer intrinsic subtype classification, clinical use and future trends', *American Journal of Cancer Research*.

Denchi, E. L. and De Lange, T. (2007) 'Protection of telomeres through

independent control of ATM and ATR by TRF2 and POT1', *Nature*, 448(7157), pp. 1068–1071. doi: 10.1038/nature06065.

Deng, Z. *et al.* (2010) 'TERRA RNA Binding to TRF2 Facilitates Heterochromatin Formation and ORC Recruitment at Telomeres Zhong Deng1, Julie Norseen1, Andreas Wiedmer1, Harold Riethman1, and Paul M. Lieberman1,2 1 The Wistar Institute 3601 Spruce Street Philadelphia, PA 19104 Abs', 35(4), pp. 403–413. doi: 10.1016/j.molcel.2009.06.025.TERRA.

Denissenko, M. F. *et al.* (1997) 'Cytosine methylation determines hot spots of DNA damage in the human P53 gene', *Proceedings of the National Academy of Sciences of the United States of America*, 94(8), pp. 3893–3898. doi: 10.1073/pnas.94.8.3893.

Denkert, C. *et al.* (2017) 'Molecular alterations in triple-negative breast cancer—the road to new treatment strategies', *The Lancet*. doi: 10.1016/S0140-6736(16)32454-0.

Dent, R. *et al.* (2007) 'Triple-negative breast cancer: Clinical features and patterns of recurrence', *Clinical Cancer Research*, 13(15). doi: 10.1158/1078-0432.CCR-06-3045.

Devreotes, P. and Horwitz, A. R. (2015) 'Signaling networks that regulate cell migration', *Cold Spring Harbor Perspectives in Biology*, 7(8), pp. 1–16. doi: 10.1101/cshperspect.a005959.

Diehl, M. C. *et al.* (2011) 'Elevated TRF2 in advanced breast cancers with short telomeres', *Breast Cancer Research and Treatment*, 127(3), pp. 623–630.

Dimitrova, N. *et al.* (2008) '53BP1 promotes non-homologous end joining of telomeres by increasing chromatin mobility', *Nature*, 456(7221). doi: 10.1038/nature07433.

Ding, N. *et al.* (2015) 'Respiratory cancers and pollution', *European Review for Medical and Pharmacological Sciences*, 19(1), pp. 31–37.

Ding, X. *et al.* (2007) 'SUN1 Is Required for Telomere Attachment to

Nuclear Envelope and Gametogenesis in Mice', *Developmental Cell*, 12(6), pp. 863–872. doi: 10.1016/j.devcel.2007.03.018.

Djojosubroto, M. W. *et al.* (2003) 'Erratum: Telomeres and telomerase in aging, regeneration and cancer (Molecules and Cells 15, 2 (164-175))', *Molecules and Cells*, 16(1), p. 142.

Doksani, Y. *et al.* (2013) 'XSuper-resolution fluorescence imaging of telomeres reveals TRF2-dependent T-loop formation', *Cell*, 155(2). doi: 10.1016/j.cell.2013.09.048.

Dong, W. *et al.* (2009) 'Sp1 upregulates expression of TRF2 and TRF2 inhibition reduces tumorigenesis in human colorectal carcinoma cells', *Cancer Biology and Therapy*, 8(22). doi: 10.4161/cbt.8.22.9880.

Doyle, A. D. *et al.* (2009) 'One-dimensional topography underlies three-dimensional fi brillar cell migration', *Journal of Cell Biology*, 184(4), pp. 481–490. doi: 10.1083/jcb.200810041.

Du, F. Le *et al.* (2015) 'Is the future of personalized therapy in triple-negative breast cancer based on molecular subtype?', *Oncotarget*, 6(15). doi: 10.18632/oncotarget.3849.

Erdel, F. *et al.* (2017) 'Telomere Recognition and Assembly Mechanism of Mammalian Shelterin', *Cell Reports*, 18(1). doi: 10.1016/j.celrep.2016.12.005.

Eriksen, K. T. *et al.* (2014) 'Dietary cadmium intake and risk of breast, endometrial and ovarian cancer in danish postmenopausal women: A prospective cohort study', *PLoS ONE*, 9(6). doi: 10.1371/journal.pone.0100815.

Fairall, L. *et al.* (2001) 'Structure of the TRFH dimerization domain of the human telomeric proteins TRF1 and TRF2', *Molecular Cell*, 8(2). doi: 10.1016/S1097-2765(01)00321-5.

Fedchenko, N. and Reifenrath, J. (2014) 'Different approaches for interpretation and reporting of immunohistochemistry analysis results in the bone tissue - a review', *Diagnostic pathology*, 9, p. 221. doi:

10.1186/s13000-014-0221-9.

Feldser, D. M. and Greider, C. W. (2007) 'Short Telomeres Limit Tumor Progression In Vivo by Inducing Senescence', *Cancer Cell*, 11(5). doi: 10.1016/j.ccr.2007.02.026.

Feng, J. *et al.* (1995) 'The RNA component of human telomerase', *Science*, 269(5228). doi: 10.1126/science.7544491.

Feuerhahn, S. *et al.* (2015) 'No DDRama at chromosome ends: TRF2 takes centre stage', *Trends in Biochemical Sciences*. doi: 10.1016/j.tibs.2015.03.003.

Flores, I., Cayuela, M. L. and Blasco, M. A. (2005) 'Molecular biology: Effects of telomerase and telomere length on epidermal stem cell behavior', *Science*, 309(5738). doi: 10.1126/science.1115025.

Folker, E. S. *et al.* (2011) 'Lamin A variants that cause striated muscle disease are defective in anchoring transmembrane actin-associated nuclear lines for nuclear movement', *Proceedings of the National Academy of Sciences of the United States of America*, 108(1), pp. 131–136.

Fradet-Turcotte, A. *et al.* (2013) '53BP1 is a reader of the DNA-damage-induced H2A Lys 15 ubiquitin mark', *Nature*, 499(7456). doi: 10.1038/nature12318.

Fruleux, A. and Hawkins, R. J. (2016) 'Physical role for the nucleus in cell migration', *Journal of Physics Condensed Matter*, 28(36).

Fumagalli, M. *et al.* (2012) 'Telomeric DNA damage is irreparable and causes persistent DNA-damage-response activation', *Nature Cell Biology*, 14(4). doi: 10.1038/ncb2466.

Gadad, S. S. *et al.* (2021) 'PARP-1 Regulates Estrogen-Dependent Gene Expression in Estrogen Receptor α–Positive Breast Cancer Cells', *Molecular Cancer Research*, pp. 1–12. doi: 10.1158/1541-7786.mcr-21-0103.

Galati, A. *et al.* (2012) 'TRF2 controls telomeric nucleosome

organization in a cell cycle phase-dependent manner', *PLoS ONE*, 7(4). doi: 10.1371/journal.pone.0034386.

García-Cao, I. *et al.* (2006) 'Increased p53 activity does not accelerate telomere-driven ageing', *EMBO Reports*, 7(5). doi: 10.1038/sj.embor.7400667.

Gaullier, G. *et al.* (2015) 'A higher-order entity formed by the flexible assembly of RAP1 with TRF2', *Nucleic Acids Research*, 44(4). doi: 10.1093/nar/gkv1531.

Greider, C. W. (2012) 'Wnt regulates TERT - Putting the horse before the cart', *Science*. doi: 10.1126/science.1223785.

Griffith, J. D. *et al.* (1999) 'Mammalian telomeres end in a large duplex loop', *Cell*, 97(4), pp. 503–514. doi: 10.1016/S0092-8674(00)80760-6.

Guilliam, T. A. and Yeeles, J. T. P. (2020) 'An updated perspective on the polymerase division of labor during eukaryotic DNA replication', *Critical Reviews in Biochemistry and Molecular Biology*. doi: 10.1080/10409238.2020.1811630.

Hakin-Smith, V. *et al.* (2003) 'Alternative lengthening of telomeres and survival in patients with glioblastoma multiforme', *Lancet*, 361(9360), pp. 836–838. doi: 10.1016/S0140-6736(03)12681-5.

Hamanaka, R. B. and Mutlu, G. M. (2018) 'Particulate Matter Air Pollution: Effects on the Cardiovascular System', *Frontiers in Endocrinology*. doi: 10.3389/fendo.2018.00680.

Hanaoka, S., Nagadoi, A. and Nishimura, Y. (2009) 'Comparison between TRF2 and TRF1 of their telomeric DNA-bound structures and DNA-binding activities', *Protein Science*, 14(1). doi: 10.1110/ps.04983705.

Harbeck, N. and Gnant, M. (2017) 'Breast cancer', *The Lancet*. doi: 10.1016/S0140-6736(16)31891-8.

Harley, C. B. (2008) 'Telomerase and cancer therapeutics', *Nature Reviews Cancer*. doi: 10.1038/nrc2275.

Hayashi, M. T. *et al.* (2015) 'Cell death during crisis is mediated by mitotic telomere deprotection', *Nature*, 522(7557). doi: 10.1038/nature14513.

Henson, J. D. *et al.* (2005) 'A robust assay for alternative lengthening of telomeres in tumors shows the significance of alternative lengthening of telomeres in sarcomas and astrocytomas', *Clinical Cancer Research*, 11(1), pp. 217–225.

Herrera, E., Samper, E. and Blasco, M. A. (1999) 'Telomere shortening in mTR(-/-) embryos is associated with failure to close the neural tube', *EMBO Journal*, 18(5). doi: 10.1093/emboj/18.5.1172.

Hiatt, R. A., Haslam, S. Z. and Osuch, J. (2009) 'The breast cancer and the environment research centers: Transdisciplinary research on the role of the environment in breast cancer etiology', *Environmental Health Perspectives*, 117(12), pp. 1814–1822. doi: 10.1289/ehp.0800120.

Higa, M. *et al.* (2017) 'TRF2 recruits ORC through TRFH domain dimerization', *Biochimica et Biophysica Acta - Molecular Cell Research*, 1864(1), pp. 191–201.

Hoffmeyer, K. *et al.* (2012) 'Wnt/β-catenin signaling regulates telomerase in stem cells and cancer cells', *Science*, 336(6088). doi: 10.1126/science.1218370.

Horikawa, I., Fujita, K. and Harris, C. C. (2011) 'p53 governs telomere regulation feedback too, via TRF2', *Aging*, 3(1). doi: 10.18632/aging.100271.

Horn, S. *et al.* (2013) 'TERT promoter mutations in familial and sporadic melanoma', *Science*, 339(6122). doi: 10.1126/science.1230062.

Houben, J. M. J. *et al.* (2008) 'Telomere length assessment: Biomarker of chronic oxidative stress?', *Free Radical Biology and Medicine*. doi: 10.1016/j.freeradbiomed.2007.10.001.

Hu, C. *et al.* (2017) 'Structural and functional analyses of the

mammalian TIN2-TPP1-TRF2 telomeric complex', *Cell Research*, 27(12). doi: 10.1038/cr.2017.144.

Hu, J. *et al.* (2012) 'Antitelomerase therapy provokes ALT and mitochondrial adaptive mechanisms in cancer', *Cell*, 148(4). doi: 10.1016/j.cell.2011.12.028.

Huff, J. *et al.* (2007) 'Cadmium-induced cancers in animals and in humans', *International Journal of Occupational and Environmental Health*, 13(2), pp. 202–212. doi: 10.1179/oeh.2007.13.2.202.

Jafri, M. A. *et al.* (2016) 'Roles of telomeres and telomerase in cancer, and advances in telomerase-targeted therapies', *Genome Medicine*, 8(1). doi: 10.1186/s13073-016-0324-x.

Jeffy, B. D., Chirnomas, R. B. and Romagnolo, D. F. (2002) 'Epigenetics of breast cancer: Polycyclic aromatic hydrocarbons as risk factors', in *Environmental and Molecular Mutagenesis*. doi: 10.1002/em.10051.

Jo, Y. J. *et al.* (2020) 'Particulate Matter Exposure During Oocyte Maturation: Cell Cycle Arrest, ROS Generation, and Early Apoptosis in Mice', *Frontiers in Cell and Developmental Biology*, 8. doi: 10.3389/fcell.2020.602097.

Kaleli, S., Deveci, A. and Guney Eskiler, G. (2018) 'Which Environment Makes Cancer?', *Oncology Research and Reviews*, 1(3), pp. 1–4. doi: 10.15761/orr.1000115.

Karlseder, J. *et al.* (2004) 'The telomeric protein TRF2 binds the ATM Kinase and Can Inhibit the ATM-dependent DNA damage response', *PLoS Biology*, 2(8). doi: 10.1371/journal.pbio.0020240.

Kawanishi, S. and Oikawa, S. (2004) 'Mechanism of telomere shortening by oxidative stress', in *Annals of the New York Academy of Sciences*. doi: 10.1196/annals.1297.047.

Key, T. J. *et al.* (2002) 'The effect of diet on risk of cancer', *Lancet*. doi: 10.1016/S0140-6736(02)09958-0.

Key, T. J. *et al.* (2020) 'Diet, nutrition, and cancer risk: What do we know and what is the way forward?', *The BMJ*, 368. doi: 10.1136/bmj.m511.

Khatau, S. B. *et al.* (2012) 'The distinct roles of the nucleus and nucleus-cytoskeleton connections in three-dimensional cell migration', *Scientific Reports*, 2. doi: 10.1038/srep00488.

Kibe, T. *et al.* (2010) 'Telomere Protection by TPP1 Is Mediated by POT1a and POT1b', *Molecular and Cellular Biology*, 30(4). doi: 10.1128/mcb.01498-09.

Kidiyoor, G. R. *et al.* (2020) 'ATR is essential for preservation of cell mechanics and nuclear integrity during interstitial migration', *Nature Communications*, 11(1), pp. 1–16.

Kim, H. *et al.* (2017) 'Systematic analysis of human telomeric dysfunction using inducible telosome/shelterin CRISPR/Cas9 knockout cells', *Cell Discovery*, 3. doi: 10.1038/celldisc.2017.34.

Kim, Y. *et al.* (2015) 'Variability of phenology and fluxes of water and carbon with observed and simulated soil moisture in the Ent Terrestrial Biosphere Model (Ent TBM version 1.0.1.0.0)', *Geoscientific Model Development*, 8(12), pp. 3837–3865. doi: 10.5194/gmd-8-3837-2015.

Kohn, H. I. (1990) 'Health Effects of Exposure to Low Levels of Ionizing Radiation (BEIR V)', *Radiation Research*, 124(2). doi: 10.2307/3577873.

Konishi, A., Izumi, T. and Shimizu, S. (2016) 'TRF2 protein interacts with core histones to stabilize chromosome ends', *Journal of Biological Chemistry*, 291(39), pp. 20798–20810. doi: 10.1074/jbc.M116.719021.

Korsh, J. *et al.* (2015) 'Polycyclic Aromatic Hydrocarbons and Breast Cancer: A Review of the Literature', *Breast Care*. doi: 10.1159/000436956.

Korten, I., Ramsey, K. and Latzin, P. (2017) 'Air pollution during pregnancy and lung development in the child', *Paediatric Respiratory*

Reviews, 21, pp. 38–46. doi: 10.1016/j.prrv.2016.08.008.

Koual, M. *et al.* (2020) 'Environmental chemicals, breast cancer progression and drug resistance', *Environmental Health: A Global Access Science Source*, 19(1), pp. 1–25. doi: 10.1186/s12940-020-00670-2.

Kumar, P. and Aggarwal, R. (2016) 'An overview of triple-negative breast cancer', *Archives of Gynecology and Obstetrics*, 293(2), pp. 247–269. doi: 10.1007/s00404-015-3859-y.

Kyo, S. and Inoue, M. (2002) 'Complex regulatory mechanisms of telomerase activity in normal and cancer cells: How can we apply them for cancer therapy?', *Oncogene*, 21(4). doi: 10.1038/sj.onc.1205163.

De Lange, T. (2009) 'How telomeres solve the end-protection problem', *Science*, 326(5955), pp. 948–952. doi: 10.1126/science.1170633.

De Lange, T. (2018) 'Shelterin-mediated telomere protection', *Annual Review of Genetics*, 52(1), pp. 223–247. doi: 10.1146/annurev-genet-032918-021921.

Lee, R. E. and Cubbin, C. (2002) 'Neighborhood context and youth cardiovascular health behaviors', *American Journal of Public Health*, 92(3), pp. 428–436. doi: 10.2105/AJPH.92.3.428.

Lei, M., Podell, E. R. and Cech, T. R. (2004) 'Structure of human POT1 bound to telomeric single-stranded DNA provides a model for chromosome end-protection', *Nature Structural and Molecular Biology*, 11(12). doi: 10.1038/nsmb867.

Leri, A. *et al.* (2003) 'Ablation of telomerase and telomere loss leads to cardiac dilatation and heart failure associated with p53 upregulation', *EMBO Journal*, 22(1). doi: 10.1093/emboj/cdg013.

Lewandowska, A. M. *et al.* (2019) 'Environmental risk factors for cancer - review paper', *Annals of Agricultural and Environmental Medicine*. doi: 10.26444/aaem/94299.

Lin, E. C. (2010) 'Radiation risk from medical imaging', *Mayo Clinic Proceedings*. doi: 10.4065/mcp.2010.0260.

Lingner, J., Cooper, J. P. and Cech, T. R. (1995) 'Telomerase and DNA end replication: No longer a lagging strand problem?', *Science*. doi: 10.1126/science.7545310.

Liu, D. *et al.* (2004) 'Telosome, a mammalian telomere-associated complex formed by multiple telomeric proteins', *Journal of Biological Chemistry*, 279(49). doi: 10.1074/jbc.M409293200.

Llopis-González, A. *et al.* (2015) 'Central nervous system (CNS) cancer in children and young people in the European Union and its involvements with socio-economic and environmental factors', *Journal of the Neurological Sciences*, 359(1–2). doi: 10.1016/j.jns.2015.10.055.

Loeb, L. A. *et al.* (1984) 'Smoking and Lung Cancer: An Overview', *Cancer Research*, 44. doi: 10.1016/s0169-5002(85)80187-2.

Londoño-Vallejo, J. A. *et al.* (2004) 'Alternative Lengthening of Telomeres Is Characterized by High Rates of Telomeric Exchange', *Cancer Research*, 64(7). doi: 10.1158/0008-5472.CAN-03-4035.

Lu, W. *et al.* (2013) 'Telomeres-structure, function, and regulation', *Experimental Cell Research*, 319(2), pp. 133–141. doi: 10.1016/j.yexcr.2012.09.005.

Luo, Q. *et al.* (2016) 'Cell stiffness determined by atomic force microscopy and its correlation with cell motility', *Biochimica et Biophysica Acta - General Subjects*, 1860(9), pp. 1953–1960.

M Waheed, R., Aleksandra, N. and Matthias, R. (2018) 'Scientific Evaluation of Dietary Factors in Cancer', *Journal of Nutritional Medicine and Diet Care*, 4(1). doi: 10.23937/2572-3278.1510029.

Macacu, A. *et al.* (2015) 'Active and passive smoking and risk of breast cancer: a meta-analysis', *Breast Cancer Research and Treatment*. doi: 10.1007/s10549-015-3628-4.

Maciejowski, J. *et al.* (2015) 'Chromothripsis and Kataegis Induced by

Telomere Crisis', *Cell*, 163(7). doi: 10.1016/j.cell.2015.11.054.

El Maï, M. *et al.* (2014) 'The telomeric protein TRF2 regulates angiogenesis by binding and activating the PDGFRβ promoter', *Cell Reports*, 9(3), pp. 1047–1060. doi: 10.1016/j.celrep.2014.09.038.

Maloisel, L., Fabre, F. and Gangloff, S. (2008) 'DNA Polymerase δ Is Preferentially Recruited during Homologous Recombination To Promote Heteroduplex DNA Extension', *Molecular and Cellular Biology*, 28(4), pp. 1373–1382. doi: 10.1128/mcb.01651-07.

Manisalidis, I. *et al.* (2020) 'Environmental and Health Impacts of Air Pollution: A Review', *Frontiers in Public Health*. doi: 10.3389/fpubh.2020.00014.

Di Maro, S. *et al.* (2014) 'Shading the TRF2 recruiting function: A new horizon in drug development', *Journal of the American Chemical Society*, 136(48), pp. 16708–16711. doi: 10.1021/ja5080773.

Martens, D. S. and Nawrot, T. S. (2016) 'Air Pollution Stress and the Aging Phenotype: The Telomere Connection', *Current environmental health reports*, 3(3). doi: 10.1007/s40572-016-0098-8.

Martin-Ruiz, C. M. *et al.* (2005) 'Telomere length in white blood cells is not associated with morbidity or mortality in the oldest old: A population-based study', *Aging Cell*, 4(6), pp. 287–290. doi: 10.1111/j.1474-9726.2005.00171.x.

McElligott, R. and Wellinger, R. J. (1997) 'The terminal DNA structure of mammalian chromosomes', *EMBO Journal*, 16(12), pp. 3705–3714. doi: 10.1093/emboj/16.12.3705.

Meijering, E., Dzyubachyk, O. and Smal, I. (2012) 'Methods for cell and particle tracking', *Methods in Enzymology*, 504, pp. 183–200.

Mendez, W. M. *et al.* (2017) 'Relationships between arsenic concentrations in drinking water and lung and bladder cancer incidence in U.S. Counties', *Journal of Exposure Science and Environmental Epidemiology*, 27(3), pp. 235–243. doi: 10.1038/jes.2016.58.

Mentella, M. C. *et al.* (2019) 'Cancer and mediterranean diet: A review', *Nutrients*. doi: 10.3390/nu11092059.

Di Micco, R. *et al.* (2021) 'Cellular senescence in ageing: from mechanisms to therapeutic opportunities', *Nature Reviews Molecular Cell Biology*. doi: 10.1038/s41580-020-00314-w.

Miri, M. *et al.* (2019) 'Air pollution and telomere length in adults: A systematic review and meta-analysis of observational studies', *Environmental Pollution*, 244, pp. 636–647. doi: 10.1016/j.envpol.2018.09.130.

Mondello, C., Smirnova, A. and Giulotto, E. (2010) 'Gene amplification, radiation sensitivity and DNA double-strand breaks', *Mutation Research - Reviews in Mutation Research*. doi: 10.1016/j.mrrev.2010.01.008.

Von Morgen, P. and Maciejowski, J. (2018) 'The ins and outs of telomere crisis in cancer', *Genome Medicine*. doi: 10.1186/s13073-018-0596-4.

Mori, K. *et al.* (2020) 'Smoking and bladder cancer: review of the recent literature', *Current opinion in urology*, 30(5). doi: 10.1097/MOU.0000000000000804.

Muñoz, P. *et al.* (2005) 'XPF nuclease-dependent telomere loss and increased DNA damage in mice overexpressing TRF2 result in premature aging and cancer', *Nature Genetics*, 37(10). doi: 10.1038/ng1633.

Muñoz, P., Blanco, R. and Blasco, M. A. (2006) 'Role of the TRF2 telomeric protein in cancer and ageing', *Cell Cycle*, 5(7), pp. 718–721. doi: 10.4161/cc.5.7.2636.

Murnane, J. P. *et al.* (1994) 'Telomere dynamics in an immortal human cell line', *EMBO Journal*, 13(20). doi: 10.1002/j.1460-2075.1994.tb06822.x.

Nabetani, A. and Ishikawa, F. (2009) 'Unusual Telomeric DNAs in

Human Telomerase-Negative Immortalized Cells', *Molecular and Cellular Biology*, 29(3). doi: 10.1128/mcb.00603-08.

Naidu, R. *et al.* (2021) 'Chemical pollution: A growing peril and potential catastrophic risk to humanity', *Environment International*. doi: 10.1016/j.envint.2021.106616.

Nakanishi, K. *et al.* (2003) 'Expression of mRNAs for telomeric repeat binding factor (TRF)-1 and TRF2 in atypical adenomatous hyperplasia and adenocarcinoma of the lung', *Clinical Cancer Research*, 9(3), pp. 1105–1111.

Nassour, J., Schmidt, T. T. and Karlseder, J. (2020) 'Telomeres and Cancer: Resolving the Paradox', *Annual Review of Cancer Biology*, 5, pp. 59–77. doi: 10.1146/annurev-cancerbio-050420-023410.

Nastały, P. *et al.* (2020) 'Role of the nuclear membrane protein Emerin in front-rear polarity of the nucleus', *Nature Communications*, 11(1), pp. 1–12. doi: 10.1038/s41467-020-15910-9.

Ng, R. *et al.* (2020) 'Smoking, drinking, diet and physical activity - Modifiable lifestyle risk factors and their associations with age to first chronic disease', *International Journal of Epidemiology*, 49(1). doi: 10.1093/ije/dyz078.

Nielsen, L. S. *et al.* (2014) 'Occupational asbestos exposure and lung cancer - A systematic review of the literature', *Archives of Environmental and Occupational Health*. doi: 10.1080/19338244.2013.863752.

Nikitina, T. and Woodcock, C. L. (2004) 'Closed chromatin loops at the ends of chromosomes', *Journal of Cell Biology*, 166(2), pp. 161–165. doi: 10.1083/jcb.200403118.

O'Hagan, R. C. *et al.* (2002) 'Telomere dysfunction provokes regional amplification and deletion in cancer genomes', *Cancer Cell*, 2(2). doi: 10.1016/S1535-6108(02)00094-6.

Okamoto, K. *et al.* (2013) 'A two-step mechanism for TRF2-mediated

chromosome-end protection', *Nature*, 494(7438), pp. 502–505.

Okunola A, A. *et al.* (2019) 'Public and Environmental Health Effects of Plastic Wastes Disposal: A Review', *Journal of Toxicology and Risk Assessment*, 5(2). doi: 10.23937/2572-4061.1510021.

Östlund, C. *et al.* (2019) 'Pathogenic mutations in genes encoding nuclear envelope proteins and defective nucleocytoplasmic connections', *Experimental Biology and Medicine*, 244(15), pp. 1333–1344. doi: 10.1177/1535370219862243.

Paeschke, K., McDonald, K. R. and Zakian, V. A. (2010) 'Telomeres: Structures in need of unwinding', *FEBS Letters*. doi: 10.1016/j.febslet.2010.07.007.

Pal, D. *et al.* (2015) 'Over-expression of telomere binding factors (TRF1 & TRF2) in renal cell carcinoma and their inhibition by using SiRNA induce apoptosis, reduce cell proliferation and migration invitro', *PLoS ONE*, 10(3), pp. 1–12. doi: 10.1371/journal.pone.0115651.

Palm, W. and De Lange, T. (2008) 'How shelterin protects mammalian telomeres', *Annual Review of Genetics*. doi: 10.1146/annurev.genet.41.110306.130350.

Parkinson, E. K. (1996) 'Do telomerase antagonists represent a novel anti-cancer strategy?', *British Journal of Cancer*, 73(1), pp. 1–4. doi: 10.1038/bjc.1996.1.

Parsa, N. (2012) 'Environmental factors inducing human cancers', *Iranian Journal of Public Health*.

Pennarun, G. *et al.* (2021) 'Increase in lamin B1 promotes telomere instability by disrupting the shelterin complex in human cells.', *Nucleic acids research*, pp. 1–20.

Pernaut, C., Lopez, F. and Ciruelos, E. (2018) 'Standard Neoadjuvant Treatment in Early/Locally Advanced Breast Cancer', *Breast Care*. doi: 10.1159/000491759.

Perrem, K. *et al.* (2001) 'Coexistence of Alternative Lengthening of Telomeres and Telomerase in hTERT-Transfected GM847 Cells', *Molecular and Cellular Biology*, 21(12). doi: 10.1128/mcb.21.12.3862-3875.2001.

Petersen, S., Saretzki, G. and Von Zglinicki, T. (1998) 'Preferential accumulation of single-stranded regions in telomeres of human fibroblasts', *Experimental Cell Research*, 239(1). doi: 10.1006/excr.1997.3893.

Petti, E. *et al.* (2019) 'SFPQ and NONO suppress RNA:DNA-hybrid-related telomere instability', *Nature Communications*, 10(1).

Peuscher, M. H. and Jacobs, J. J. L. (2011) 'DNA-damage response and repair activities at uncapped telomeres depend on RNF8', *Nature Cell Biology*, 13(9). doi: 10.1038/ncb2326.

Pfeiffer, V. and Lingner, J. (2013) 'Replication of telomeres and the regulation of telomerase', *Cold Spring Harbor Perspectives in Biology*. doi: 10.1101/cshperspect.a010405.

Portier, C. J. (2020) 'A comprehensive analysis of the animal carcinogenicity data for glyphosate from chronic exposure rodent carcinogenicity studies', *Environmental Health: A Global Access Science Source*. doi: 10.1186/s12940-020-00574-1.

Prioleau, M. N. and MacAlpine, D. M. (2016) 'DNA replication origins—Where do we begin?', *Genes and Development*. doi: 10.1101/gad.285114.116.

Pudrovska, T., Anishkin, A. and Shen, Y. (2012) 'Early-life socioeconomic status and the prevalence of breast cancer in later life', *Research on Aging*, 34(3). doi: 10.1177/0164027511415632.

Reddel, R. (2014) 'Telomere Maintenance Mechanisms in Cancer: Clinical Implications', *Current Pharmaceutical Design*, 20(41), pp. 6361–6374. doi: 10.2174/13816128206661406301010 47.

Rizvi, S., Raza, S. T. and Mahdi, F. (2015) 'Telomere Length

Variations in Aging and Age-Related Diseases', *Current Aging Science*, 7(3). doi: 10.2174/1874609808666150122153151.

Rizzo, A. *et al.* (2017) 'SIRT6 interacts with TRF2 and promotes its degradation in response to DNA damage', *Nucleic Acids Research*, 45(4), pp. 1820–1834. doi: 10.1093/nar/gkw1202.

Romano, G. H. *et al.* (2013) 'Environmental Stresses Disrupt Telomere Length Homeostasis', *PLoS Genetics*, 9(9). doi: 10.1371/journal.pgen.1003721.

Ronckers, C. M., Erdmann, C. A. and Land, C. E. (2005) 'Radiation and breast cancer: A review of current evidence', *Breast Cancer Research*. doi: 10.1186/bcr970.

Rouda, S. and Skordalakes, E. (2007) 'Structure of the RNA-Binding Domain of Telomerase: Implications for RNA Recognition and Binding', *Structure*, 15(11). doi: 10.1016/j.str.2007.09.007.

Ruis, P. *et al.* (2021) 'TRF2-independent chromosome end protection during pluripotency', *Nature*, 589(7840), pp. 103–109. doi: 10.1038/s41586-020-2960-y.

S. Coughlin, S. (2015) 'The Impact of the Natural, Social, Built, and Policy Environments on Breast Cancer', *Journal of Environment and Health Science*. doi: 10.15436/2378-6841.15.020.

Sabatier, L. *et al.* (2005) 'The loss of a single telomere can result in instability of multiple chromosomes in a human tumor cell line', *Molecular Cancer Research*, 3(3). doi: 10.1158/1541-7786.MCR-04-0194.

Salvati, E. *et al.* (2014) 'Evidence for G-quadruplex in the promoter of vegfr-2 and its targeting to inhibit tumor angiogenesis', *Nucleic Acids Research*, 42(5), pp. 2945–2957. doi: 10.1093/nar/gkt1289.

Sasco, A. J., Secretan, M. B. and Straif, K. (2004) 'Tobacco smoking and cancer: A brief review of recent epidemiological evidence', in *Lung Cancer*. doi: 10.1016/j.lungcan.2004.07.998.

Schmidt, C. W. (2020) 'Telomere length and air pollution: Observations in women who use biomass cookstoves', *Environmental Health Perspectives*. doi: 10.1289/EHP6445.

Schmutz, I. *et al.* (2017) 'TRF2 binds branched DNA to safeguard telomere integrity', *Nature Structural and Molecular Biology*, 24(9), pp. 734–742.

Schmutz, I. and De Lange, T. (2016) 'Shelterin', *Current Biology*, 26(10), pp. R397–R399. doi: 10.1016/j.cub.2016.01.056.

Sfeir, A. *et al.* (2009) 'Mammalian Telomeres Resemble Fragile Sites and Require TRF1 for Efficient Replication', *Cell*, 138(1). doi: 10.1016/j.cell.2009.06.021.

Sfeir, A. *et al.* (2010) 'Loss of Rap1 induces telomere recombination in the absence of NHEJ or a DNA damage signal', *Science*, 327(5973). doi: 10.1126/science.1185100.

Shammas, M. A. (2011) 'Telomeres, lifestyle, cancer, and aging', *Current Opinion in Clinical Nutrition and Metabolic Care*, 14(1), pp. 28–34. doi: 10.1097/MCO.0b013e32834121b1.

Shay, J. W. and Wright, W. E. (2005) 'Senescence and immortalization: Role of telomeres and telomerase', *Carcinogenesis*. doi: 10.1093/carcin/bgh296.

Siegel, R. L., Miller, K. D. and Jemal, A. (2020) 'Cancer statistics, 2020', *CA: A Cancer Journal for Clinicians*, 70(1), pp. 7–30. doi: 10.3322/caac.21590.

Simonet, T. *et al.* (2011) 'The human TTAGGG repeat factors 1 and 2 bind to a subset of interstitial telomeric sequences and satellite repeats', *Cell Research*, 21(7), pp. 1028–1038.

Smogorzewska, A. *et al.* (2002) 'DNA ligase IV-dependent NHEJ of deprotected mammalian telomeres in G1 and G2', *Current Biology*, 12(19). doi: 10.1016/S0960-9822(02)01179-X.

Smogorzewska, A. and De Lange, T. (2004) 'Regulation of telomerase

by telomeric proteins', *Annual Review of Biochemistry*. doi: 10.1146/annurev.biochem.73.071403.160049.

Stansel, R. M., De Lange, T. and Griffith, J. D. (2001) 'T-loop assembly in vitro involves binding of TRF2 near the 3′ telomeric overhang', *EMBO Journal*, 20(19). doi: 10.1093/emboj/20.19.5532.

Steensel, B. van and Lange, T. de (1997) 'Control of telomere length by the human telomeric protein TRF1 Bas', *Nature*, 385(February), pp. 740–743.

Van Steensel, B., Smogorzewska, A. and De Lange, T. (1998) 'TRF2 protects human telomeres from end-to-end fusions', *Cell*, 92(3), pp. 401–413. doi: 10.1016/S0092-8674(00)80932-0.

Subhawong, A. P. *et al.* (2009) 'The alternative lengthening of telomeres phenotype in breast carcinoma is associated with HER-2 overexpression', *Modern Pathology*, 22(11), pp. 1423–1431. doi: 10.1038/modpathol.2009.125.

Takai, H., Smogorzewska, A. and De Lange, T. (2003) 'DNA damage foci at dysfunctional telomeres', *Current Biology*, 13(17). doi: 10.1016/S0960-9822(03)00542-6.

Takai, K. K. *et al.* (2010) 'In vivo stoichiometry of shelterin components', *Journal of Biological Chemistry*, 285(2), pp. 1457–1467. doi: 10.1074/jbc.M109.038026.

Takai, K. K. *et al.* (2011) 'Telomere Protection by TPP1/POT1 Requires Tethering to TIN2', *Molecular Cell*, 44(4). doi: 10.1016/j.molcel.2011.08.043.

Tan, M. C. B., Goedegebuure, S. P. and Eberlein, T. J. (2012) 'Tumor Biology and Tumor Markers', in *Sabiston Textbook of Surgery*. doi: 10.1016/b978-1-4377-1560-6.00030-5.

Tavera-Mendoza, L. E. and Brown, M. (2017) 'A less invasive method for orthotopic injection of breast cancer cells into the mouse mammary gland', *Laboratory Animals*, 51(1), pp. 85–88.

Tomita, K. and Cooper, J. P. (2006) 'The Meiotic Chromosomal Bouquet: SUN Collects Flowers', *Cell*, 125(1), pp. 19–21. doi: 10.1016/j.cell.2006.03.020.

Trybek, T. *et al.* (2020) 'Telomeres and telomerase in oncogenesis (review)', *Oncology Letters*, 20(2), pp. 1015–1027. doi: 10.3892/ol.2020.11659.

U.S.DHSS (2010) *How Tobacco Smoke Causes Disease The Biology and Behavioral Basis for Smoking-Attributable Disease A Report of the Surgeon General*, *Public Health*.

Vagia, E., Mahalingam, D. and Cristofanilli, M. (2020) 'The landscape of targeted therapies in TNBC', *Cancers*. doi: 10.3390/cancers12040916.

Valdes, A. M. *et al.* (2005) 'Obesity, cigarette smoking, and telomere length in women', *Lancet*, 366(9486), pp. 662–664. doi: 10.1016/S0140-6736(05)66630-5.

De Vitis, M., Berardinelli, F. and Sgura, A. (2018) 'Telomere length maintenance in cancer: At the crossroad between telomerase and alternative lengthening of telomeres (ALT)', *International Journal of Molecular Sciences*. doi: 10.3390/ijms19020606.

Wahba, H. A. and El-Hadaad, H. A. (2015) 'Current approaches in treatment of triple-negative breast cancer', *Cancer Biology and Medicine*. doi: 10.7497/j.issn.2095-3941.2015.0030.

Walton, R. T. *et al.* (2016) 'Air pollution, ethnicity and telomere length in east London schoolchildren: An observational study', *Environment International*, 96. doi: 10.1016/j.envint.2016.08.021.

Wang, F. *et al.* (2007) 'The POT1-TPP1 telomere complex is a telomerase processivity factor', *Nature*, 445(7127). doi: 10.1038/nature05454.

Wang, L. *et al.* (2018) 'Dual roles of TRF1 in tethering telomeres to the nuclear envelope and protecting them from fusion during meiosis', *Cell*

Death and Differentiation, 25(6), pp. 1174–1188.

Wang, R. C., Smogorzewska, A. and De Lange, T. (2004) 'Homologous recombination generates t-loop-sized deletions at human telomeres', *Cell*, 119(3). doi: 10.1016/j.cell.2004.10.011.

Wang, Z. and Xiaoying, W. U. (2021) 'Abnormal function of telomere protein TRF2 induces cell mutation and the effects of environmental tumor-promoting factors (Review)', *Oncology Reports*, 46(2), pp. 1–20. doi: 10.3892/OR.2021.8135.

Watson, M., Holman, D. M. and Maguire-Eisen, M. (2016) 'Ultraviolet Radiation Exposure and Its Impact on Skin Cancer Risk', *Seminars in Oncology Nursing*. doi: 10.1016/j.soncn.2016.05.005.

Wellinger, R. J. (2014) 'In the end, what's the problem?', *Molecular Cell*. doi: 10.1016/j.molcel.2014.03.008.

White, A. J. *et al.* (2016) 'Exposure to multiple sources of polycyclic aromatic hydrocarbons and breast cancer incidence', *Environment International*, 89–90. doi: 10.1016/j.envint.2016.02.009.

Williams, D. R., Mohammed, S. A. and Shields, A. E. (2016) 'Understanding and effectively addressing breast cancer in African American women: Unpacking the social context', *Cancer*. doi: 10.1002/cncr.29935.

Wolff, A. C. *et al.* (2014) 'Recommendations for human epidermal growth factor receptor 2 testing in breast cancer: American society of clinical oncology/college of American pathologists clinical practice guideline update', *Archives of Pathology and Laboratory Medicine*, 138(2). doi: 10.5858/arpa.2013-0953-SA.

Wood, A. M. *et al.* (2014) 'TRF2 and lamin A/C interact to facilitate the functional organization of chromosome ends', *Nature Communications*, 5.

Wright, W. E., Pereira-Smith, O. M. and Shay, J. W. (1989) 'Reversible cellular senescence: implications for immortalization of normal human

diploid fibroblasts.', *Molecular and Cellular Biology*, 9(7). doi: 10.1128/mcb.9.7.3088.

Wright, W. E. and Shay, J. W. (1992) 'The two-stage mechanism controlling cellular senescence and immortalization', *Experimental Gerontology*, 27(4). doi: 10.1016/0531-5565(92)90069-C.

Wu, P. and de Lange, T. (2008) 'No Overt Nucleosome Eviction at Deprotected Telomeres', *Molecular and Cellular Biology*, 28(18). doi: 10.1128/mcb.01764-07.

Yang, D. *et al.* (2011) 'Human telomeric proteins occupy selective interstitial sites', *Cell Research*, 21(7), pp. 1013–1027.

Yang, X. *et al.* (2015) 'Knockdown of telomeric repeat binding factor 2 enhances tumor radiosensitivity regardless of telomerase status', *Journal of Cancer Research and Clinical Oncology*, 141(9). doi: 10.1007/s00432-015-1911-8.

Yeager, T. R. *et al.* (1999) 'Telomerase-negative immortalized human cells contain a novel type of promyelocytic leukemia (PML) body', *Cancer Research*, 59(17).

Yin, J. *et al.* (2020) 'Impact of environmental factors on gastric cancer: A review of the scientific evidence, human prevention and adaptation', *Journal of Environmental Sciences (China)*. doi: 10.1016/j.jes.2019.09.025.

Yin, L. *et al.* (2020) 'Triple-negative breast cancer molecular subtyping and treatment progress', *Breast Cancer Research*, 22(1), pp. 1–13. doi: 10.1186/s13058-020-01296-5.

Yuan, X., Larsson, C. and Xu, D. (2019) 'Mechanisms underlying the activation of TERT transcription and telomerase activity in human cancer: old actors and new players', *Oncogene*. doi: 10.1038/s41388-019-0872-9.

Von Zglinicki, T. (2002) 'Oxidative stress shortens telomeres', *Trends in Biochemical Sciences*. doi: 10.1016/S0968-0004(02)02110-2.

Zhang, J. M. and Zou, L. (2020) 'Alternative lengthening of telomeres: From molecular mechanisms to therapeutic outlooks', *Cell and Bioscience*, 10(1), pp. 1–9. doi: 10.1186/s13578-020-00391-6.

Zhang, L. *et al.* (2019) 'Exposure to glyphosate-based herbicides and risk for non-Hodgkin lymphoma: A meta-analysis and supporting evidence', *Mutation Research - Reviews in Mutation Research*. doi: 10.1016/j.mrrev.2019.02.001.

Zhao, B. *et al.* (2018) 'Air pollution and telomere length: A systematic review of 12,058 subjects', *Cardiovascular Diagnosis and Therapy*, 8(4). doi: 10.21037/cdt.2018.06.05.

Zizza, P. *et al.* (2019) 'TRF2 positively regulates SULF2 expression increasing VEGF - A release and activity in tumor microenvironment', *Nucleic Acids Research*, 47(7), pp. 3365–3382.